Distribution Agreement

In presenting this thesis or dissertation as a partial fulfillment of the requirements for an advanced degree from Emory University, I hereby grant to Emory University and its agents the non-exclusive license to archive, make accessible, and display my thesis or dissertation in whole or in part in all forms of media, now or hereafter known, including display on the world wide web. I understand that I may select some access restrictions as part of the online submission of this thesis or dissertation. I retain all ownership rights to the copyright of the thesis or dissertation. I also retain the right to use in future works (such as articles or books) all or part of this thesis or dissertation.

Signature:

_____ _____

Donghai Liang Date

Development and Evaluation of External and Internal Methods for Assessing Exposures to Traffic Related Air Pollution

By

Donghai Liang
Doctor of Philosophy
Environmental Health Sciences

_____

Jeremy Sarnat, ScD
Advisor

_____

Armistead Russell, PhD
Committee Member

_____

Stefanie Sarnat, ScD
Committee Member

_____

Tianwei Yu, PhD
Committee Member

Accepted:

_____

Lisa A. Tedesco, Ph.D.
Dean of the James T. Laney School of Graduate Studies

_____

Date

Development and Evaluation of External and Internal Methods for Assessing Exposures to Traffic Related Air Pollution

By

Donghai Liang
MPH, Yale University, 2014
BS, Peking University, 2012

Advisor: Jeremy Sarnat, ScD

An abstract of
A dissertation submitted to the Faculty of the
James T. Laney School of Graduate Studies of Emory University
in partial fulfillment of the requirements for the degree of Doctor of Philosophy
in Environmental Health Sciences
2018

Abstract

Development and Evaluation of External and Internal Methods for Assessing Exposures to Traffic Related Air Pollution
By Donghai Liang

Introduction

Short- and long-term exposures to traffic pollution have been linked to numerous adverse health endpoints. While various approaches have been proposed to model traffic exposures and corresponding health response, few have systematically examined how well these approaches reflect actual and biologically-relevant exposures along a complete emissions-to-dose pathway. The overarching goal of this dissertation is to develop and evaluate external and internal methods for assessing exposures to traffic related air pollution (TRAP). To achieve this goal, two large prospective panel-studies were conducted. In the first study, the Dorm Room Inhalation to Vehicle Emissions (DRIVE) study, I examined spatiotemporal variability trends and assessed the potential for bias and errors when using a roadside monitor as a primary traffic pollution exposure surrogate, in lieu of more spatially-refined, proximal exposure indicators (Aim1). Using data from the DRIVE study, I also examined the feasibility of using high-resolution metabolomics (HRM) as means of assessing internal exposures, through the identification of traffic pollution-related metabolites (Aim 2). Finally, in the second study, the Atlanta Commuters Exposure (ACE-2) study, I applied high-resolution environmental metabolomics to examine and develop metabolic signals that are most predictive of TRAP exposure or the corresponding effects, and to investigate the potential effect modification of asthma on modifying the metabolic responses to TRAP exposures (Aim 3).

Methods

For Aim 1, I measured several single TRAP indicators with high spatial and temporal resolution at six indoor and outdoor sites ranging from 0.01 to 2.3 km away from a major highway artery. I examined spatiotemporal variability trends of these TRAP indicators and estimated errors when using a roadside monitor as a primary traffic pollution exposure surrogate for use in epidemiologic studies. For Aim 2, 54 students living in dormitories either near (20 m) or far (1.4 km) from the highway conducted personal sampling and contributed bio samples (plasma and saliva) during the DRIVE study. Untargeted HRM were used to identify potential metabolic pathways associated with traffic-related air pollutants in the panel. For Aim 3, we conducted extensive exposure assessment on 27 air pollutants during each commute session and conducted high-resolution metabolomics profiling on blood samples from the commuters prior to and after the commute in ACE-2 study. I further evaluated metabolite and metabolic pathway alternations using an untargeted metabolome-wide association study (MWAS) framework with pathway analyses and chemical annotation.

Results

In Aim 1, Pollutant levels measured during DRIVE showed a low impact of this highway hotspot source. Patterns of correlation among the sites also varied by pollutant and time of day. Pronounced attenuation of observed changes in health effects were found when using measured pollutant from the near-road monitor as a surrogate for true exposure, and the magnitude varied substantially over the course of the day. In Aim 2, I identified and verified biological perturbations associated with primary traffic pollutant, including arginine, histidine, γ-linolenic acid, and hypoxanthine.

Observed response was consistent with endogenous metabolic signaling related to oxidative stress, inflammation, and nucleic acid damage and repair. In Aim 3, I observed significant and robust metabolic perturbations associated with TRAP exposure among commuters in ACE-2 study. I confirmed the chemical identity of 45 unique metabolites enriched in these metabolic pathways, including inflammatory amino acids such as arginine, histidine, and methionine. Many of these molecules were not only associated with multiple TRAPs, but also responded differentially among asthmatic and healthy participants.

Conclusions

Collectively, the aims and analyses for this dissertation centered on a highly chemically-speciated set of external and internal measurements of traffic pollution, in a range of near road microenvironments. Caution should be taken when using near-road monitoring network observations, alone, to investigate health effects of traffic pollutants. Using the high-resolution environmental metabolomics platform, we observed significant and robust metabolic perturbations associated with TRAP exposure in two independent panels. I identified xenobiotic-mediated oxidative stress and acute inflammatory response related pathways and metabolites. These results motivate future studies geared towards development of metabolic markers for reflecting TRAP exposures, their corresponding effects, and the asthma etiology.

Development and Evaluation of External and Internal Methods for Assessing Exposures to Traffic Related Air Pollution

By

Donghai Liang
MPH, Yale University, 2014
BS, Peking University, 2012

Advisor: Jeremy Sarnat, ScD

A dissertation submitted to the Faculty of the
James T. Laney School of Graduate Studies of Emory University
in partial fulfillment of the requirements for the degree of Doctor of Philosophy
in Environmental Health Sciences
2018

Acknowledgement

Looking back at my amazing journey as a doctoral student, I still cannot believe it has been four years. I cherish every moment spent here at Emory and I am so blessed to have so many guidance, support and great help throughout my doctoral training.

First and foremost, I'd like to thank my dear advisor, Dr. Jeremy Sarnat, for his tremendous support, insightful guidance, and brilliant mentorship, without whom I cannot learn and accomplish so much. Word fails me to express my deepest gratitude to his mentorship and friendship throughout this amazing journey. I am also very lucky to have three awesome committee members, Ted, Stefanie, and Tianwei to point me to the right direction from the very beginning of my training.

In addition, I want to sincerely thank Rachel, Jen, Chandresh, Roby and Howard for their consistent support and help in accompanying me conduct the research projects since day one. In addition, I want to take this chance to thank all my collaborators for giving me the opportunities to work together with them on several amazing studies. I am especially grateful for all EH faculty and staff, and I want to thank many of them to serve as volunteers for one of my ongoing climate change project.

I am also thrilled to be a part of a fantastic PhD cohort, and every now and then I learn a great deal from my talented peers and I am really thankful for all their friendship, with special thanks to Molly, Qingyang, Dongni, Sam, Kostya and Naser. I also want to thank all my great friends from my childhood and high school, Peking University and Yale University, for their constant moral support and encouragement.

Finally, I want to thank my family, my parents and in-laws for their eternal love and support, especially my 83-year old grandmother who took great care of me for my first 18 years.

Last, and most importantly, I want to thank my wife, Jingxuan Zhao. I am so lucky to have met Jingxuan right here three years ago, and have gone through so many ups and downs on this journey together. Thank you for making my life shine and bright.

Table of Contents

INTRODUCTION

The association between ambient air pollution and excess morbidity and mortality has been well-established over several decades (Brunekreef and Holgate 2002; Dockery et al. 1993; Kampa and Castanas 2008; Pope III et al. 2002; Schwartz and Dockery 1992; Wilson and Spengler 1996). Traffic emissions is a significant source of urban air pollution and has been linked to both short-term and long-term adverse health effects (Kim et al. 2004; Künzli et al. 2000; Laumbach and Kipen 2012; Zmirou et al. 2004). Although many epidemiologic studies have found positive associations with traffic exposure, less is known about the specific components of traffic that impact health. Thus, improving exposure assessment to TRAP is particularly critical for developing more targeted regulation to better protect public health (Health Effects Institute 2010). Similar to other major air pollution sources, unbiased estimates of risk associated with traffic emissions is heavily dependent on accurately characterizing both exposure and health along a complete dose-to-response pathway. For primary traffic emission exposures, in particular, an added challenge lies in its chemical and physical heterogeneity, consisting of hundreds of different organic and inorganic components. While near-road monitoring offers opportunities for conducting direct measurements of freshly emitted traffic-related pollution, it is unclear how well these sites reflect near-road levels at varying proximities to the traffic source. Specifically, despite the recent progress in assessing the spatial representativeness of urban air quality monitoring stations (Santiago et al. 2013; Martín et al. 2015), questions remain regarding the comparability of spatiotemporal variability patterns of primary pollutants from traffic at near-road sites to those at varying distances from highways (Batterman et al. 2014b; Beckerman et al. 2008; Zhu et al. 2002), and whether these near-road measurements offer accurate means of assigning population exposures to traffic pollution. An additional concern relates to the use of outdoor monitors as surrogates of exposure for the general population that spends the majority (>85%) of their time indoors (Lim et al. 2012). Precise and accurate population exposure assignment is essential for quantifying and limiting measurement errors in epidemiologic studies, which stem both from the lack of spatial

representativeness in outdoor monitors as well as indoor-outdoor exposure discrepancies (Dionisio et al. 2014; Zeger et al. 2000).

Beyond the challenges involving external characterization of traffic pollution mixtures, measuring internal, biologically-relevant exposures and corresponding responses also remains difficult, due to the lack of sensitive biomarkers, individual susceptibility, impact of the pre-existing condition, and complexity of numerous endogenous pathways that may mediate the responses. Given their ability to conduct accurate assessment on both external exposure and internal responses, panel-based exposure studies have proved to be an effective platform to investigate the health effects of traffic pollution in humans using realistic exposures mixtures (Delfino et al. 2006; Delfino et al. 2008; McCreanor et al. 2007; Sarnat et al. 2012). Nevertheless, results from these previous panel-based studies have been inconsistent, with plausible findings on responses associated with inflammation and oxidative stress in some studies (Riediker et al. 2004; Zuurbier et al. 2010) and null responses in others (Chiu et al. 2016; Wu et al. 2014), mainly due to the lack of robust and specific biomarkers that accurately reflect TRAP exposure or the corresponding effects (Rylance et al. 2013).

Environmental metabolomics, involving the identification and quantitation of thousands of metabolites associated with endogenous and exogenous processes, holds promise as a powerful tool to improve internal exposure estimation to complex environmental mixtures (Bundy et al. 2009; Lankadurai et al. 2013; Miller and Jones 2014; Simpson and McKelvie 2009; Viant 2008). Analytical and scientific uncertainties in its application (Hines et al. 2007; Morrison et al. 2007), however, have limited its use for measuring individual sources, such as primary traffic pollution. Moreover, considerable questions remain concerning specific metabolites and pathways most predictive of TRAP exposure and the adverse responses, as well as the potential effect modification of pre-existing condition on modifying the responses to TRAP exposure.

To address these knowledge gaps associated with measuring exposure and response to primary traffic pollution, two large prospective panel-studies were conducted. The first study, the Dorm Room Inhalation to Vehicle Emissions (DRIVE) study, focused on examining the spatiotemporal variability trends of

traditional single TRAP indicators and assessed the potential for bias and errors when using a roadside monitor as a primary traffic pollution exposure surrogate, in lieu of more spatially refined, proximal exposure indicators (**Aim1**). In addition, high-resolution environmental metabolomics was conducted to identify traffic pollution-related pathways and metabolites in the DRIVE study (**Aim 2**). The second study, the Atlanta Commuters Exposure (ACE-2) study, applied high-resolution environmental metabolomics to examine and develop metabolic signals that are most predictive of TRAP exposure or the corresponding effects, and to investigate the potential effect modification of asthma on modifying the metabolic responses to TRAP exposures (**Aim 3**).

DISSERTATION AIMS

Overarching Aim: To improve understanding of TRAP exposures and health effects using high-dimensional external and internal data on TRAP mixtures and metabolomics.

Aim 1 examines the spatiotemporal variability trends of traditional single TRAP indicators and assesses the potential for bias and errors when using a roadside monitor as a primary traffic pollution exposure surrogate, in lieu of more spatially refined, proximal exposure indicators.

Aim 2 examines whether differences in exposures to primary traffic pollution are associated with corresponding metabolomics changes in a panel of human participants living at different proximity to congested highway.

Aim 3 examines and develops metabolic signals that are most predictive of TRAP exposure or the corresponding effects, and investigates the potential modification of metabolic responses to TRAP exposures by asthma status.

Collectively, the aims and analyses for this dissertation center on a highly chemically-speciated set of external and internal measurements of traffic pollution, in a range of near road microenvironments. The overarching goal will be to empirically validate the use of differing approaches for estimating primary traffic emission exposures. These analyses serve to clarify emission-to-exposure pathway dynamics, characterize the spatiotemporal variability of traditional single TRAP indicators in a changing environment, and examine the suitability of using near road indicators as primary traffic exposure surrogates in panel-based and small cohort epidemiological studies. In addition, in examining the link between these metrics and corresponding internal metabolic profiles, I anticipate highly novel results that may lead to the development of new biologically based primary traffic indicators. Ultimately, the results from this dissertation may inform more targeted regulation of traffic related pollution with the ultimate goal of reducing the public health burden attributable to air pollution.

REFERENCES

1. Brunekreef B, Holgate ST. 2002. Air pollution and health. The Lancet 360:1233-1242.
2. Bundy JG, Davey MP, Viant MR. 2009. Environmental metabolomics: A critical review and future perspectives. Metabolomics 5:3-21.
3. Chiu Y-HM, Garshick E, Hart JE, Spiegelman D, Dockery DW, Smith TJ, et al. 2016. Occupational vehicle-related particulate exposure and inflammatory markers in trucking industry workers. Environmental research 148:310-317.
4. Delfino RJ, Staimer N, Gillen D, Tjoa T, Sioutas C, Fung K, et al. 2006. Personal and ambient air pollution is associated with increased exhaled nitric oxide in children with asthma. Environ Health Perspect 114:1736-1743.
5. Delfino RJ, Staimer N, Tjoa T, Gillen D, Kleinman MT, Sioutas C, et al. 2008. Personal and ambient air pollution exposures and lung function decrements in children with asthma. Environ Health Perspect 116:550-558.
6. Dockery DW, Pope CA, Xu X, Spengler JD, Ware JH, Fay ME, et al. 1993. An association between air pollution and mortality in six us cities. New England journal of medicine 329:1753-1759.
7. Health Effects Institute PotHEoT-RAP. 2010. Traffic-related air pollution: A critical review of the literature on emissions, exposure, and health effects:Health Effects Institute.
8. Hines A, Oladiran GS, Bignell JP, Stentiford GD, Viant MR. 2007. Direct sampling of organisms from the field and knowledge of their phenotype: Key recommendations for environmental metabolomics. Environmental Science & Technology 41:3375-3381.
9. Kampa M, Castanas E. 2008. Human health effects of air pollution. Environmental pollution 151:362-367.
10. Kim JJ, Smorodinsky S, Lipsett M, Singer BC, Hodgson AT, Ostro B. 2004. Traffic-related air pollution near busy roads: The east bay children's respiratory health study. American journal of respiratory and critical care medicine 170:520-526.

11. Künzli N, Kaiser R, Medina S, Studnicka M, Chanel O, Filliger P, et al. 2000. Public-health impact of outdoor and traffic-related air pollution: A european assessment. The Lancet 356:795-801.
12. Lankadurai BP, Nagato EG, Simpson MJ. 2013. Environmental metabolomics: An emerging approach to study organism responses to environmental stressors. Environmental Reviews 21:180-205.
13. Laumbach RJ, Kipen HM. 2012. Respiratory health effects of air pollution: Update on biomass smoke and traffic pollution. Journal of allergy and clinical immunology 129:3-11.
14. McCreanor J, Cullinan P, Nieuwenhuijsen MJ, Stewart-Evans J, Malliarou E, Jarup L, et al. 2007. Respiratory effects of exposure to diesel traffic in persons with asthma. New England Journal of Medicine 357:2348-2358.
15. Miller GW, Jones DP. 2014. The nature of nurture: Refining the definition of the exposome. toxicological sciences 137:1-2.
16. Morrison N, Bearden D, Bundy JG, Collette T, Currie F, Davey MP, et al. 2007. Standard reporting requirements for biological samples in metabolomics experiments: Environmental context. Metabolomics 3:203-210.
17. Pope III CA, Burnett RT, Thun MJ, Calle EE, Krewski D, Ito K, et al. 2002. Lung cancer, cardiopulmonary mortality, and long-term exposure to fine particulate air pollution. Jama 287:1132-1141.
18. Riediker M, Cascio WE, Griggs TR, Herbst MC, Bromberg PA, Neas L, et al. 2004. Particulate matter exposure in cars is associated with cardiovascular effects in healthy young men. American journal of respiratory and critical care medicine 169:934-940.
19. Rylance J, Gordon SB, Naeher LP, Patel A, Balmes JR, Adetona O, et al. 2013. Household air pollution: A call for studies into biomarkers of exposure and predictors of respiratory disease. American Journal of Physiology-Lung Cellular and Molecular Physiology 304:L571-L578.
20. Sarnat SE, Raysoni AU, Li WW, Holguin F, Johnson BA, Luevano SF, et al. 2012. Air pollution and acute respiratory response in a panel of asthmatic children along the u.S.-mexico border. Environmental Health Perspectives 120:437-444.
21. Schwartz J, Dockery DW. 1992. Increased mortality in philadelphia associated with daily air pollution concentrations. American review of respiratory disease 145:600-604.
22. Simpson MJ, McKelvie JR. 2009. Environmental metabolomics: New insights into earthworm ecotoxicity and contaminant bioavailability in soil. Analytical and bioanalytical chemistry 394:137-149.
23. Viant MR. 2008. Recent developments in environmental metabolomics. Mol BioSyst 4:980-986.
24. Wilson R, Spengler JD. 1996. Particles in our air: Concentrations and health effects:Harvard School of Public Health Cambridge, MA.
25. Wu W, Muller R, Berhane K, Fruin S, Liu F, Jaspers I, et al. 2014. Inflammatory response of monocytes to ambient particles varies by highway proximity. American journal of respiratory cell and molecular biology 51:802-809.
26. Zmirou D, Gauvin S, Pin I, Momas I, Sahraoui F, Just J, et al. 2004. Traffic related air pollution and incidence of childhood asthma: Results of the vesta case-control study. Journal of Epidemiology and Community Health 58:18-23.
27. Zuurbier M, Hoek G, Oldenwening M, Lenters V, Meliefste K, van den Hazel P, et al. 2010. Commuters' exposure to particulate matter air pollution is affected by mode of transport, fuel type, and route. Environmental health perspectives 118:783.

CHAPTER 1

Errors associated with the use of roadside monitoring in the estimation of acute traffic pollutant-related health effects

Donghai Liang, Rachel Golan, Jennifer L Moutinho, Howard H Chang, Roby Greenwald, Stefanie E Sarnat, Armistead Russell, Jeremy A Sarnat

Liang D, Golan R, Moutinho JL, Chang HH, Greenwald R, Sarnat SE, Russell AG, Sarnat JA. 2018. Errors associated with the use of roadside monitoring in the estimation of acute traffic pollutant-related health effects. *Environmental Research*. 2018 Aug 31;165:210-9.

ABSTRACT

Near-road monitoring creates opportunities to provide direct measurement on traffic-related air pollutants and to better understand the changing near-road environment. However, how such observations represent traffic-related air pollution exposures for estimating adverse health effect in epidemiologic studies remains unknown. A better understanding of potential exposure measurement error when utilizing near-road measurement is needed for the design and interpretation of the many observational studies linking traffic pollution and adverse health.

The Dorm Room Inhalation to Vehicle Emission (DRIVE) study conducted near-road measurements of several single traffic indicators at six indoor and outdoor sites ranging from 0.01 to 2.3 km away from a heavily-trafficked (average annual daily traffic over 350,000) highway artery between September 2014 to January 2015. We examined spatiotemporal variability trends and assessed the potential for bias and errors when using a roadside monitor as a primary traffic pollution exposure surrogate, in lieu of more spatially-refined, proximal exposure indicators.

Pollutant levels measured during DRIVE showed a low impact of this highway hotspot source. Primary pollutant species, including NO, CO, and BC declined to near background levels by 20 to 30 m from the highway source. Patterns of correlation among the sites also varied by pollutant and time of day. NO_2, specifically, exhibited spatial trends that differed from other single-pollutant primary traffic indicators. This finding provides some indication of limitations in the use of NO_2 as a primary traffic exposure indicator in panel-based health effect studies. Interestingly, roadside monitoring of NO, CO, and BC tended to be more strongly correlated with sites, both near and far from the road, during morning rush hour periods, and more weakly correlated during other periods of the day. We found pronounced attenuation of observed changes in health effects when using measured pollutant from the near-road monitor as a surrogate for true exposure, and the magnitude varied substantially over the course of the day. Caution should be taken when using near-road monitoring network observations, alone, to investigate health effects of traffic pollutants.

KEYWORDS

Measurement Error; Traffic-related Air Pollution; Air Pollution Epidemiology; Pollutant Spatial Gradients; Acute Health Effects

INTRODUCTION

Epidemiologic evidence exists linking traffic-related air pollution (TRAP) with a range of acute and chronic health effects, with particular concern for those living in close proximity to heavily-trafficked roadways (Health Effects Institute 2010; Künzli et al. 2000). The recent establishment of an EPA-supported near-road monitoring network, was aimed to improve assessment of exposure to primary traffic emissions for urban populations, especially for individuals living near highways (Batterman 2013). The 75 near-road monitoring sites are mostly located within 30 meters of highly-trafficked highways.

While near-road monitoring offers opportunities for conducting direct measurements of freshly-emitted traffic-related pollution, it is unclear how well these sites reflect near-road levels at varying proximities to the traffic source. Specifically, despite the recent progress in assessing the spatial representativeness of urban air quality monitoring stations (Santiago et al. 2013; Martín et al. 2015), questions remain regarding the comparability of spatiotemporal variability patterns of primary pollutants from traffic at near-road sites to those at varying distances from highways (Batterman et al. 2014b; Beckerman et al. 2008; Zhu et al. 2002), and whether these near-road measurements offer accurate means of assigning exposures to traffic pollution. An additional concern relates to the use of outdoor monitors as surrogates of exposure for population that spend the majority (>85%) of their time indoors (Lim et al. 2012). Precise and accurate exposure assignment is essential for quantifying and reducing measurement errors, which stem both from the lack of spatial representativeness in outdoor monitors as well as indoor-outdoor exposure discrepancies (Dionisio et al. 2014; Zeger et al. 2000).

Epidemiologic studies utilizing panel-based and small cohort study designs have been particularly useful for examining short-term health effects of air pollution exposures within near-road settings, given their ability to measure a range of exposure and health endpoints on an individual-level (Delfino et al. 2006; Delfino et al. 2008; McCreanor et al. 2007; Sarnat et al. 2012). For these study designs, in particular, inter-individual variability in mobility and activity patterns can result in varying times spent near traffic pollution sources. The ability to monitor study participants at closer proximities may, consequently, be especially

important for accurately modeling differing levels of exposure to TRAPs and reducing exposure misclassification. Adding to this challenge is the growing evidence that the near-road environment is changing rapidly (Blanchard et al. 2013a, b; Henneman et al. 2015; Vijayaraghavan et al. 2014), due mainly to general reductions in primary automotive emissions. Today, primary traffic source contributions, fate and transport dynamics, and exposure factors for primary traffic pollutants likely differ from those reported historically. Zhai et al. (2017), for example, estimated that mobile source PM impacts decreased by about 30% between 2002 and 2013 in Georgia (Zhai et al. 2017), while national reductions in on road emissions decreased 49% (U.S. EPA). NO_x emissions decreased 51% in Georgia and 45% nationally during the same period. Substantial gaps exist in our understanding of how TRAPs vary in space and time in this changed near-road environment and whether near-road measurements can represent exposure to primary traffic emissions for broader population.

To address these research gaps and more closely examine emerging trends related to characterizing traffic pollution exposures, we conducted the Dorm Room Inhalation to Vehicle Emissions (DRIVE) study, an extensive near-road field-monitoring campaign. The focus of DRIVE centered around a prominent near-road environment in Atlanta, GA, with the goal of understanding the impact of a highway on its adjacent environment, and the potential implications for conducting and interpreting traffic pollution epidemiology for individuals living within this setting. The current analysis, specifically, assesses relationships between outdoor and indoor primary traffic exposure indicators within an approximate 5 km^2 spatial domain. To address the above research gaps, we report spatiotemporal variability patterns at sites within this domain and present findings from a simulated panel-based epidemiologic study of individuals living in close proximities to these sources.

METHODS

The DRIVE study was conducted on and around the Georgia Institute of Technology (GIT) campus in Atlanta, GA, at outdoor and indoor monitoring sites adjacent to one of the most heavily trafficked highway arteries in the US (a section of highway, where Interstates 75 and 85 merge in a 16-lane corridor with

average annual daily traffic over 350,000 vehicles). Intensive field sampling was conducted from September 2014 to January 2015. This location was, in many ways, ideal for an examination of traffic emission impacts within an urban near-road domain, given our ability to conduct simultaneous measurements at multiple monitors at varying linear distances from this major traffic source.

Sampling was conducted at six dedicated monitoring sites (four outdoor and two indoor) ranging from less than 0.01 to 2.3 km away from the highway (Figure 1.1). The main near-road sampling site ('Roadside' or RDS) consisted of a highly instrumented trailer with an inlet at a distance of 10 m from the closest highway center lane. Urban background outdoor pollutant concentrations away from the road were collected at the Southeastern Aerosol Research and Characterization (SEARCH) network at the Jefferson Street center monitoring site (CMS) located 2.3 km west of the highway (Hansen et al. 2006). Measurements from the Jefferson Street CMS have been used previously to generate population exposure estimates in analyses examining short-term associations between air pollution and daily morbidity (Darrow et al. 2008; Darrow et al. 2011; Metzger et al. 2003a; Metzger et al. 2003b; S Sarnat et al. 2008; SE Sarnat et al. 2008; Sarnat et al. 2010; Strickland et al. 2010; Tolbert et al. 2000) and is generally considered to be representative of Atlanta urban background pollutant concentrations and composition (Edgerton et al. 2005; Liu et al. 2005; Solomon et al. 2003). Two additional outdoor sites, along with two indoor sites, were located at the two student dormitories on the GIT campus: the 'Near Dorm', approximately 20 m west of the highway, and the 'Far Dorm', approximately 1.4 km west of the highway.

Primary instrumentation

We measured pollutants to provide information related to the particulate and gaseous composition of primary traffic emissions and characterize the regional pollution. The pollutants we measured included traditional single-species traffic-related indicators: black carbon (BC), carbon monoxide (CO), nitric oxide (NO), nitrogen dioxide (NO_2), nitrogen oxides (NO_x), and fine particulate matter or particles with diameters less than 2.5 micrometers ($PM_{2.5}$) (See Appendix, Table S1.1 and S2 for a complete list of measured pollutants). BC, CO, NO, NO_2 and NO_x were measured continuously or semi-continuously at each sampling

location. In addition to these measurements, we conducted quartz and Teflon filter-based measurements for particle mass integrated over 48h durations. A total of 55 instruments were deployed, providing air pollutant concentration data at time scales from minutes to weekly means (Appendix Table S1.1). The RDS, which served as the roadside reference monitor, was instrumented with the widest range of samplers as well as a meteorological station. The sampling height for the RDS monitoring station was 3 m off the ground, and 4 m for the meteorological station. At the Near Dorm site, instrumentation was placed in a dorm room, which was used as an administrative office, situated adjacent to occupied student rooms. At the Far Dorm site, sampling was conducted in an unoccupied bedroom of a two-bedroom suite. Sampling equipment located inside each dorm were identical (Appendix Table S1.1) and a three-way valve was used to alternate sampling between indoor and outdoor air. The outdoor sampling inlet tube was located approximately 0.5 m off the ground for the Near Dorm and 1.5 m off the ground for the Far Dorm. The indoor sampling inlet tube was raised approximately 0.25 m off the flooring for both of the dormitories.

All field instrumentation used to measure continuous pollutant concentrations were evaluated, refurbished if needed, and calibrated prior to field sampling. In order to compare concurrent pollutant measurements across the multiple sampling sites and ensure accurate concentrations during the sampling period, instruments measuring the same pollutant parameters were also co-located both before and after the sampling period and consistently calibrated throughout the 13-week field sampling period. Final concentration data reported were adjusted based on the time-weighted average of the calibration curves and the collocated measurements.

Data analysis

We compared the traditional single-pollutant TRAP indicators, BC, CO, NO, NO_2, and $PM_{2.5}$, across the six monitoring sites: the RDS site, near dorm residence outdoor site (NRO), near dorm residence indoor site (NRI), far dorm residence outdoor site (FRO), far dorm residence indoor site (FRI), and the urban background Jefferson Street center monitoring site (CMS). We computed descriptive statistics for each of the traffic indicators over these six monitoring sites, on both hourly and daily temporal averaging scales.

We conducted additional inter-site correlation analyses examining the Spearman's correlation between pollutant concentrations (24h and 1h means) measured at RDS and each of the other non-RDS sites, given the non-normality of the pollutant distributions.

Assessment of TRAP spatiotemporal variability

We considered the following regression model for examining spatiotemporal variability in pollutant levels among the outdoor monitoring sites:

$$\text{Log}\,(\text{Ratio}_{st}) = \beta_1 \text{Distance}_{st} + \beta_2 Z_{st} + \beta_3 \text{Distance}_{st} * Z_{st} + \theta_t + \varepsilon_{st} \qquad \text{(Eq. 1.1)}$$

where Ratio_{st} denotes the log ratio of the pollutant concentration measured at site $'s'$ during hour $'t'$ to the pollutant concentration at the RDS site during hour $'t'$. Here $'s'$ indexed the three additional outdoor monitoring locations: NRO, FRO, and CMS. $'\beta_1'$ is the coefficient for the proximity from the monitoring site s to the RDS site (distance). $'\beta_2'$ is the coefficient for factor Z_{st} including time period of the day (categorical), temperature, wind speed, relative humidity, wind direction (categorical), day of the week (categorical) and traffic counts. These factors were included in separate models predicting the ratios for each pollutant. Interactions between distance from the monitoring site to the RDS site (i.e. the spatial gradient) and each factor, represented by $'\beta_3'$, was also examined to quantify the effect modification by each factor on the distance-driven gradient on TRAPs and we scaled it into percentage decrease in outdoor pollutant concentration for greater physical interpretability (per 200 meters). Finally, $'\theta_t'$ is the time-specific random intercepts used to capture potential variations in each sampling dates not explained by $'Z_{st}'$; and ε_{st} represents residual normally-distributed random error.

Panel study measurement error simulation

For the purpose of the current analysis aims, impact of measurement error was calculated for each TRAP when using the level at RDS as an error-prone surrogate of the pollutant level at other non-RDS sites. For each TRAP, we considered measurements at each of the non-RDS location (i.e., NRI, NRO, FRI, FRO, and CMS) as true exposures (measured without error), while measurements at RDS site served as the

exposure surrogate assigned to a hypothetical participant in an epidemiologic survey. Measurement error, thus, may be introduced due to the presence of pollutant spatial gradients or additional microenvironmental contributions not reflected within the surrogate metric. We quantified measurement error, **δ**, as the absolute difference between the RDS measurements and each of the other five non-RDS sites measurements, and generated the following measurement error terms: $\delta_{CMS,}$ δ_{NRO}, $\delta_{NRI,}$ δ_{FRO} and δ_{FRI}. For example, measurement error due to the spatial difference between central monitoring site (which represents urban background), and near-road site (which represents traffic emission) was represented as $\delta_{CMS} = CMS - RDS$. Mean and variance were also calculated for these five types of measurement errors for all five TRAPs: BC, CO, NO, NO_2, and $PM_{2.5}$.

To examine the impact of measurement error when using near-road measurements on estimating the health responses associated with traffic emissions within a small panel study, we used empirical health response estimates of a widely used biomarker, forced expiratory volume in 1 second (FEV_1), which was associated with pre-post exposure to traffic emission in a highly cited small panel study in London (McCreanor et al. 2007). We averaged the percent change (health responses estimates from McCreanor et al. 2007) of FEV_1 after exposure to TRAPs and used β = -0.41 for percent change in FEV_1 per interquartile range (IQR) increase in each of the TRAPs for the simulation. Linear regression models were used to simulate FEV_1:

$$E(Y_t) = \propto + \beta_1 pollution_{i,t} + \varepsilon_t \qquad \text{(Eq. 1.2)}$$

where Y_t is the percent change in FEV_1 on day t. For each pollutant i, daily averages (24-hr average) of same-day concentrations were used. Percent changes in health outcomes were drawn from Gaussian distributions and fitted using the simulated true exposures (each of the non-RDS measurements) or the error-prone exposures (RDS measurements) with two linear models: one using the simulated true exposure, and another using the error-prone exposure. Simulations were run 1,000 times in each scenarios and impact of measurement error were calculated (Appendix A). We should emphasize that for each of these simulated models, we view the TRAP pollutant metric as merely serving as an indicator of some component of

primary traffic pollution observed to be causally associated with respiratory response. For example, models including CO as the TRAP indicator, should not necessarily be interpreted as reflecting a true causal association between CO and FEV_1. Rather, for this model, CO is serving as a general indicator of exposure to this multipollutant source.

Since numerous panel-based epidemiologic designs measure pollutant levels over short periods of time (e.g., 1h means) to assess associations involving hyper-acute biological responses (Golan et al. 2017; McCreanor et al. 2007; Shields et al. 2013), it is possible that exposure measurements may also be prone to errors over this temporal scale. Thus, we also simulated and characterized hourly-resolved impact of measurement error for each of the five TRAPs (Appendix A). All statistical analyses were completed in R, version 3.3.1 (R Foundation for Statistical Computing; http://www.r-project.org/).

RESULTS

Analytic time series, where valid measurements were available across the six monitoring sites, varied by pollutant, and ranged between 48 and 121 sampling-days (Appendix Table S1.2). Mean pollutant concentrations measured at the RDS site were typically elevated above the urban background level; however, concentrations were not as high as those reported in previous near-road field studies (Beckerman et al. 2008; Kozawa et al. 2009; MacNaughton et al. 2014). The key pollutant species measured at the near-road site were NO, NO_2, CO, BC, and $PM_{2.5}$, with mean concentrations (standard deviation) over the entire study period of 20.9 (15.6) ppb, 30.3 (10.9) ppb, 0.43 (0.14) ppm, 1.9 (1.0) $\mu g/m^3$, and 7.9 (2.7) $\mu g/m^3$, respectively (Appendix Table S1.3).

Spatial gradient analysis.

With the exception of NO_2 and $PM_{2.5}$, all of the measured pollutants exhibited pronounced gradients of decreasing concentration with distance from the highway, with steepest gradients shown within the first 20 meters (Figure 1.2, Appendix Table S1.3). We observed a mean difference of 200 ppb for CO, 0.8 $\mu g/m^3$ for BC, and 17 ppb for NOx, between the RDS and FRO sites. Conversely, NO_2 spatial gradients were not

apparent within the 1.3 km DRIVE sampling domain, with mean NO_2 levels approximately 30.3 ppb at the RDS site and 21.6 ppb at the FRO site. There was some indication of lower mean NO_2 levels at the urban background site (CMS), located 2.3 km from the highway, with levels averaging 14.5 ppb during DRIVE sampling.

We examined diurnal concentration profiles for each pollutant at the varying sampling locations (Figure 1.3). We observed RDS peak CO concentrations at 7 am, followed by peaks occurring slightly later in the morning, between 8 and 9 am, at sampling locations further away from the highway, highlighting dispersion and transport processes near the highway. Similar to CO, morning peak concentrations at the RDS site for ambient NO occurred mainly around 7 am and reached a daily maximum of about 35 ppb. Steep gradients were observed within 30 m of the highway in the BC concentrations at the RDS site, with 0.5 $\mu g/m^3$ greater than all the other sites. For BC, while no spatial gradient was observed between the NRO and FRO sites, all sites exhibited similar diurnal profiles with a pronounced concentration peak between 7 am and 10 am, and another less pronounced peak during the evening.

Inter-site Spearman's correlations (r_S) were used to examine how well temporal variability at the RDS site reflected corresponding variability of the pollutants at varying distances from the highway (Table 1.1). When assessing 24h-integrated pollutant concentrations, correlations varied considerably by distance to the highway and pollutant. Generally, NO_2 concentrations measured at the RDS were more strongly correlated across the sampling domain than BC, CO, and NO, with observed Spearman's correlations greater than 0.7 between the RDS site and the other ambient sites for NO_2. For BC, CO, and NO, we observed stronger correlations with the RDS site for sites closer to the RDS than for those further away (correlation of 0.6-0.8 between RDS and NRO, and 0.3-0.5 between RDS and FRO, respectively). Hourly-resolved correlation analysis showed that the strengths of linear association varied markedly throughout the day (Figure 1.4). This was most apparent for the primary traffic pollutant NO, where correlations between RDS and all other sites were strong through the sampling domain during rush hour periods (6 – 10 am), but declining in strength (r_S: 0.0 – 0.3) between 12 pm and 8 pm between RDS and FRO.

Spatiotemporal regression model analysis

To further quantify the degree of pollutant spatial heterogeneity, including factors contributing to variations in the gradients, we conducted regression analyses modeling the log ratio of the pollutant concentration measured at all other sites to that measured at the RDS site as a function of distance to the RDS site (Table 1.2 and Appendix Table S1.5). We specifically examined temporal, meteorological, and traffic count as potential modifiers of an observed distance-driven concentration gradient. As expected, results show that 'distance' from the highway served as a robust independent predictor of the pollutant spatial gradient, with negative associations observed for all pollutants; here, larger estimates for percentage decrease indicate a more pronounced spatial gradient (or decay) in pollutant concentrations with increasing distance from the highway.

Most factors we examined also served to modify pollutant spatial gradients. For example, we found significant modification by time of day, with the most pronounced gradients (i.e., with largest percentage decrease estimates) occurring during mid-day hours (10 am- 3 pm) across pollutants. Additionally, for all pollutants, 'midnight' and 'early morning' periods (12 am -5 am) exhibited the most gradual pollutant decay (i.e., with smallest percentage decrease coefficients).

Hourly-resolved spatial gradients were further modified by wind speed and traffic count at the highway (Table 1.2). Interaction terms for wind speed were consistently larger than 1% for decrease in concentrations for all pollutants, indicating that hours with higher wind speed exhibited a stronger spatial decay gradient. Interaction terms between 'distance' and traffic count were also significant for CO spatial gradient (0.23% decrease in concentrations per 200 meters), showing that spatial gradients were more pronounced during hours with higher traffic counts (10 am- 3pm). Across pollutants, the impact of 'distance' was generally strongest for NO compared to other pollutants, suggesting that NO concentrations exhibited stronger spatial gradients compared to the other pollutants, a finding which is consistent with the rapid oxidation of NO to other NO_x species (e.g., NO_2).

Measurement error simulation analysis

We then used the empirical findings from the spatial- and temporal variability analyses to model potential bias that may occur when using the pollutant concentration from the RDS monitor as an exposure surrogate for a small panel study setting, compared to more spatially-refined, proximal exposure measures. Generally, we observed magnitudes of error increasing with increasing distance from the highway (Appendix Table S1.4), resulting in greater relative attenuation in the estimation of pre-post changes in FEV_1 (Table 1.3). With CO as an example, we estimated that using CO at RDS as an exposure surrogate, in place of the assuming true NRO CO concentrations, located 20m from the highway, introduced 18.1% attenuation in the model effect estimates, and 49.2% attenuation in effect estimates when using RDS in lieu of FRO CO levels. Assuming a true effect estimate to be a -0.41% decrease in FEV_1 per IQR increase in pollutant concentration (McCreanor et al. 2007), our observed attenuation levels when using RDS measurements translate to reduced FEV_1 underestimated to -0.34%, -0.21%, and -0.26% for NRO, FRO, and CMS, respectively. This trend was consistent across all pollutant species. Further, greater attenuation generally existed when we assumed the indoor measurements to be the true exposures. For the models that account for indoor-outdoor differences due to pollutant infiltration, the magnitude of observed attenuation in the simulated epidemiologic models also varied by pollutant species, with less attenuation for CO and NO_2 (34% and 49% at FRO respectively) compared to BC (68% at FRO).

We also examined the presence and effect of hourly-resolved measurement error on observed pollution-FEV_1 associations. Results from these models have implications for panel-based epidemiologic studies which assess both pollutant levels and acute responses over short durations (i.e., hourly), and may be more susceptible to rapidly-changing errors resulting from diurnal pollutant spatiotemporal variability patterns. Four ambient sites were selected for this analysis, including RDS (as the reference site), NRO, FRO, and CMS. As shown in Figure 1.5, for these models, percent attenuation due to measurement error estimates were lowest during morning rush hour (8 am) at all of the sites (e.g., percent attenuation for models including CO was 9.2%, 18.2% and 27.1% for NRO, FRO, and CMS respectively). During other hours, in contrast, moderate to high attenuation was observed in the βs (β_1 in Eq. 1.2), especially during the

afternoon hours (i.e. percentage attenuation = 43.8%, 77.1% and 65.6% at 4 pm for NRO, FRO, and CMS respectively).

DISCUSSION

We conducted the Atlanta DRIVE study, in part, to comprehensively characterize a traffic pollution hotspot adjacent to a residential area and assess how patterns of TRAP spatiotemporal variability may affect exposure assignment and health risk estimation within epidemiological study designs examining short-term exposure and acute response. The current analysis is particularly pertinent given the fact that in the US alone, more than 45 million people live, work, or attend school within 100 meters of a major road (US EPA), along with the recent establishment of a comprehensive US network of near-road monitors to better characterize this microenvironment (Batterman 2013).

Broadly, the results from the over 2,800 hours of measurements collected during DRIVE study period point to complex and highly dynamic conditions within and adjacent to this near-road microenvironment, intersected by one of the largest and most trafficked highways in the US (Darnell 2017; Ultee 2016). Based on these measurements, we offer several key findings with implications for both assigning exposure and estimating health response associated with TRAP.

Firstly, the measured concentrations of traditional primary traffic indicators, BC, CO, and NO, were low relative to historic levels. While still elevated above background levels, the impact of the highway on the adjacent sampling domain was less pronounced than reported in numerous prior investigations at or near this site (Baldasano et al. 2003; Cohan et al. 2007; Hu et al. 2010; S Sarnat et al. 2008). Moreover, during four months of continuous sampling, we measured pollutant concentrations decreasing rapidly with increasing distance from the highway. BC, CO, and NO levels all declined to near background levels within 20 to 50 m from the highway. Spatial gradients varied substantially during the course of a day, with greater primary impacts from the highway occurring during morning rush hour periods. Notably, the heterogeneous spatial variability patterns were also reflected in varying strength of temporal correlation throughout the

day. Daily correlations were largely driven by morning rush hour (7 – 9 am) values, with substantially weaker roadside to near-road correlations occurring during other hours of the day. For NO, in particular, roadside concentrations were virtually uncorrelated with corresponding NO levels at many of the other sites between 3 and 8 pm. These are periods of higher thermally-driven turbulence and dispersion. Further, regression analysis found that distance from highway was a dominant explanatory variable. While neither of these findings is wholly unexpected, the degree of reduced correlation during the afternoon is important in terms of interpreting how well near-road observations reflect temporal variability patterns in other locations.

The DRIVE results suggest that the spatial environment over which a near-road monitor can be used to assess temporal variability patterns in TRAP concentrations is limited. Thus, for epidemiological studies that specifically model highly resolved exposure and response, it may not be sufficient to rely on near-road monitoring as an exposure surrogate. Reduced correlation may be due, in part, to site-specific instrument uncertainty or other unspecified pollutant contributions at a given site, but the trend to weaker linear associations during the afternoon for all the single-pollutant primary traffic indicators at the more distant monitors suggests that additional observations and/or modeling tools should be used to characterize pollutant dynamics over such scales if a study is relying on capturing the temporal exposure trends (Santiago et al. 2017; Sanchez et al. 2017). Collectively, the spatiotemporal analysis findings highlighted the changing impact of the highway source on the adjacent domain during the course of a day.

A final, somewhat unexpected, key finding related to differences in the spatiotemporal behavior of NO_2, as compared to that of other single-pollutant traffic indicators. During DRIVE sampling, NO_2 levels did not exhibit as strong a spatial gradient as for CO and BC. Absolute NO_2 concentrations were moderately homogeneous from the RDS site to the FRO site due, in part, to kinetic limitations in the photochemical reactions required to convert the NO-dominant primary NOx, emitted from automobiles, to NO_2. It is possible that some of the stoichiometric dynamics involved are related, more broadly, to the lower primary traffic emissions associated with a changing near-road environment. The NO_2 findings from the DRIVE study provide some indication that this historic traffic indicator may serve as a less useful surrogate of

traffic than the other primary single-pollutant indicators, NO, CO, or BC, given its divergent near-road spatiotemporal variability patterns. The decrease in primary NO_2 associated with tailpipe emissions likely contribute to its reduced utility as a source indicative tracer. A detailed analysis into the role and behavior of NO_2 within the DRIVE sampling is being conducted.

With these findings, it is, thus, reasonable to question how well roadside monitors reflect adjacent pollutant concentrations within a range of near-road proximities, as well as their utility as potential exposure surrogates within epidemiologic studies examining health effects near busy roads. Exposure surrogates that are not representative of population or individual exposures may result in exposure misclassification, leading to biased or uncertain estimates of risk (Batterman et al. 2014a; Kioumourtzoglou et al. 2014). To investigate this issue, we conducted a simulation examining short-term primary traffic pollution exposure (i.e., daily and hourly) and acute respiratory response (i.e., changes in FEV_1) modeled on the design used in the influential Oxford Road study (McCreanor et al. 2007). Specifically, we were interested in evaluating the potential impact of spatiotemporal variability in this setting and how those patterns propagate through a panel-based epidemiologic study.

Broadly, we observed substantial attenuation in the observed β estimates across simulated models with different primary TRAPs. Importantly, attenuation was substantial even for models that assumed true exposure to be the concentration measured at NRO site, located only 10m from the RDS site. In each of these cases, we should note that the attenuation in the β's can be interpreted as underestimated association of health response. For instance, a moderate attenuation in the β coefficients of 30%.means that IQR increases in TRAP are truly associated with a corresponding 0.29% decrement in FEV_1 as compared to the observed 0.41% decrement. Additionally, for CO, NO, and BC, we observed that indoor environments exhibited greater attenuation in β compared to the corresponding outdoor environments, due to the variability in the infiltration of ambient air pollutants into the indoor environment and the contribution of indoor pollution sources.

Our findings showing diurnal variations in roadside to near road pollutant correlations, suggest further that the suitability of a roadside monitor as an accurate exposure surrogate may also be contingent on the

timing of the measurement periods during the course of a day. Protocols that measure pollutants and health endpoints in varying exposure windows from day to day, may lead to the introduction of differing degrees of error. The trend of weaker linear associations during the afternoon for all the TRAPs at the more distant monitors with RDS measurements suggests that additional observations and/or modeling tools should be used to characterize pollutant dynamics over such scales if a study is relying on capturing the accurate temporal exposure trends.

It is important to emphasize that variations in diurnal correlation patterns, however, are not necessarily captured when using 24h-integrated exposure metrics. As a consequence, panel studies that rely on hourly and sub-daily exposure metrics (McCreanor et al. 2007; Sarnat et al. 2014; Zhang et al. 2009; Ladva et al. 2017), exhaled nitric oxide (McCreanor et al. 2007; Sarnat et al. 2014; Sarnat et al. 2012; Zhang et al. 2009), and heart-rate variability (de Paula Santos et al. 2005; Schwartz et al. 2005; Shields et al. 2013), may also be prone to measurement error due to the temporal variability of pollutant.

Results from the hourly-resolved simulations confirm that the impact of measurement error varies substantially by time of day. The modeled effect estimates reflect this spatiotemporal variation between the highway and the adjacent site, when errors are propagated through an epidemiologic model commonly used in panel-based designs. During morning rush hours, when the impact of traffic sources was most pronounced across a relatively large spatial domain (> 1000 m), near-road measurements were more appropriate for reflecting levels of primary traffic across near-road environments, with relatively low attenuated impact on our selected health endpoints. This was not the case, however, during other periods of the day, when locations far away from the traffic sources would exhibited moderate to high percent attenuation in simulated FEV_1. Thus, for panel or small cohort studies involving participants living near busy highways, similar to the DRIVE study participants, these findings suggest that decisions regarding temporal averaging time (e.g., 24h, 1h, or moving averages) may be critical for accurately modeling true health effect associations.

Several inherent limitations in this analysis warrant attention. First, as with any monitoring study conducted within a single geographic domain, it is difficult to generalize the current findings to other near-

road environments. Moreover, the DRIVE sampling domain is idiosyncratic in that the section of the I-75/I-85 highways that intersect the study location, includes a higher proportion of light duty gasoline vehicles compared to heavy duty diesel vehicles than many highways. Additionally, the DRIVE sampling was conducted during a 4-month period. Meteorological factors, which will affect photochemistry-driven pollutant formation and other transport processes, were, correspondingly, limited to conditions and seasonal patterns similar to those during DRIVE field sampling. It is worth noting, however, that the sampling start and end dates were intentionally designed to maximize variability in meteorological conditions, and sampling did occur in a wide range of temperature (-2 to 26 °C), relative humidity (32% to 99%), wind (0.21 to 2.55 m/s), and precipitation conditions (0 to 25.4 mm/hr). In addition, the pollutant levels we measured during this extensive monitoring period were consistent with measurements from the US EPA's near-road monitoring network pollutant trends analysis and emissions estimates (Blanchard et al. 2013a; EPA 2015).

Second, although our findings may be generally applicable to domains with predominantly traffic-related local sources, the impact of the traffic emissions was low, which is a key finding we attribute to a changing near-road environment. The extent of the attenuation between use of data from the near-road monitoring site compared to more proximal residential locations might, consequentially, vary substantially for regions with relatively higher traffic emissions (i.e. developing countries with rapidly growing vehicle fleets). In our analysis, we assumed the congested I-75/I-85 highway to be the predominant source of TRAP and calculated the distance from each residence site to the highway as the proximity between the exposure source and the contact. While contribution from local arterial sources may have masked the true gradients of TRAPs, the total traffic volumes at the local arterial roadways surrounding the far resident location were much less compared to the highway (annual average daily traffic of 6,990 and 353,700 respectively). Finally, for our simulated epidemiologic analyses, we only consider single pollutant as the predictor for the simplicity of interpretation, while inclusion of multiple pollutants, with correlated measurement error, in the models simultaneously might introduce additional insights (Dionisio 2016).

CONCLUSIONS

To our knowledge, this is among the first studies to quantify the effects of measurement error due to spatial and temporal variation of TRAPs and examine how well a near-road monitoring site can serve as a proxy to estimate traffic pollutant related health effects in epidemiology studies. Pollutant levels measured during DRIVE showed a relatively low impact of the 16-lane interstate highway compared to historic near-road field data. Spatial gradients of TRAPs varied substantially during the course of a day, with greater primary impacts from the highway occurring during morning rush hour periods. NO_2, specifically, exhibited spatial trends that differed from other single-pollutant primary traffic indicators. This finding provides some indication of limitations in the use of NO_2 as a primary traffic exposure indicator in panel-based health effect studies. We found pronounced attenuation of observed changes in health effects when using measured pollutant level from the near-road monitor as a surrogate for true exposure. Moreover, the extent of attenuation associated with increasing distance from the traffic hotspot varied across pollutant species and over the course of the day. Together, results from the DRIVE monitoring and simulated epidemiologic analyses indicate that for panel-based studies, the use of near-road measurements as surrogates of exposure to primary traffic pollution may result in substantial under-estimates of health response and potential risk. We observed this to be true for even sites located within 20 m of the highway sources and increasing with distance from the highway and within indoor environments. Collectively, these results provide indication that caution should be taken when using near-road monitoring network to investigate health effects of traffic pollutants in future studies.

ACKNOWLEDGEMENT

Support for this project were provided through a contract with the Health Effects Institute (RFA #4942-RFA13-1/14-3). The field study conducted as part of this study benefitted greatly from the assistance of many students, staff, and faculty at both Georgia Tech and Emory. Specific thanks go to C. Cornwell, K. Parada, S. Shim, K. Johnson and E. Yang for their tremendous help in conducting the field study. We want to thank Dr. R. Weber, Dr. V. Verma, and Ms. D. Gao for their measurements of oxidative potential of ambient fine particles via DTT assay. We are indebted to Dr. J. Schauer (U. Wisconsin) for loaning us several instruments to supplement our sampling network. We would also like to thank Dr. Seung-Hyun Cho from RTI, Inc. for her collaboration on this project. The Georgia EPD allowed us access to their roadside monitoring site and helped provide data from those monitors, and we particularly thank Ken Buckley for his assistance with this. The study used on the instrumentation assembled for field studies conducted as part of the Southeastern Center for Air Pollution and Epidemiology (SCAPE), which was funded by a US Environmental Protection Agency STAR grant R834799. The information in this document may not necessarily reflect the views of the Agency and no official endorsement should be inferred. R Golan gratefully acknowledges support by a post-doctoral fellowship from the Environment and Health Fund, Jerusalem, Israel. We acknowledge NSF for providing a fellowship to JM, and Prof. Russell made use of funds provided by a generous gift from Howard T. Tellepson. We owe a debt of gratitude to the numerous administrators at Georgia Tech for allowing us to conduct this study on campus and in their residence hall facilities.

REFERENCE

1. Baldasano J, Valera E, Jimenez P. 2003. Air quality data from large cities. Science of the Total Environment 307:141-165.
2. Batterman S. 2013. The near-road ambient monitoring network and exposure estimates for health studies. EM (Pittsburgh, Pa) 2013:24.
3. Batterman S, Burke J, Isakov V, Lewis T, Mukherjee B, Robins T. 2014a. A comparison of exposure metrics for traffic-related air pollutants: Application to epidemiology studies in detroit, michigan. International journal of environmental research and public health 11:9553-9577.
4. Batterman S, Chambliss S, Isakov V. 2014b. Spatial resolution requirements for traffic-related air pollutant exposure evaluations. Atmospheric Environment 94:518-528.
5. Beckerman B, Jerrett M, Brook JR, Verma DK, Arain MA, Finkelstein MM. 2008. Correlation of nitrogen dioxide with other traffic pollutants near a major expressway. Atmospheric Environment 42:275-290.
6. Blanchard CL, Hidy GM, Tanenbaum S, Edgerton ES, Hartsell BE. 2013a. The southeastern aerosol research and characterization (search) study: Temporal trends in gas and pm concentrations and composition, 1999-2010. Journal of the Air & Waste Management Association 63:247-259.
7. Blanchard CL, Hidy GM, Tanenbaum S, Edgerton ES, Hartsell BE. 2013b. The southeastern aerosol research and characterization (search) study: Spatial variations and chemical climatology, 1999-2010. Journal of the Air & Waste Management Association 63:260-275.
8. Cohan DS, Boylan JW, Marmur A, Khan MN. 2007. An integrated framework for multipollutant air quality management and its application in georgia. Environmental management 40:545-554.
9. Darnell C. 2017. Connector or disconnector: Analyzing impacts of the interstate 75/85 connector on historic neighborhoods in atlanta, georgia:Clemson University.
10. Darrow LA, Klein M, Correa A, Flanders WD, Waller L, Marcus M, et al. 2008. Ambient air pollution and preterm birth in atlanta, 1994-2004: A time-series analysis. Birth Defects Res A 82:367-367.
11. Darrow LA, Klein M, Strickland MJ, Mulholland JA, Tolbert PE. 2011. Ambient air pollution and birth weight in full-term infants in atlanta, 1994-2004. Environmental Health Perspectives 119:731-737.
12. de Paula Santos U, Braga ALF, Giorgi DMA, Pereira LAA, Grupi CJ, Lin CA, et al. 2005. Effects of air pollution on blood pressure and heart rate variability: A panel study of vehicular traffic controllers in the city of sao paulo, brazil. European heart journal 26:193-200.
13. Delfino RJ, Staimer N, Gillen D, Tjoa T, Sioutas C, Fung K, et al. 2006. Personal and ambient air pollution is associated with increased exhaled nitric oxide in children with asthma. Environ Health Perspect 114:1736-1743.
14. Delfino RJ, Staimer N, Tjoa T, Gillen D, Kleinman MT, Sioutas C, et al. 2008. Personal and ambient air pollution exposures and lung function decrements in children with asthma. Environ Health Perspect 116:550-558.
15. Dionisio KL, Baxter LK, Chang HH. 2014. An empirical assessment of exposure measurement error and effect attenuation in bipollutant epidemiologic models. Environmental health perspectives 122:1216.
16. Edgerton ES, Hartsell BE, Saylor RD, Jansen JJ, Hansen DA, Hidy GM. 2005. The southeastern aerosol research and characterization study: Part ii. Filter-based measurements of fine and coarse particulate matter mass and composition. Journal of the Air & Waste Management Association 55:1527-1542.
17. EPA U. 2015. Aerminute user's guide.

18. Golan R, Ladva C, Greenwald R, Krall JR, Raysoni AU, Kewada P, et al. 2017. Acute pulmonary and inflammatory response in young adults following a scripted car commute. Air Quality, Atmosphere & Health:1-14.
19. Hansen DA, Edgerton E, Hartsell B, Jansen J, Burge H, Koutrakis P, et al. 2006. Air quality measurements for the aerosol research and inhalation epidemiology study. Journal of the Air & Waste Management Association 56:1445-1458.
20. Health Effects Institute PotHEoT-RAP. 2010. Traffic-related air pollution: A critical review of the literature on emissions, exposure, and health effects:Health Effects Institute.
21. Henneman LRF, Holmes HA, Mulholland JA, Russell AG. 2015. Meteorological detrending of primary and secondary pollutant concentrations: Method application and evaluation using long-term (2000-2012) data in atlanta. Atmospheric Environment 119:201-210.
22. Hu Y, Chang ME, Russell AG, Odman MT. 2010. Using synoptic classification to evaluate an operational air quality forecasting system in atlanta. Atmospheric Pollution Research 1:280-287.
23. Kioumourtzoglou M-A, Spiegelman D, Szpiro AA, Sheppard L, Kaufman JD, Yanosky JD, et al. 2014. Exposure measurement error in pm 2.5 health effects studies: A pooled analysis of eight personal exposure validation studies. Environmental Health 13:2.
24. Kozawa KH, Fruin SA, Winer AM. 2009. Near-road air pollution impacts of goods movement in communities adjacent to the ports of los angeles and long beach. Atmospheric Environment 43:2960-2970.
25. Künzli N, Kaiser R, Medina S, Studnicka M, Chanel O, Filliger P, et al. 2000. Public-health impact of outdoor and traffic-related air pollution: A european assessment. The Lancet 356:795-801.
26. Ladva, C.N., Golan, R., Greenwald, R., Yu, T., Sarnat, S.E., Flanders, W.D., Uppal, K., Walker, D.I., Tran, V., Liang, D. and Jones, D.P., 2017. Metabolomic profiles of plasma, exhaled breath condensate, and saliva are correlated with potential for air toxics detection. Journal of breath research, 12(1), p.016008.
27. Lim, S.S., Vos, T., Flaxman, A.D., Danaei, G., Shibuya, K., Adair-Rohani, H., AlMazroa, M.A., Amann, M., Anderson, H.R., Andrews, K.G. and Aryee, M., 2012. A comparative risk assessment of burden of disease and injury attributable to 67 risk factors and risk factor clusters in 21 regions, 1990–2010: a systematic analysis for the Global Burden of Disease Study 2010. The lancet, 380(9859), pp.2224-2260.
28. Liu W, Wang YH, Russell A, Edgerton ES. 2005. Atmospheric aerosol over two urban-rural pairs in the southeastern united states: Chemical composition and possible sources. Atmospheric Environment 39:4453-4470.
29. MacNaughton P, Melly S, Vallarino J, Adamkiewicz G, Spengler JD. 2014. Impact of bicycle route type on exposure to traffic-related air pollution. Science of the Total Environment 490:37-43.
30. Martín, F., Santiago, J.L., Kracht, O., García, L. and Gerboles, M., 2015. FAIRMODE Spatial representativeness feasibility study. JRC Technical Report (Report EUR 27385) 2015.
31. McCreanor J, Cullinan P, Nieuwenhuijsen MJ, Stewart-Evans J, Malliarou E, Jarup L, et al. 2007. Respiratory effects of exposure to diesel traffic in persons with asthma. New England Journal of Medicine 357:2348-2358.
32. Metzger KB, Tolbert PE, Klein M, Peel JL, Flanders WD. 2003a. Case-crossover analyses of cardiovascular emergency department visits and ambient air quality, atlanta, georgia, 1993-2000. Epidemiology 14:S66-S66.
33. Metzger KB, Tolbert PE, Klein M, Peel JL, Flanders WD, Todd KH, et al. 2003b. Ambient air pollution and emergency department visits for specific cardiovascular conditions, atlanta, georgia, 1993-2000. Am J Epidemiol 157:S27-S27.
34. Sanchez B, Santiago JL, Martilli A, Martin F, Borge R, Quaassdorff C, de la Paz D, 2017. Modelling NOx concentration through CFD-RANS model in an urban hot-spot using high

resolution traffic emissions and meteorology from a mesoscale model. Atmospheric Environment 163, 155-165.
35. Santiago, J.L., Martín, F. and Martilli, A., 2013. A computational fluid dynamic modelling approach to assess the representativeness of urban monitoring stations. Science of the total environment, 454, pp.61-72.
36. Santiago JL, Borge R, Martin F, de la Paz D, Martilli A, Lumbreras J, 2017. Evaluation of a CFD based approach to estimate pollutant distribution within a real urban canopy by means of passive samplers. Science of the Total Environment 576, 46-58.
37. Sarnat JA, Golan R, Greenwald R, Raysoni AU, Kewada P, Winquist A, et al. 2014. Exposure to traffic pollution, acute inflammation and autonomic response in a panel of car commuters. Environmental research 133:66-76.
38. Sarnat S, Klein M, Sarnat J, Flanders W, Waller L, Mulholland J, et al. 2008. The impact of exposure measurement error in a time-series analysis of air pollution and emergency department visits in atlanta, georgia. Epidemiology 19:S347.
39. Sarnat SE, Klein M, Sarnat JA, Flanders WD, Waller L, Mulholland JA, et al. 2008. The impact of exposure measurement error in a time-series analysis of air pollution and emergency department visits in atlanta, georgia. Epidemiology 19:S347-S347.
40. Sarnat SE, Klein M, Sarnat JA, Flanders WD, Waller LA, Mulholland JA, et al. 2010. An examination of exposure measurement error from air pollutant spatial variability in time-series studies. J Expo Sci Env Epid 20:135-146.
41. Sarnat SE, Raysoni AU, Li WW, Holguin F, Johnson BA, Luevano SF, et al. 2012. Air pollution and acute respiratory response in a panel of asthmatic children along the u.S.-mexico border. Environmental Health Perspectives 120:437-444.
42. Schwartz J, Litonjua A, Suh H, Verrier M, Zanobetti A, Syring M, et al. 2005. Traffic related pollution and heart rate variability in a panel of elderly subjects. Thorax 60:455-461.
43. Shields KN, Cavallari JM, Hunt MJO, Lazo M, Molina M, Molina L, et al. 2013. Traffic-related air pollution exposures and changes in heart rate variability in mexico city: A panel study. Environmental Health 12:7.
44. Solomon PA, Chameides W, Weber R, Middlebrook A, Kiang CS, Russell AG, et al. 2003. Overview of the 1999 atlanta supersites project. J Geophys Res 108:10.1029/2001JD001458.
45. Strickland MJ, Darrow LA, Klein M, Flanders WD, Sarnat JA, Waller LA, et al. 2010. Short-term associations between ambient air pollutants and pediatric asthma emergency department visits. American Journal of Respiratory and Critical Care Medicine 182:307-316.
46. Tolbert PE, Mulholland JA, MacIntosh DL, Xu F, Daniels D, Devine OJ, et al. 2000. Air quality and pediatric emergency room visits for asthma in atlanta, georgia. Am J Epidemiol 151:798-810.
47. Ultee JD. 2016. The potential of express bus to serve peak travel demand to outlying employment centers: A case study of the atlanta region:Georgia Institute of Technology.
48. Vijayaraghavan K, DenBleyker A, Ma L, Lindhjem C, Yarwood G. 2014. Trends in on-road vehicle emissions and ambient air quality in atlanta, georgia, USA, from the late 1990s through 2009. Journal of the Air & Waste Management Association 64:808-816.
49. Zeger SL, Thomas D, Dominici F, Samet JM, Schwartz J, Dockery D, et al. 2000. Exposure measurement error in time-series studies of air pollution: Concepts and consequences. Environmental health perspectives 108:419.
50. Zhai X, Mulholland JA, Russell AG, Holmes HA. 2017. Spatial and temporal source apportionment of pm 2.5 in georgia, 2002 to 2013. Atmospheric Environment 161:112-121.
51. Zhang J, McCreanor JE, Cullinan P, Chung KF, Ohman-Strickland P, Han I-K, et al. 2009. Health effects of real-world exposure to diesel exhaust in persons with asthma. Research report (Health Effects Institute):5-109; discussion 111-123.
52. Zhu YF, Hinds WC, Kim S, Shen S, Sioutas C. 2002. Study of ultrafine particles near a major highway with heavy-duty diesel traffic. Atmospheric Environment 36:4323-4335.

CHAPTER 1 TABLES AND FIGURES

Table 1.1. Inter-site Spearman's correlations for each single traffic pollutant indicators between road site monitor (RDS) and each of the other non-RDS monitoring sites

	BC	CO	NO	NO_2	NO_x	$PM_{2.5}$
$r_{RDS-NRO}$	0.59	0.66	0.75	0.79	0.85	0.90
$r_{RDS-NRI}$	0.52	0.67	0.53	0.72	0.80	0.65
$r_{RDS-FRO}$	0.39	0.50	0.41	0.81	0.61	0.93
$r_{RDS-FRI}$	0.34	0.52	0.34	0.79	0.62	0.91
$r_{RDS-CMS}$	0.64	0.48	0.55	0.70	0.64	0.94

Acronym: RDS, Road site; NRO, Near-road residence outdoor; NRI, Near-road residence indoor; FRO, Far-road residence outdoor; FRI, Far-road residence indoor; CMS, Center monitoring site.

Table 1.2. Effect modification by various factors on the percentage decrease in outdoor pollutant concentrations per 200 meters away from the near road monitoring site ^

	BC	**CO**	**NO**	**NO_2**
Categorical Factors[#]				
Time Period				
Morning Rush Hour (6am-9am)	3.63%	6.37%*	9.08%**	4.69%
Mid-day (10am-3pm)	5.19%**	9.66%**	15.24%*	8.68%**
Evening Rush Hour (4pm-7pm)	3.63%[&,**]	7.64%[&,**]	17.12%[&,**]	4.71%[&,**]
Late Evening (8pm-11pm)	3.05%	6.57%*	12.50%**	3.68%**
Midnight & Early Morning (12am-5am)	2.63%**	5.58%**	11.13%**	3.65%**
Wind Direction (relative to RDS site)				
Westerly	3.78%[&,**]	7.73%[&,**]	16.59%[&,**]	8.70%[&,**]
Northerly	0.91%*	4.21%**	3.80%**	2.47%**
Easterly (towards GIT campus)	3.03%	6.15%*	10.94%**	4.02%**
Southerly	5.27%	8.07%	15.80%	6.60%**
Date of Week				
Weekday	3.30%[&,**]	7.11%[&,**]	12.46%[&,**]	4.67%[&,**]
Weekend	4.14%*	6.92%	15.01%**	5.64%**
Continuous Factors[##]				
Temperature (per 10 F)	-0.15%	0.87%**	1.77%**	1.28%**
Relative Humidity (%)	0.06%**	-0.02%*	-0.05%**	-0.05%**
Wind Speed (mph)	0.54%**	1.57%**	2.87%**	1.00%**
Traffic Counts (per 1,000)	0.18%**	0.23%**	0.12%	0.28%**

^ Modification assessed using distance*factor product terms, with each factor tested in different models;
[#] Categorical factor results present the effect of distance (per 200 meters from highway) on pollutant concentrations for each level of the factor; [##] Continuous factor results present the interaction term parameter estimate;
[&] Reference category showing magnitude and significance of 'distance' main effect (note: results for other levels of each category present the magnitude of the 'distance' effect and whether the effect is significantly different from the reference category); ** p-Value <0.001; * p-Value<0.05.

Table 1.3. Percentage of attenuation of percent change in FEV_1 in a simulated panel study* (N=60) between road site monitor (RDS) and each of the other monitoring sites.

Monitoring Sites	Distance to RDS (in meters)	BC (ug/m^3) N=39		CO (ppm) N=77		NO (ppb) N=77		NO_2 (ppb) N=77		$PM_{2.5}$# (ug/m^3) N=28	
		Assumed true effect estimate β= -0.41 per IQR increase in pollutant concentration									
		β_{error}	$\%_{Attenuation}$	β_{error}	$\%_{Attenuation}$	β_{error}	$\%_{Attenuation}$	β_{error}	$\%_{Attenuation}$	β_{error}	$\%_{Attenuation}$
δ_{NRO}	10	-0.144	64.9%	-0.336	18.1%	-0.351	14.4%	-0.331	19.2%	-0.546	-33.3%
δ_{NRI}	10	-0.158	61.5%	-0.315	23.1%	-0.157	61.6%	-0.401	2.2%	-0.450	-9.9%
δ_{FRO}	1,390	-0.159	61.2%	-0.208	49.2%	-0.271	34.0%	-0.277	32.5%	-0.628	-53.2%
δ_{FRI}	1,390	-0.131	68.1%	-0.215	47.6%	-0.124	69.9%	-0.347	15.4%	-0.534	-30.2%
δ_{CMS}	2,290	-0.215	47.5%	-0.266	35.2%	-0.322	21.5%	-0.195	52.5%	-0.566	-38.0%

Acronym: RDS, Road site; NRO, Near-road residence outdoor; NRI, Near-road residence indoor; FRO, Far-road residence outdoor; FRI, Far-road residence indoor; CMS, Center monitoring site; IQR, interquartile range.

* The small panel study was simulated based on previous field study (McCreanor et, al. 2007). Post-exposure changes in FEV_1 was simulated using a single pollutant linear model with a percent change of -0.41 and 1.05 per interquartile range.

Only 48 hour integrated sampling of $PM_{2.5}$ was available for RDS. A total of 28 samples were available.

Figure 1.1. Map of sampling locations for the DRIVE study on the campus of the Georgia Institute of Technology (GIT) in Atlanta, GA. The section of highways represents where Interstates 75 and 85 come together, with more than 350,000 vehicles passing by every day. Roadside site serve as a near-road-monitoring site and Jefferson St site was a center monitoring site that was 2.3 km away from this traffic hotspot. Two additional outdoor sites, along with two indoor sites, were located at the two student dormitories: 'Near Dorm', approximately 20 m west of the highway, and 'Far Dorm', approximately 1.4 km west of the highway.

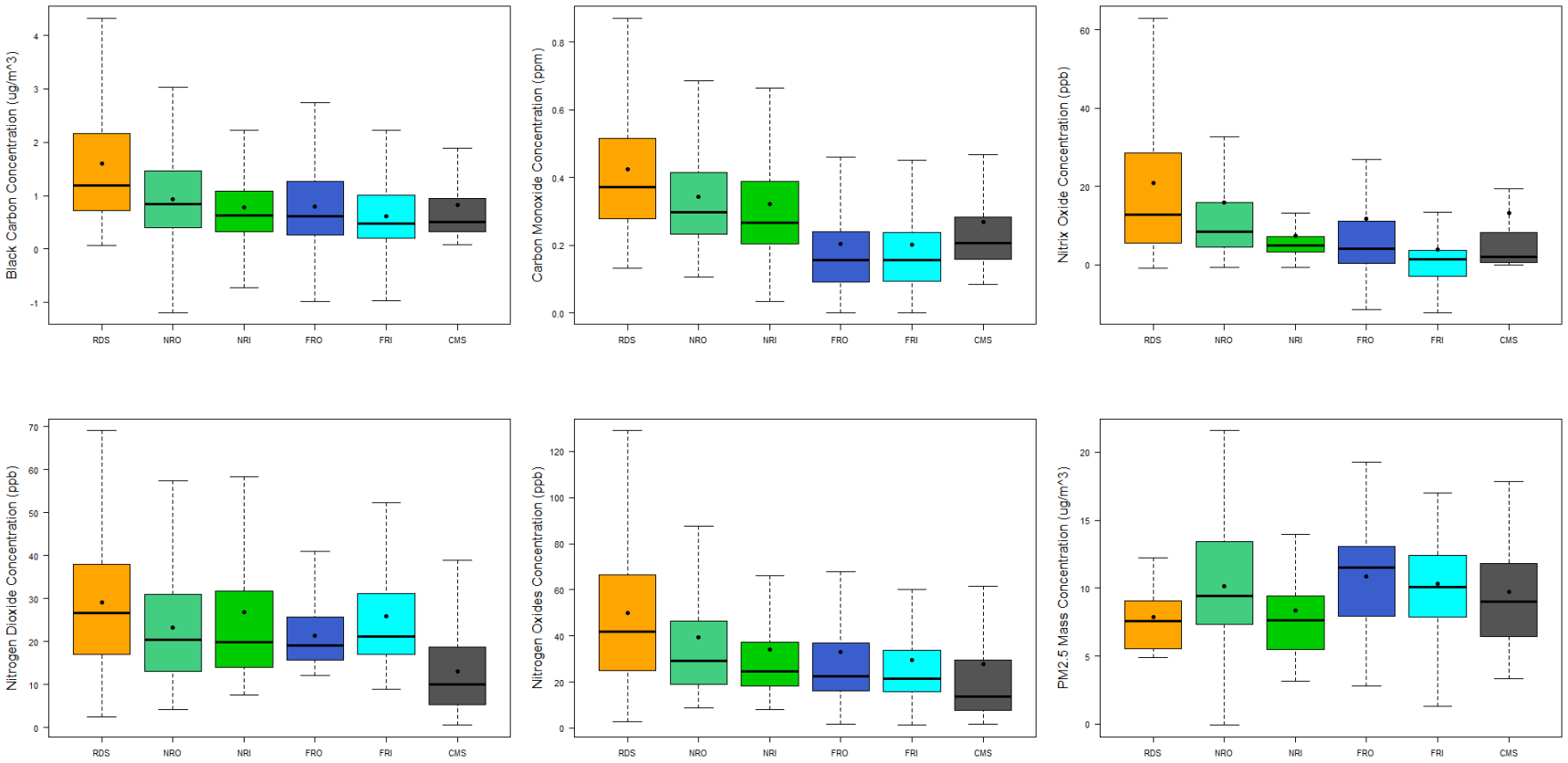

Figure 1.2. Boxplots presenting the distribution of BC, CO, NO, NO_2, NO_x, and $PM_{2.5}$ concentrations during September 8th, 2014 to January 5th, 2015 at outdoor and indoor sampling locations, ordered in increasing distance from the highway source: (1) RDS: Near-highway stationary site [10m], (2) NRO: Near Dorm outside [20 m], (3) NRI: Near Dorm inside [20 m], (4) FRO: Far Dorm outside [1.4 km], (5) FRI: Far Dorm inside [1.4 km], and (6) CMS: urban background [2.3 km]. The horizontal line within the box indicates the median, boundaries of the box indicate the 25_{th}- and 75_{th} -percentile, the whiskers are the 5_{th} and 95_{th} percentile, and the "•" marked in the box indicates the mean.

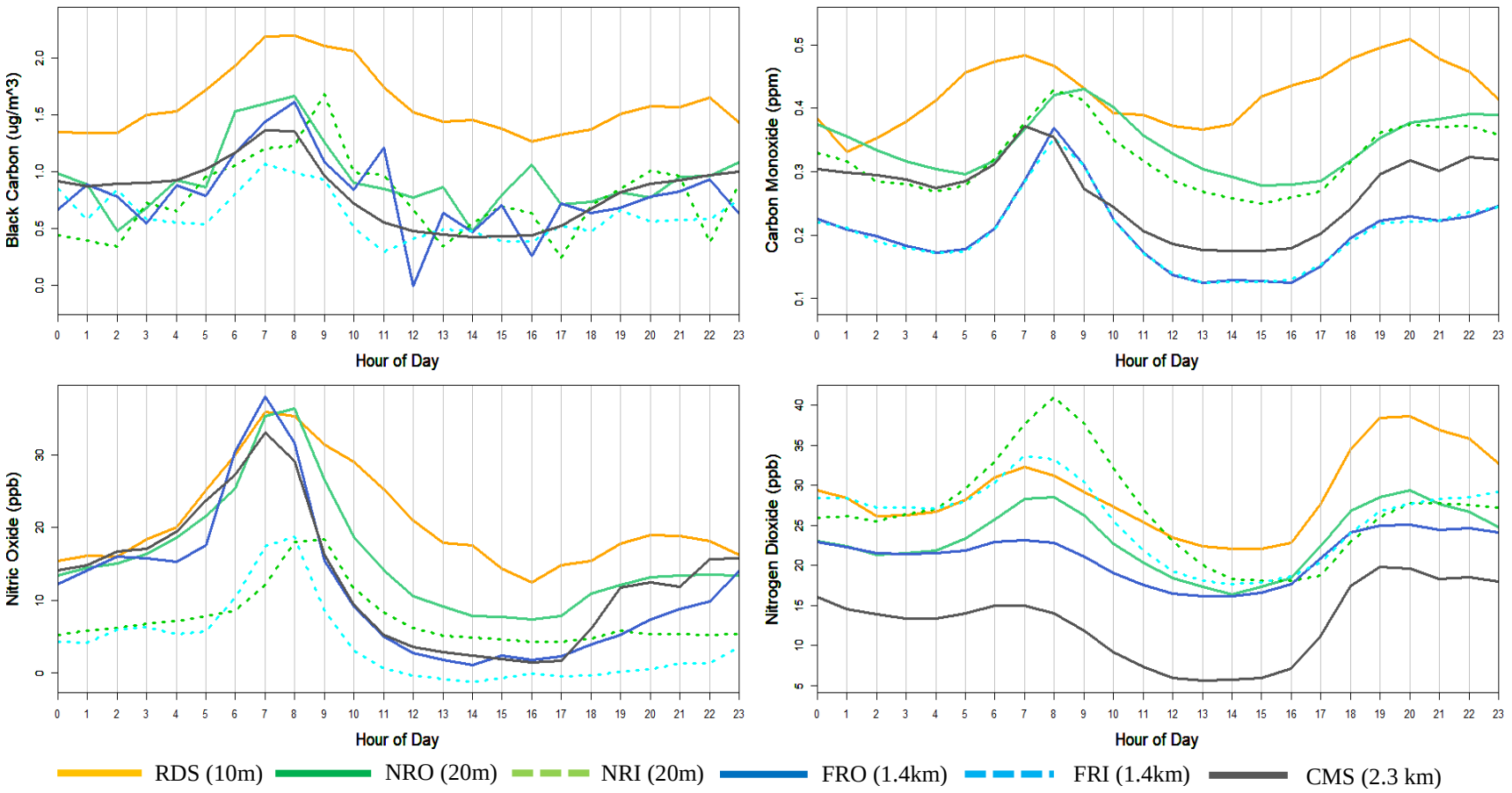

Figure 1.3. Diurnal profile plots presenting mean hourly concentrations of BC, CO, NO, and NO_2 at outdoor and indoor sites during September 8th, 2014 to January 5th, 2015: (1) RDS: Near-highway stationary site [10m], (2) NRO: Near Dorm outside [20 m], (3) NRI: Near Dorm inside [20 m], (4) FRO: Far Dorm outside [1.4 km], (5) FRI: Far Dorm inside [1.4 km], and (6) CMS: urban background [2.3 km].

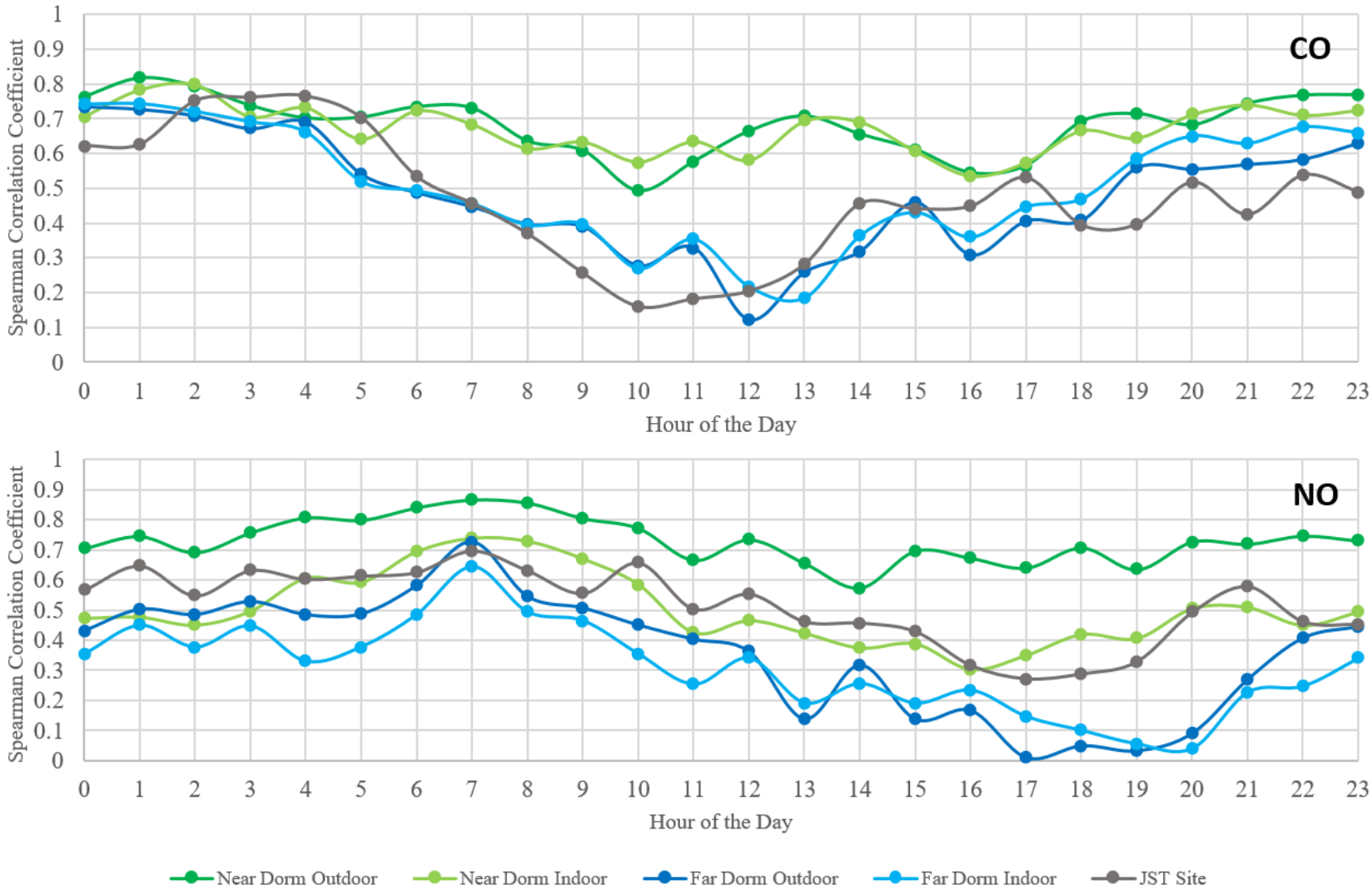

Figure 1.4. Spearman correlations (y-axis) between measurements at the RDS site and all other sites by hour of the day (x-axis).

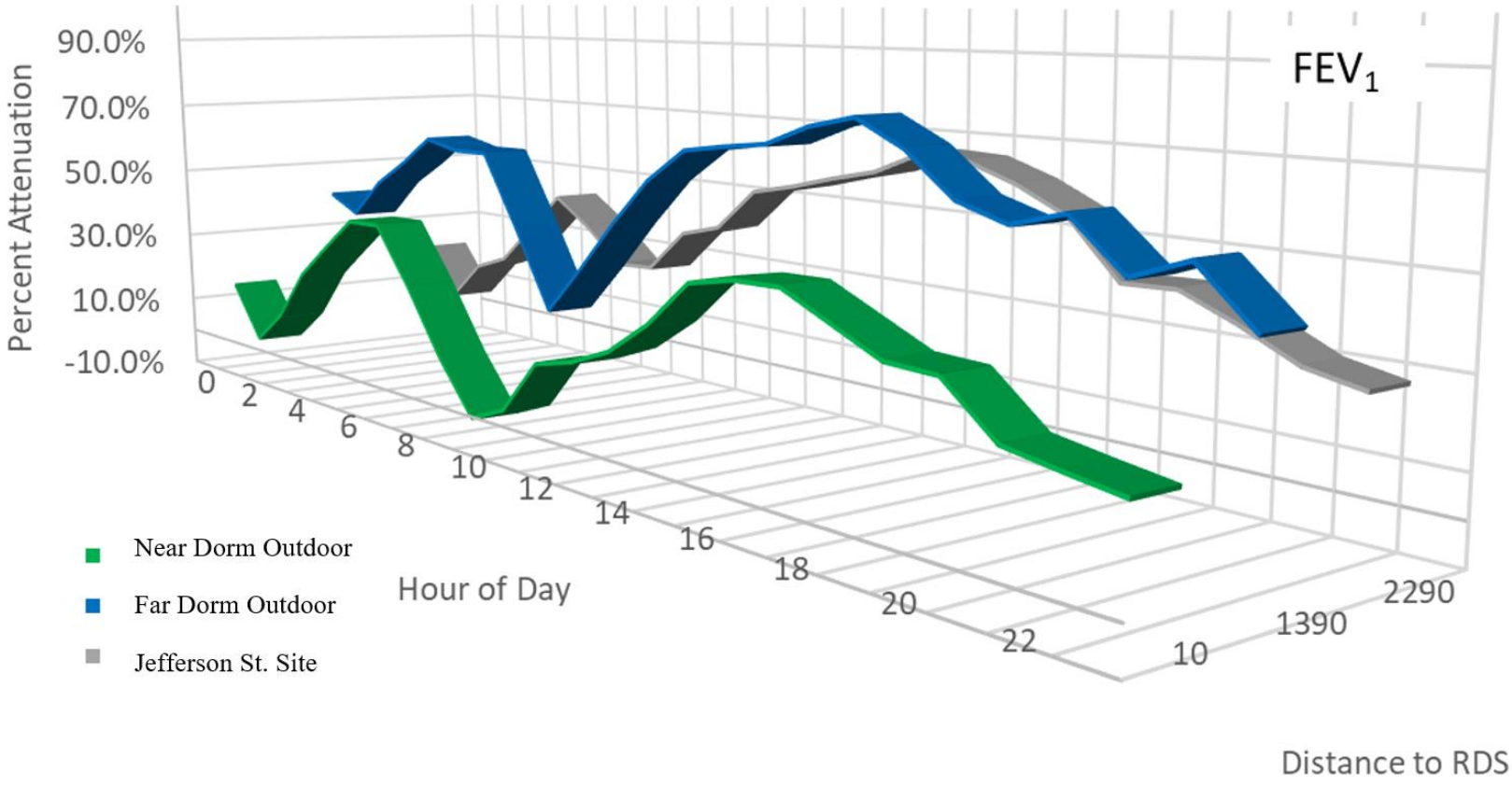

Figure 1.5. Hourly percentage of attenuation of percent change in FEV_1 associated with mean hourly CO level in a simulated panel study* (N=60) between road site monitor (RDS) and each of the other monitoring sites.

*Hourly post-exposure changes in FEV_1 was simulated using a single pollutant linear model with a percent change of -0.41 per interquartile range of CO.

CHAPTER 1 SUPPLEMENTAL MATERIALS

Table S1.1. Summary of measurements conducted at each monitoring location.

Tier	Site	Pollutant	Instrument Model	Frequency (n=target sample #)
Outdoor	RDS	CO	Thermo 48i	Continuous
		$NO\text{-}NO_2$	Teledyne 200A	Continuous
		$PM_{2.5}$ BC	Magee Scientific Aethalometer	Continuous
		$PM_{2.5}$ Mass	Gravimetric	Integrated (48-hr) - 2/wk
	NRO, FRO	CO	Teledyne 300E	Continuous
		$NO\text{-}NO_2$	Thermo 42C Low Source	Continuous
		$PM_{2.5}$ BC	microAeth AE51	Continuous
		$PM_{2.5}$ Mass	Gravimetric	Integrated (48-hr) - 2/wk
	CMS	CO	*	Continuous
		$NO\text{-}NO_2$	*	Continuous
		$PM_{2.5}$ BC	*	Continuous
		$PM_{2.5}$ Mass	*	Continuous
Indoor	NRI, FRI	CO	Teledyne 300E	Continuous
		$NO\text{-}NO_2$	Thermo 42C Low Source	Continuous
		$PM_{2.5}$ BC	microAeth AE51	Continuous
		$PM_{2.5}$ Mass	Gravimetric	Integrated (48-hr) - 2/wk

Acronym: RDS, Road site; NRO, Near-road residence outdoor; NRI, Near-road residence indoor; FRO, Far-road residence outdoor; FRI, Far-road residence indoor; CMS, Center monitoring site.

*Info on the instrument model used in the center monitoring site was unavailable.

Table S1.2**.** Instrumentation used at each sampling location and completeness of each data parameter.

Sampling Site	**Distance from Highway**	**Black Carbon**	**Carbon Monoxide**	**NO-NO_2-NOx**	**$PM_{2.5}$ Mass**	**Weather Data**
Near Highway	10 m	X/O	X	X	O	X
		79%/78%	76%	93%	78%	61%
Near Dorm	20 m	X/O	X	X	O	--
		34%/94%	77%	82%	94%	
Far Dorm	1.4 km	X/O	X	X	O	--
		34%/100%	66%	65%	100%	
Jefferson St.	2.3 km	X	X	X	--	X
		100%	92%	92%		96%

X = Continuous, completeness based on ratio of hours with valid data and total hours from Sept 8th to Jan 5th (n = 2880 hours); O = Integrated 48-hour, completeness based on ratio of 48-hr periods with valid data and target number of 48-hr periods during Sept 8th to Jan 5th (n = 26 periods); -- = parameter not measured

Table S3. Descriptive statistics of average traffic pollutant concentrations across multiple monitoring sites

Monitoring Sites	Distance to Highway (in meters)	BC (ug/m^3)		CO (ppm)		NO (ppb)		NO_2 (ppb)		$PM_{2.5}$[#] (ug/m^3)	
		N=39		N=77		N=77		N=77		N=28	
		Mean±SD	IQR	Mean±SD	IQR	Mean±SD	IQR	Mean±SD	IQR	Mean±SD	IQR
RDS	10	1.9±1.0	1.2	0.43±0.14	0.18	20.9±15.6	15.5	30.3±10.9	16.6	7.9±2.7[#]	3.4
NRO	20	0.8±1.0	0.8	0.35±0.13	0.13	16.6±16.8	11.3	25.2±9.4	12.0	11.3±4.2	5.5
NRI	20	0.8±0.6	0.6	0.33±0.13	0.14	7.6±8.9	5.7	29.2±15.9	19.0	9.3±4.1	5.4
FRO	1,400	0.7±0.6	0.8	0.22±0.13	0.12	12.8±16.1	18.5	21.6±4.6	7.1	12.1±4.6	5.4
FRI	1,400	0.6±0.5	0.7	0.21±0.13	0.12	4.6±11.8	8.3	26.4±8.2	12.3	10.4±4.4	4.4
CMS	2,300	1.0±0.6	0.7	0.29±0.14	0.15	15.7±19.3	17.2	14.5±6.3	9.3	10.7±4.0	5.8

Acronym: RDS, Road site; NRO, Near-road residence outdoor; NRI, Near-road residence indoor; FRO, Far-road residence outdoor; FRI, Far-road residence indoor; CMS, Center monitoring site; IQR, interquartile range.

[#] Only 48 hour integrated sampling of $PM_{2.5}$ was available for RDS. A total of 28 samples were available.

Table S4. Descriptive statistics of absolute differences on traffic pollution exposures between road site monitor (RDS) and each of the other monitoring sites.

Monitoring Sites	Distance to RDS (in meters)	BC (ug/m^3)		CO (ppm)		NO (ppb)		NO_2 (ppb)		$PM_{2.5}$[#] (ug/m^3)	
		N=39		N=77		N=77		N=77		N=28	
		Mean	Variance	Mean	Variance	Mean	Variance	Mean	Variance	Mean	Variance
δ_{NRO}	10	-1.14	1.29	-0.08	0.00	-4.31	25.17	-5.13	50.74	3.37	4.25
δ_{NRI}	10	-1.15	0.69	-0.11	0.00	-13.33	86.30	-1.07	138.35	1.38	9.71
δ_{FRO}	1,390	-1.17	0.74	-0.22	0.01	-8.17	131.59	-8.68	57.26	4.26	5.24
δ_{FRI}	1,390	-1.28	0.82	-0.22	0.01	-16.33	148.76	-3.86	37.32	2.48	4.92
δ_{CMS}	2,290	-0.88	0.59	-0.14	0.01	-5.21	128.89	-15.78	47.39	2.85	2.89

Acronym: RDS, Road site; NRO, Near-road residence outdoor; NRI, Near-road residence indoor; FRO, Far-road residence outdoor; FRI, Far-road residence indoor; CMS, Center monitoring site.

[#] Only 48 hour integrated sampling of $PM_{2.5}$ was available for RDS. A total of 28 samples were available.

Table S5. Effect modification by various factors on the percentage decrease in outdoor pollutant concentrations per 200 meters away from the near road monitoring site ^

	BC	**CO**	**NO**	**NO_2**
Categorical Factors[#]				
Time Period	R^2=0.30	R^2=0.27	R^2=0.29	R^2=0.37
Morning Rush Hour (6am-9am)	3.63% (2.66%, 4.58%)	6.37%* (5.56%, 7.16%)	9.08%** (7.03%, 11.09%)	4.69% (2.67%, 6.71%)
Mid-day (10am-3pm)	5.19%** (4.40%, 5.98%)	9.66%** (9.00%, 10.31%)	15.24%* (13.60%, 16.84%)	8.68%** (7.15%, 9.23%)
Evening Rush Hour (4pm-7pm)	3.63%[&,]** (3.03%, 4.23%)	7.64%[&,]** (7.15%, 8.13%)	17.12%[&,]** (15.93%, 18.29%)	4.71%[&,]** (3.55%, 5.87%)
Late Evening (8pm-11pm)	3.05% (2.25%, 3.84%)	6.57%* (5.90%,7.24%)	12.50%** (10.84%, 14.13%)	3.68%** (2.88%, 4.48%)
Midnight & Early Morning (12am-5am)	2.63%** (1.88%, 3.38%)	5.58%** (4.95%, 6.21%)	11.13%** (9.55%, 12.68%)	3.65%** (2.70%, 4.60%)
Wind Direction (relative to RDS site)	R^2=0.32	R^2=0.23	R^2=0.30	R^2=0.38
Westerly	3.78%[&,]** (2.27%, 5.26%)	7.73%[&,]** (6.58%, 8.87%)	16.59%[&,]** (13.87%, 19.23%)	8.70%[&,]** (7.87%, 9.52%)
Northerly	0.91%* (-1.74%, 3.49%)	4.21%** (2.23%, 6.14%)	3.80%** (-1.60%, 8.91%)	2.47%** (0.95%, 3.96%)
Easterly (towards GIT campus)	3.03% (1.48%, 4.56%)	6.15%* (4.94%, 7.34%)	10.94%** (796%, 13.84%)	4.02%** (3.12%, 4.90%)
Southerly	5.27% (3.70%, 6.82%)	8.07% (6.83%, 9.28%)	15.80% (12.89%, 18.62%)	6.60%** (5.70%, 7.49%)
Date of Week	R^2=0.29	R^2=0.25	R^2=0.27	R^2=0.36

Weekday	3.30%[&,**] (3.02%, 3.58%)	7.11%[&,**] (6.88%, 7.35%)	12.46%[&,**] (11.87%, 13.06%)	4.67%[&,**] (4.49%, 4.86%)
Weekend	4.14%* (3.59%, 4.70%)	6.92% (6.45%, 7.38%)	15.01%** (13.88%, 16.12%)	5.64%** (5.30%, 6.60%)
Continuous Factors[##]				
	R^2=0.29	R^2=0.24	R^2=0.29	R^2=0.38
Temperature (per 10 F)	-0.15% (-0.37%, 0.08%)	0.87%** (0.70%, 1.04%)	1.77%** (1.32%, 2.23%)	1.28%** (1.15%, 1.41%)
	R^2=0.29	R^2=0.23	R^2=0.26	R^2=0.35
Relative Humidity (%)	0.06%** (0.04%, 0.07%)	-0.02%* (-0.03%, 0.00%)	-0.05%** (-0.08%, -0.02%)	-0.05%** (-0.06%, -0.05%)
	R^2=0.29	R^2=0.25	R^2=0.27	R^2=0.36
Wind Speed (mph)	0.54%** (0.33%, 0.74%)	1.57%** (1.40%, 1.74%)	2.87%** (2.44%, 3.30%)	1.00%** (0.87%, 1.12%)
	R^2=0.33	R^2=0.26	R^2=0.27	R^2=0.39
Traffic Counts (per 1,000)	0.18%** (0.12%, 0.23%)	0.23%** (0.19%, 0.28%)	0.12% (-0.01%, 0.24%)	0.28%** (0.25%, 0.32%)

^ Modification assessed using distance*factor product terms, with each factor tested in different models;
[#] Categorical factor results present the effect of distance (per 200 meters from highway) on pollutant concentrations for each level of the factor; [##] Continuous factor results present the interaction term parameter estimate;
[&] Reference category showing magnitude and significance of 'distance' main effect (note: results for other levels of each category present the magnitude of the 'distance' effect and whether the effect is significantly different from the reference category); ** p-Value <0.001; * p-Value<0.05.

Appendix A

Simulating impact of measurement error within a small panel epidemiologic framework.

Small panel studies have been particularly useful for examining short-term pollutant exposures and acute biological responses by measuring a range of clinical and sub-clinical exposure and health endpoints on an individual-level. Given that small panel studies assign individual exposure level by obtaining measurements from central, urban or near-road monitoring sites, exposure measurement error may be introduced due to the spatial variability of the pollutants and differences between monitored concentrations and personal exposure, thus potentially impacting the effect estimate of pollutant on biological response. For the purpose of the current analysis aims, impact of measurement error was calculated for each of the TRAPs when using the level at RDS as an error-prone surrogate of the pollutant level at other non-RDS sites. It is important to note that no assumption was made between the true health risk associated and any of the specific single traffic pollutant; each single traffic pollutant may serve as an indicator of either the true causal agent, a causal mixture, or the traffic source itself that cause the adverse health effects. We defined exposure error, **δ**, as the absolute difference between two exposure metrics on the same time scale (daily or hourly). The RDS measurements were compared to each of the other five exposure metrics to generate the following five exposure error terms: δ_{CMS}, δ_{NRO}, δ_{NRI}, δ_{FRO} and δ_{FRI}. The exposure error due to the spatial difference between central monitoring site and near-road traffic hotspot was represented by $\delta_{\mathrm{CMS}} = \mathrm{CMS} - \mathrm{RDS}$, given that our near-road monitoring site captures traffic impacts, while the measurement at CMS represents urban background average. Similarly, there were exposure errors introduced due to the distance between near-road traffic hotspot and the outdoor environment at the two residence sites, which were represented by $\delta_{\mathrm{NRO}} = \mathrm{NRO} - \mathrm{RDS}$ and $\delta_{\mathrm{FRO}} = \mathrm{FRO} - \mathrm{RDS}$ respectively. In addition, exposure error was also introduced when the microenvironment changed from ambient to indoor, where residents spent 90% of their time every day. These exposure errors are presented by $\delta_{\mathrm{NRI}} = \mathrm{NRI} - \mathrm{RDS}$ and $\delta_{\mathrm{FRI}} = \mathrm{FRI} - \mathrm{RDS}$ for the two residential sites respectively. Mean and variance were calculated for these five types of exposure errors for all five pollutants.

For each pollutant, we viewed pollutant level measured at each of the non-RDS location (NRI, NRO, FRI, FRO, and CMS) as true exposure (measured without error). Pollutant level measured at RDS site served as the exposure that would be used to conduct a health study; exposure error is introduced because of spatial gradient or with additional discrepancies due to microenvironment. To simulate true daily exposures for each pollutant at various non-RDS locations, we randomly sampled, with replacement, the pollutant levels measured at each site during the four-month DRIVE field campaign. Then to simulate daily RDS exposures, we used a linear model fitted between each non-RDS site and the RDS site; for example, for NDO serving as the true exposure, the model is given by

$$\widetilde{\mathrm{RDS}_t} = \theta_{1,\mathrm{NDO}} + \theta_{2,\mathrm{NDO}} * \mathrm{NDO}_t + \varepsilon_{\mathrm{NDO},t} \qquad \text{(Eq. S1)}$$

where t indexes day; and θ_1 and θ_2 represent additive and multiplicative error between the two exposure metrics; and $\varepsilon_{\mathrm{NDO},t}$ are independent normal residual errors. The above model parameters were estimated using NDO_t and RDS_t measurements from DRIVE. For each Monte Carlo simulation, an error-prone exposure mean for each day was simulated by using the true exposures at each of the non-RDS sites as the predictor (i.e., NDO) and a realization of the coefficients (θ_1 and θ_2) drawn from their asymptotic bivariate normal distribution. Finally, a daily residual error (ε_t) was subsequently drawn from a univariate normal distribution, and then added with the mean to obtain the full error-prone near-road exposure value.

To examine the impact of measurement error in estimating the health responses associated with traffic emissions in small panel study, we utilized health response estimates of a widely used biomarker, first force expiratory volume (FEV_1), which was associated with pre-post exposure to traffic emission from a highly cited small panel study (McCreanor et al. 2007) for the health response simulation. We averaged the percent change (health responses estimates in J. McCreanor et al. 2007) of FEV_1 after exposure to traffic pollutants (EC, NO_2, and $PM_{2.5}$) and used β=-0.41 for percent change in FEV_1 per IQR increase in each of the single pollutant for the simulation. Linear regression models were used to simulate FEV_1:

$$\mathrm{E}(\mathrm{Y}_t) = \propto + \beta_1 \mathrm{pollution}_{i,t} + \varepsilon_t \qquad \text{(Eq. S2)}$$

where Y_t is the percent change in FEV_1 on day t. For each pollutant i, daily averages (24-hr average) of same-day concentrations were used. For each pollutant, we viewed pollutant level measured at each of the non-RDS location (NRI, NRO, FRI, FRO, and CMS) as true exposure (measured without error). Impact of measurement error was estimated via simulation. Percent changes in health outcomes were drawn from Gaussian distributions and fitted using the simulated true exposures or the error-prone exposures with two linear models (Eq. S2): one using the simulated the true exposure, and another using the error-prone exposure. This resulted in two sets of estimated β: $\hat{\beta}_{\text{true}}$ and $\hat{\beta}_{\text{error}}$. The above simulation was run 1,000 times for each pollutant and non-RDS site. In order to determine if the presence of measurement error induces bias and a loss of precision, the mean over the 1,000 estimates for each β was calculated and used as the overall point-estimate associated with each pollutant pair and measurement error scenario. As an example, the effect estimate β for the main pollutant i in the true exposure scenario, was calculated as:

$$\overline{\beta}_{\text{true}} = \exp\left(\frac{\sum_{n=1}^{N} \hat{\beta}_{\text{true,n}}}{N}\right) \quad \text{(Eq. S3)}$$

Similarly, the β for the error-prone scenario was calculated as:

$$\overline{\beta}_{\text{error}} = \exp\left(\frac{\sum_{n=1}^{N} \hat{\beta}_{\text{error,n}}}{N}\right) \quad \text{(Eq. S4)}$$

where n index the simulation iteration and $N = 1{,}000$. Percentage of Bias of the β for each single pollutant at each non-RDS site was calculated. For pollutant i at site s in the error-prone scenario, we define:

$$\%\ \text{Bias}_{s,i} = \left(1 - \frac{\overline{\beta}_{\text{error,i}}}{(-0.41)}\right) * 100\% \quad \text{(Eq. S5)}$$

where $\overline{\beta}_{\text{error}}$ is defined in Equation S4.

Since some small panel-based epidemiologic designs measured pollutant level over a short period of time (1-hour average, etc) when the biological responses were collected, the exposure measurement in this epidemiologic setting might also be prone to temporal variability of traffic pollutants. Thus, we also

characterized hourly-resolved percent attenuation for each of the five single pollutants. The methods remained the same as described above in both models, except that to calculate the hourly percentage of attenuation, we used hourly pollutant concentration instead of 24-hr average pollutant concentration.

CHAPTER 2

Use of High-Resolution Metabolomics for the Identification of Metabolic Signals Associated with Traffic-Related Air Pollution

Donghai Liang, Jennifer Moutinho, Tianwei Yu, Rachel Golan, Chandresh Ladva, Megan Niedzwiecki, Douglas Walker, Stefanie Ebelt Sarnat, Howard H. Chang, Roby Greenwald, Dean Jones, Armistead Russell, Jeremy A. Sarnat

ABSTRACT

High-resolution metabolomics (HRM) is emerging as a sensitive tool for measuring environmental exposures and biological responses. The aim of this analysis is to assess the ability of high-resolution metabolomics (HRM) to reflect internal exposures to complex traffic-related air pollution mixtures.

We used untargeted HRM profiling to characterize plasma and saliva collected from participants in the Dorm Room Inhalation to Vehicle Emission (DRIVE) study to identify metabolic pathways associated with traffic emission exposures. We measured a suite of traffic-related pollutants at multiple ambient and indoor sites at varying distances from a major highway artery for 12 weeks in 2014. In parallel, 54 students living in dormitories near (20 m) or far (1.4 km) from the highway contributed plasma and saliva samples. Untargeted HRM profiling was completed for both plasma and saliva samples; metabolite and metabolic pathway alternations were evaluated using a metabolome-wide association study (MWAS) framework with pathway analyses.

Weekly levels of traffic pollutants were significantly higher at the near dorm when compared to the far dorm ($p<0.05$ for all pollutants). In total, 20,766 metabolic features were extracted from plasma samples and 29,013 from saliva samples. 45% of features were detected and shared in both plasma and saliva samples. 1,291 unique metabolic features were significantly associated with at least one or more traffic indicator, including black carbon, carbon monoxide, nitrogen oxides and fine particulate matter ($p < 0.05$ for all significant features), after controlling for confounding and false discovery rate. Pathway analysis of metabolic features associated with traffic exposure indicated elicitation of inflammatory and oxidative stress related pathways, including leukotriene and vitamin E metabolism. We confirmed the chemical identities of 10 metabolites associated with traffic pollutants, including arginine, histidine, γ-linolenic acid, and hypoxanthine.

We identified and verified biological perturbations associated with primary traffic pollutant. Observed response was consistent with endogenous metabolic signaling related to oxidative stress, inflammation, and nucleic acid damage and repair. Collectively, the current findings provide support for the use of untargeted HRM in the development of metabolic biomarkers of traffic pollution exposure and response.

KEYWORDS

High Resolution Metabolomics; Traffic Related Air Pollution; Metabolic Perturbations; Oxidative Stress; Inflammation; Biomarkers

INTRODUCTION

Recent interest in air pollution health effects and regulatory intervention has shifted towards adopting multipollutant perspectives (Greenbaum and Shaikh 2010; Johns et al. 2012; Mauderly et al. 2010; Solomon et al. 2012; Vedal and Kaufman 2011). For highly heterogeneous sources, including traffic-related air pollution (TRAP), a multipollutant framework provides new opportunities to characterize biologically-relevant exposures. Improving exposure assessment to traffic emissions is particularly critical given the abundance of observational and controlled studies reporting associations between traffic sources and numerous adverse health effects (Health Effects Institute 2010).

High resolution metabolomics (HRM), involving the identification and quantitation of thousands of metabolites associated with endogenous and exogenous processes, holds specific promise as a powerful tool to improve internal exposure estimation to complex environmental mixtures (Bundy et al. 2009; Lankadurai et al. 2013; Miller and Jones 2014; Simpson and McKelvie 2009; Viant 2008). We (Ladva et al. 2017), and others (Breitner et al. 2016; Martens et al. 2017; Menni et al. 2015; Surowiec et al. 2016; Vlaanderen et al. 2017), have begun to examine the capability of HRM to capture metabolomic perturbations following exposures to ambient air pollutants. Currently, analytical and scientific uncertainties in HRM application, however, have limited its use for measuring the response to exposures from individual sources, such as TRAP (Hines et al. 2007; Morrison et al. 2007). Moreover, most environmental HRM applications, to date, have either been conducted in cohorts of several thousand or in smaller panels of individuals exposed to highly elevated concentrations of specific chemicals in occupational settings.

To address these research gaps and uncertainties, we conducted the Dorm Room Inhalation to Vehicle Emission (DRIVE) study. DRIVE was an intensive 12-week filed study that focused on assessing a complete emission-to-exposure pathway of traffic pollution. The present analysis utilized the extensive repeated biomonitoring (plasma and saliva) in a panel of 54 college students living in dormitories either

near (20 m) or far (1.4 km) from the highway. We used untargeted metabolomics-wide association analyses to assess whether changes in specific metabolic profiles in plasma or saliva samples are observed in relation to TRAP. Comprehensive pathway analysis and chemical validation were conducted to identify specific metabolic patterns and to further investigate potentially biologically relevant indicators to primary traffic exposures. In examining the link between TRAPs and corresponding internal metabolic profiles, we aimed to generate results that lead to the development of new biologically based primary traffic indicators. Such indicators could inform more targeted regulation of traffic-related pollution with the ultimate goal of reducing the public health burden attributable to air pollution.

METHODS

We conducted the DRIVE study to measure traditional and multipollutant traffic indicators along an emissions-to-dose exposure pathway. The centerpiece of this study was an intensive field sampling campaign that took place between September 8th, 2014 and January 5th, 2015. As part of this campaign, we measured a suite of traffic- and non-traffic-related pollutants at 6 outdoor and 2 indoor monitoring sites on the campus of the Georgia Institute of Technology (GIT) in Atlanta, GA, adjacent to the Downtown Connector ('the Connector'), one of the most heavily trafficked highway arteries in the US (Fig 1). While numerous smaller roadways surround the GIT campus, the Connector is the dominant mobile emissions source, with an annual average daily traffic (AADT) count of 305,365 vehicles during 2014, approximately 15 times that of the adjacent roads.

In addition to the field sampling, we recruited 54 GIT students living in one of two dormitories, located at different proximities from the highway, to participate in repeated personal biomonitoring. The current analysis examined a subset of the measurements collected, specifically those related to traffic pollution indicators in these study participants and corresponding metabolic response.

Exposure assessment

Measurements included, but were not limited to, several, ubiquitous primary traffic-related pollutants using a range of sampling platforms. A detailed description of the DRIVE study design, as well as the sampling methods can be found elsewhere (Sarnat submitted; Liang submitted). For the current analysis, we used exposure measurements conducted at two student dormitories located at different proximities from the highway, including two outdoor sites and two indoor sites: 'Near Dorm', approximately 20 m west of the Connector, and 'Far Dorm', approximately 1.4 km west of the Connector (Figure 2.1).

Sampling instrumentation located inside each dorm was identical, and utilized a three-way valve to alternate sampling between indoor and outdoor air. A complete list of the instruments used to conduct the exposure assessment is provided as Supplemental Material. Broadly, at each sampling location, we measured a suite of traditional primary traffic-related pollutants continuously including black carbon (BC), carbon monoxide (CO), nitric oxide (NO), nitrogen dioxide (NO_2), and nitric oxides (NO_x). In addition to the continuous and semi-continuous measurements, we conducted 48-hour quartz and Teflon filter-based measurements for particle mass. A total of 10 instruments were utilized, providing air pollutant concentration data at time scales from minutes to averages of over a week. All field instrumentation used to measure continuous pollutant concentrations were evaluated, refurbished if needed, and calibrated prior to field sampling. In order to compare concurrent pollutant measurements across the multiple sampling sites and ensure accurate concentrations during the sampling period, instruments measuring the same pollutant parameters were also co-located both before and after the sampling period and consistently calibrated throughout the 13-week intensive field sampling period. Calibration was done by varying the blend of pollutant gas from a cylinder of known concentration with a cylinder of zero air at given flow rates (Bios, DryCal). Instrument collocations were conducted, for continuous NO-NO_2-NO_x, CO, and integrated $PM_{2.5}$ mass and reflectance over a multi-day period, both before and after field sampling to assess method precision and potential instrument offset.

In the Near Dorm, we placed sampling instrumentation in a first-floor dorm room that was being used as an administrative office. The room had a microwave, dorm-size refrigerator, and a small space heater running periodically. The Near Dorm building was five stories high, built in 1961, and most recently renovated in 2002. The first floor was used for administrative offices and the top four floors were occupied student rooms (typically two students per room). Each floor of the Near Dorm was laid out similarly with about 12 double rooms (11' x 15') and a single shared bathroom. Each floor also had a single larger utility room (33' x 15'); used as a conference room on the first floor, an exercise room on the second floor, and a kitchenette on the third through fifth floors. The outdoor and indoor sampling inlet tubes were located approximately 0.5 and 0.25m off the ground, respectively

In the Far Dorm, we conducted sampling in one-half of a two-bedroom suite on the first floor of the five-story building built in 1984. There were seven suites on each floor and each suite shared a bathroom. Each floor also shared a small kitchen. The room used for sampling within the suite was not occupied during the study. The outdoor sampling inlet tube was 2 m off the ground and the indoor sampling inlet tube was raised 0.25 m off the linoleum flooring for all continuous instrumentation. Integrated, filter-based measurements were collected about 1.5 m off the floor, which was about the height of the window used for the outdoor sampling inlet. Both buildings used two-pipe heating and air conditioning systems that transitioned or started according to ambient air temperatures. Less heated water was produced elsewhere for heating when the outside air temperature was above 55 degrees, and less chilled water was produced for air conditioning when the temperature was below 65. The Near Dorm system made this transition automatically, while the Far Dorm system required manual conversion between A/C and heating.

Panel study recruitment

We conducted a nested panel study (from Sept 8th to Dec 15th, 2014) as a component within the indoor and outdoor monitoring campaign. We recruited a cohort of students living in the same dormitories that housed the indoor Near Dorm and Far Dorm sampling instrumentation. Recruitment occurred on-site during a 3-week period to accommodate dorm move-in dates and the start of the fall school semester, and was

conducted by researchers in accordance to pre-established protocols and the Institutional Review Board at GIT. Recruitment flyers were posted in each of the dorms and a series of informational sessions were given at each of the dorms in early August 2014. Of the 28 and 38 students who signed consent forms to participate from the Near Dorm and Far Dorm, respectively, 26 from the Near Dorm and 31 from the Far Dorm were enrolled based on an assessment of the participant's availability during the semester and likely compliance with the study protocol. During the 12-week sampling period, 2 participants from the Near Dorm and 1 from the Far Dorm dropped out of the study. No specific reasons were given for the attrition. In total, 54 students participated in the panel study.

Participants were given a baseline questionnaire detailing socio-demographic information, preliminary health, and typical time-activity patterns. Time-activity pattern data were collected through portable global positioning system (GPS) trackers that were distributed to a subset of participants (N=6) each week. The collected GPS data aided in quantifying time spent in various microenvironments and proximity to traffic sources as potential modifiers of personal exposures.

Biomonitoring and High-Resolution Metabolomics

All 54 students participated in the environmental metabolomics analysis by contributing up to four (monthly) venous blood and twelve (weekly) saliva samples. In total, 175 plasma and cell samples (average of 3.3 repeated samples per participant) and 621 2-ml vials of saliva (average of 11.5 repeated samples per participant) were collected. Metabolomics analyses were conducted on the monthly blood samples and saliva samples collected at the same time (collected on September 19th, October 24th, Nov 14th, and December 5th 2014). For each sample, 5 µL were injected and analyzed using liquid chromatography–mass spectrometry (LC/MS) techniques (Thermo Scientific™ Q Exactive™ HF hybrid quadrupole-Orbitrap). Each sample was analyzed in triplicate. Two technical columns, hydrophilic interaction liquid chromatography (HILIC) with positive ionization mode and C18 hydrophobic reversed-phase chromatography with negative ionization mode, were used to enhance the coverage of metabolic feature detection. Two quality control pooled reference plasma samples (referred to as NIST, from National

Institute of Standards and Technology, and QSTD, from Equitech) (Simon-Manso et al. 2013) were included at the beginning and end of each analytical batch of 20 samples for normalization, control for background noise, batch evaluation, and post hoc quantification. Raw data files obtained from the LC/MS instrument were converted into .mzML files using ProteoWizard. Two R packages, apLCMS and xMSanalyzer, were used to extract metabolic features with data quality control assessment and batch effect correction (Uppal et al. 2013; Yu et al. 2009). Several stringent criteria were applied to minimize the chance of degeneracy and false positive discovery. Only metabolites exhibiting a median coefficient of variation (CV) among the triplicate less than 30% and Pearson correlation greater than 0.7 were included in further analyses. Finally, all the metabolites needed to present in at least 15% of all samples (by biological media) to be included in final statistical analyses; these criteria were established in order to enhance generalizability and to reduce the possibility that the association between metabolic signals and traffic pollutant levels (the main predictor of interest, see below) were unduly influenced by individual samples or participants. Following this quality assessment, the triplicate measures of each extracted features of each sample were averaged and a log2 transformation was performed.

Data Analysis

For the primary statistical analysis, we followed an untargeted Metabolome-Wide Association Study (MWAS) workflow, where metabolic profiles were analyzed without prior knowledge of their chemical identity. Linear mixed effect models were conducted to assess associations between metabolite feature intensity (i.e., relative concentration) and levels of traffic related pollutants, controlling for random subject effects. Since nested personal exposure assessment showed that students from both dorms tended to spend the majority of their time in or around their respective dormitories (57% for Near Dorm students; 61% for Far Dorm students), we selected measurements from these locations as *a priori* surrogates of actual personal pollutant exposures. We used the weekly average outdoor or indoor level of each of the six traditional single-species air pollutants (BC, CO, NO, NO_2, NO_X, and $PM_{2.5}$) TRAP at the dormitory locations as the primary exposure indicator of interest. Models had the following form:

$$Y_{ijt} = \mu + \theta_i + \beta_{1j}Pollutant_{ikt} + \beta_{2j}Dorm_i + \beta_{3j}Age_i + \beta_{4j}Gender_i + \beta_{5j}BMI_i +$$
$$+\beta_{6j}Race_i + \beta_{7j}Movingdays_{it} + \beta_{8j}Timepoints_{it} + \varepsilon_{ijkt} \quad \text{(Eq. 2.1)}$$

where Y_{ijt} refers to intensity (i.e., relative concentration) of metabolic feature j for participant i on sampling date t. Separate models were conducted for each metabolic feature, from each of the four-biomatrix technical columns (plasma HILIC positive ions column, plasma C18 negative ions column, saliva HILIC positive ions column, and saliva C18 negative ions column). μ is the fixed-effect intercept and a random effect θ_i is included to control for potential between participant variation. $Pollutant_{ikt}$ refers to the weekly average outdoor or indoor level of the traffic related pollutant k at the dorm location for participant i on biosampling date t. $Dorm_i$ refers to the dorm location for participant i, accounting for potential differences in the non-traffic-pollutant-related factors among the participants from the two dorms. Other covariates were included to control for potential between participant differences, including age, gender (categorical), body mass index (BMI; continuous), and race (categorical). We also controlled for $Movingdays_{it}$, the total number of days between the biosample collection date and the date that participant i moved into the dorm; and $Timepoints_{it}$, the time point order (i.e., month number for plasma or saliva) when the biosample was collected from participant i on biosampling date t. ε_{ijkt} represents residual random normal error.

Hypothesis tests to identify differentially expressed features associated with specific traffic related pollutant levels (by biomatrix column) were corrected for multiple comparisons using the Benjamini-Hochberg false discovery rate ($FDR_{B\text{-}H}$) procedure at a 0.05 false positive (i.e., Type I error) threshold. Results were presented using Manhattan plots, which plot the retention time of each metabolic feature on the x-axis against the negative logarithm of its p-value for β_1 from Equation 1 on the y-axis. The significant metabolic features ($FDR_{B\text{-}H}$<0.05) associated with traffic-related pollutants were then used to conduct the pathway enrichment and metabolite annotation analyses.

Metabolic Pathway Enrichment Analysis and Metabolite Annotation

Pathway identification and module analysis were performed for significant metabolic features using mummichog (v. 1.0.5), a novel bioinformatics platform that infers and categorizes functional biological activity directly from mass spectrometry output, without prior metabolite validation (Amorim et al. 2013 134; Li et al. 2013). Mummichog analyses were conducted separately for each set of significant features from each of the 24 indoor/outdoor TRAP linear mixed models in the HILIC and C18 columns. An adjusted p-value per pathway was calculated from resampling the reference input file in mummichog using a gamma distribution which penalizes pathways with fewer reference hits, and assigning greater significance to pathways with more reference hits (Li et al. 2013). We classified pathways with adjusted p-values of <0.05 for at least three of the TRAPs models, and with at least 4 features from the experimental data matched with pathway metabolites. To further minimize the possibility of false positive discovery, candidate pathways were re-run using a subset of 6 most common forms out of the 16 standard adduct forms in mummichog (For HILIC positive ion mode, only the following adducts were considered: $M^{[+]}$, $M+H^{[+]}$, $M-H2O+H^{[+]}$, $M+Na^{[+]}$, $M+K^{[+]}$, $M+2H^{[2+]}$, and $M(C13)+2H^{[2+]}$; For C18 negative ion mode, only the following adducts were considered: $M-H^{[-]}$, $M+Cl^{[-]}$, $M+ACN-H^{[-]}$, $M+HCOO^{[-]}$, $M(C13)-H^{[-]}$, $M-H2O-H^{[-]}$, and $M+Na-2H^{[-]}$). We presented final results in a metabolic-pathway-TRAPs heat map, with each cell of the heat map representing a statistical association between each of the metabolic pathways and each of the corresponding indoor/outdoor TRAPs.

Metabolic features that were significantly associated with TRAPs ($FDR_{B-H}<0.05$) and also significantly enriched in a relevant pathway ($p<0.05$) using mummichog were annotated by matching mass m/z value for adducts commonly formed to the METLIN (https://metlin.scripps.edu/index.php), ChemSpider (http://www.chemspider.com/), Human Metabolome Database (HMDB), and Kyoto Encyclopedia of Genes and Genomes (KEGG) (http://www.genome.jp/kegg/pathway.html) databases, using a mass error threshold of 10 ppm. Tentative matches were further screened on their retention time, isotope patterns, and

peak quality by manually examining the extracted ion chromatograph (EIC). The remaining candidate features were selected for final chemical identification via Tandem Mass Spectrometry (MS/MS).

RESULTS

We collected 175 plasma and cell samples and 204 saliva samples during four time points, spaced approximately 21-35 days apart from each other, throughout the study from the 51 DRIVE participants providing blood and saliva specimens. With the exception of indoor $PM_{2.5}$, mean indoor and outdoor levels for all the pollutants were significantly higher in the Near Dorm compared to the Far Dorm during the entire study period, indicative of a substantial contrast in the potential exposure level to TRAPs among the two groups of study participants (t-test: $p < 0.05$) (Table 2.1 and Table S2.1). Baseline information collected from each participant at the commencement of sampling showed generally similar demographic characteristics among participants in both dorms, although there was a greater relative number of sophomore (i.e., 2nd year) students living in the Far Dorm compared to the Near Dorm (42.9% vs 8.7%, respectively) (Table 2.1). The total number of days the participants spent in their respective dorms prior to the first plasma collection were comparable in both dorms (86 vs 55 days, $p>0.05$).

Among the 54 participants, continuous GPS data were collected from 43 participants; 21 participants from the Near Dorm and 22 from the Far Dorm, over the course of 12 sampling weeks. As expected, there was a clear bimodal distribution between participants from the two dorms of time spent in closer proximity to the highway (Figure S2.2), supporting an observation that much of the students' time was spent within or near their respective dorms.

After data quality filtering, we extracted 20,766 metabolic features from plasma samples (13,419 in HILIC plasma column and 7,347 in C18 plasma column) and 29,013 from saliva samples (21,313 in HILIC plasma column and 7,700 in C18 plasma column). The median CV across the triplicate for each metabolic feature was 24.8%, indicating good overall data quality. A moderate fraction of features (6,667 in HILIC column and 2,812 in C18 column) were identified in both plasma and saliva samples (Figure S2.1).

Spearman correlation coefficients between these shared feature intensities identified in both plasma and saliva were 0.53 in the HILIC and 0.58 in the C18 column (across all four sampling time points: p-value < 0.0001, for all pairwise correlations). Correlations were stronger among the metabolic features with CVs less than 10% (0.64 in HILIC; 0.68 in C18). In addition, more than 45% of the extracted ions were found to have m/z matches (< 10 ppm) with metabolites identified in either the Human Metabolome Database (HMDB) or the USEPA's Mobile Air Toxics database.

We conducted and analyzed 48 sets of MWAS models (12 indoor/outdoor TRAPs among metabolic features in 2 biomatrices, each with 2 technical columns). In total, 847 and 444 unique metabolic features were associated with at least one or more of the indoor or outdoor TRAPs in the HILIC- and C18-plasma columns, respectively ($FDR_{B\text{-}H} < 0.05$). There were a similar number of significant metabolic features found in both columns for saliva samples (HILIC-saliva = 1,320 features; C18-saliva = 399 features) (Table 2.2 and Figure S2.3a-S2.3d).

We further screened each of the significant features based on their spectrum peak quality and purity by manual examination of their respective extracted ion chromatographs (EICs). By including only those spectra with unambiguous EIC peaks (63% to 95% in each biometric-technical column), we reduced the possibility of erroneously identifying a unique feature as multiple metabolites; an error known as degeneracy (Mahieu and Patti 2017). Using mummichog, we examined whether the features that were significantly associated with TRAPs co-occurred as enriched metabolites within specific metabolic pathways.

The results indicated that over 24 metabolic pathways were significantly associated with at least three or more TRAPs in plasma samples (adjusted $p<0.05$, calculated by mummichog), using either the HILIC or C18 column (Figure 2.2a). A similar number of significant metabolic pathways (N=23) were identified in saliva samples using both technical columns (Figure 2.2b). Broadly, approximately eight pathways consistently appeared to be significantly elicited across varying indoor or outdoor TRAPs models, in both plasma and saliva samples and technical columns. These include pathways predominantly associated with

xenobiotic-mediated oxidative stress and acute inflammatory response, such as leukotriene metabolism, vitamin E metabolism, and cytochrome P450 (Chow 1991; Dahlén et al. 1981; Gonzalez 2005; Henderson 1994; Morgan 1997; Singh et al. 2005). The leukotriene metabolism and vitamin E pathway, identified within these analyses, consistently appeared to be those pathways most strongly associated with a majority of the TRAPs, in each of the four biomatrices technical columns. Based on the strength and consistency of the mummichog results in showing these TRAP-related associations, we selected to focus on annotating the constituent metabolic features within these pathways, with the aim of validating the untargeted metabolomic observations.

As a means of providing additional confidence in the biochemical plausibility of the mummichog output, we excluded 34 less common (i.e., less plausible) identified adduct forms for subsequent validation. Using identified metabolite data available in KEGG, ChemSpider, HMDB, and a curated database of air toxics published by the US Environmental Protection Agency, we putatively matched 17 and 11 unique metabolic features within the leukotriene pathway and vitamin E metabolism, respectively (m/z difference < 10ppm)(Table S2.2a- S2.3d). These tentatively matched features were each significantly associated with multiple indoor or outdoor TRAPs, and exhibited relatively pure spectrum peaks with common adduct forms.

Putatively matched metabolites participating in the leukotriene pathway included leukotriene B4 (LTB4), leukotriene D4 (LTD4) and leukotriene E4 (LTE4), as well as their metabolic precursors, 12-oxo-LTB4, 20-OH-LTB4 and 20-oxo-LTE4. Also, identified within this pathway were metabolic indicators of lipid oxidation, such as 6-trans-LTB4, 12-oxo-20-dihydroxy-LTB4 and 18-carboxy-dinor-LTE4. In addition, several features were tentatively matched with other leukotriene related metabolites, including 10,11-dihydro-12R-hydroxy-LTC4, and 12-oxo-c-LTB3. Tentatively matched metabolites in the vitamin E pathway included multiple dehydrogenation carboxy products, or dehydrogenation precursors of tocotrienols and tocopherols, which maintain primary vitamin E antioxidant activities. Notably, most of the features that matched with pro-inflammatory-related metabolites were significantly and positively

associated with the TRAPs in the MWAS models; with significant and negative associations for those features linked to antioxidant processes.

Finally, we conducted tandem mass spectrometry to confirm the chemical identity of these unknown, yet putatively matched metabolic features that were both associated with the measured TRAPs as well as those enriched within TRAP exposure-relevant metabolic pathways. In total, we identified 10 metabolites using MS/MS (Table 2.3), 9 of which were indicative of endogenous metabolic signals, including arginine, histidine, γ-linolenic acid, and hypoxanthine. As noted, we observed consistent significantly negative associations ($\beta < 0$) between these anti-inflammatory metabolites with levels of TRAPs, while significantly positive association ($\beta > 0$) between TRAP and corresponding oxidative or pro-inflammatory metabolites.

DISCUSSION

Untargeted omics-based methods represent promising, yet still uncertain, means for measuring exposure and response to thousands of xenobiotic agents (Ellis et al. 2012; Park et al. 2012; Walker et al. 2016). To date, most examples of using environmental metabolomics have either been in cohorts of several thousand individuals (Ganna et al. 2016; Pallister et al. 2016), in smaller human panels exposed to highly elevated concentrations of specific chemicals in occupational settings (Dudka et al. 2014; Romano et al. 2012; Z Wang et al. 2015; Wei et al. 2013), or in cross-sectional designs (Li et al. 2017; Surowiec et al. 2016; Vlaanderen et al. 2017). Here, we specifically assessed whether changes in specific metabolic profiles associated with realistic environmental exposures, were discernable in plasma and saliva samples measured repeatedly in a relatively small, healthy, young adult panel. To our knowledge, this analysis constituted the single largest prospective longitudinal assessment examining traffic pollution related perturbations of the human metabolome.

Among the most pronounced and consistent findings from the MWAS mixed effect modeling and mummichog pathway enrichment analyses was that cumulative exposure to elevated levels of TRAPs over a multi-month period was associated with perturbations in several key biological pathways (Figure 2.2a-

2.2b). Of added importance was that the identification of the specific elicited pathways were robust to the various indoor and outdoor TRAP models, biomatrices, and in both technical columns. Moreover, a majority of the identified pathways are biologically plausible mediators of TRAP-related acute oxidative stress and inflammatory response (Baja et al. 2010; Chuang et al. 2007; Kelly 2003; Lodovici and Bigagli 2011; Nel et al. 2001). Among the pathways, those involved in leukotriene and vitamin E metabolism, in particular, consistently exhibited the strongest associations with most of the measured TRAPs in both saliva and plasma samples.

Leukotrienes, synthesized from arachidonic acid by arachidonate 5-lipoxygenase, are a family of active eicosanoid inflammatory mediators formed by leukocytes, mastocytoma cells, macrophages, and other tissues and cells in response to immunological and non-immunological stimuli (Hammarström 1983). Actively involved in asthmatic and allergic reactions and sustaining inflammatory reactions, leukotrienes are powerful biological signals, the overproduction of which is the major cause of inflammation in asthma and allergic rhinitis (Nelson et al. 2008; Salmon and Higgs 1987). Particularly, the dihydroxy fatty acid LTB4, synthesized by leukotriene A4 (LTA4) hydrolase from LTA4, is a potent chemoattractant and proinflammatory mediator that recruits cells from the immune system to produce inflammation and induces the release of lysosomal enzymes by neutrophils (Cotran et al. 1999; Devchand et al. 1996; Ford-Hutchinson et al. 1980). Numerous *in vitro* and *in vivo* studies have shown that LTB4 increases the generation of reactive oxygen species (ROS) and promotes leukocyte adherence (Biselli et al. 1996; Salas et al. 1999; Steiner et al. 2001). Moreover, perturbations in LTB4 in exhaled breath condensate have been linked to elevated NO_2 (Hüls et al. 2017; Vossoughi et al. 2014), ozone (Alfaro et al. 2007), and cigarette smoking (Carpagnano et al. 2003).

In the DRIVE MWAS models, we observed consistent, robust and positive associations between features putatively matched with LTB4 and multiple indoor or outdoor TRAPs, including BC, CO, NO and $PM_{2.5}$. In contrast, LTE4, the final cysteinyl leukotriene involved in inflammation within this pathway (Lee et al. 1983), is another important leukotriene synthesized and converted from LTA4. Compared to LTB4,

LTE4 is more stable, making it the dominant leukotriene accumulating in various biologic fluids, including breath condensation, plasma, and urine (Sala et al. 1990). Previously, urinary LTE4 levels were found to be positively associated with $PM_{2.5}$ among asthmatic children (Rabinovitch et al. 2006). Similarly in DRIVE study, significant positive associations were found between NO and features putatively matched with LTE4 in saliva samples among healthy participants. In addition, 15 primary metabolites or lipid oxidation metabolites of LTB4, LTD4 or LTE4 were putatively matched with the features that were significantly associated with multiple TRAPs (Appendix Table S2.2a-S2.2d), indicating the potential of further developing these pro-inflammatory metabolites as biomarkers to TRAPs. Furthermore, we demonstrated that the perturbations in leukotrienes related metabolites associated with exposure to air pollutants are observed among healthy people and not only in individuals with pre-existing disease such as asthma (Rabinovitch et al. 2006). In another recent study, we putatively identified 20-OH-LTB4 as a primary factor in leukotriene-mediated response in a panel study of car commuters consisting of both asthmatic and healthy participants (Ladva submitted).

Vitamin E, on the other hand, is a potent fat-soluble antioxidant that protects cells from oxidative damage (Brigelius-Flohe and Traber 1999; Cerecetto and Lopez 2007; Rigotti 2007). Acting as a peroxyl radical scavenger, vitamin E disables the generation of damaging free radicals, interrupts the propagation of reactive oxygen species, protects lipids and prevents the oxidation of polyunsaturated fatty acids (Choe and Min 2009; Traber and Stevens 2011; Whitney and Rolfes 2012). Previously, nutritional research has revealed the protective role of vitamin E in preventing or minimizing free-radical damage associated with specific diseases and lifestyle patterns, including protection against ambient $PM_{2.5}$ or ozone induced inflammatory response and oxidative stress (Bo et al. 2016; Menzel 1979; Packer 1991; Salvi 2007). In our study, 11 features were matched with vitamin E metabolites, mostly the dehydrogenation carboxy products, or precursors of dehydrogenation of tocotrienols and tocopherols, and the intensities of these antioxidants significantly decreased as levels of TRAPs increased (Appendix Table S2.3a-S2.3d).

We believe the MWAS modeling and tandem MS analyses lend additional coherence to the pathway enrichment findings. Most of the 10 metabolites we validated (70%) were endogenous molecules that participate in oxidative stress, acute inflammatory response, and DNA damage and repair processes. The findings also provide preliminary support for these validated metabolites as potential novel biomarkers of TRAP exposures. Arginine, specifically, is an α-amino acid that produces NO endogenously in the airways via NO synthase (Silkoff et al. 2000), with decreased levels associated with airway hyperresponsiveness, due to the augmentation of arginase induced by exposure to air pollution (North et al. 2011). Correspondingly, in our samples, we identified plasma arginine and found it to be significantly and inversely associated with measured BC and NO_x levels. Another promising metabolite we identified in DRIVE study is histidine, a semi-essential amino acid needed in humans. Histidine is the precursor to histamine (TABOR 1954), a vital and well-known inflammatory agent in immune responses, including the airway hyper responsiveness (Hospers et al. 2000; Liu et al. 1990). Previously in a study on examining the serum amino acid profiles in obese and non-obese women, both histidine and arginine were found to be negatively associated with inflammation and oxidative stress (Niu et al. 2012). Consistently in DRIVE, we observed a significant negative association between histidine and outdoor $PM_{2.5}$ level.

We also validated plasma hypoxanthine, a naturally occurring purine derivative that protects against oxidant-induced cell injury by inhibiting activation of nuclear poly (ADP-ribose) polymerase (Durkacz et al. 1980; Szabó 1998; Szabó and Dawson 1998). In a recent study, Vlaanderen et al also reported blood hypoxanthine perturbations associated with exposure to air pollutants, following 18 hours of exposure (Vlaanderen et al. 2017). In our study, hypoxanthine was significantly and positively associated with both indoor and outdoor CO levels. Finally, we identified □-linolenic acid (GLA) in plasma, which is an essential inhibitor in the biosynthesis of LTB4, which was putatively identified in this and in previous studies (Horrobin 1992; Mancuso et al. 1997). Here, too, the negative observed relationship between GLA and $PM_{2.5}$ levels is biochemically coherent, indicative of its inverse relationship with LTB4 expression. Collectively, we view these validated results as comprising a small, yet promising additional step in the

development of specific molecular markers for TRAP exposure. Towards this end, future work should focus on replicating the present findings, as well as in identifying metabolite biomarkers concomitantly expressed across multiple biomatrices, rather than metabolites enriched in a single matrix and columns.

Of all the extracted metabolic features, roughly 45% were matched, by m/z ratio and identified within both the plasma and saliva samples. Correlation coefficients among the shared features ranged from 0.5 - 0.9, which is consistent with our previous findings of moderate-to-strong correlation between saliva and plasma, observed in a pilot study comparing metabolic profiles in multiple biomatrices (Ladva et al. 2017). Moreover, more than 10 significant metabolic pathways elucidated in mummichog were shared by both saliva and plasma. Taken together, these results provide additional support for the possibility that saliva samples may serve as an alternative sensitive, and less invasive, biomatrix for metabolomics analysis.

Although somewhat unexpected, we also identified bis(2-ethylhexyl) phthalate (DEHP) using tandem mass spectrometry, an exogenous air pollutant identified in the EPA air toxic compounds metabolic database. DEHP was significantly and positively associated with multiple TRAPs within the MWAS results, including BC, CO and NO. DEHP is commonly found indoors as a ubiquitous chemical plasticizer component, which may also be found from the emissions of volatile organic compounds from the interior materials within new vehicles, according to a recent study (Faber et al. 2013). A less well-known source of DEHP, however, is road dust (Omar et al. 2007; Wang et al. 2013), which may explain its association with our pollutant traffic indicators within the MWAS results.

We used an MWAS approach where we modeled each of six single-pollutant indicators, independently, as surrogates of exposure to primary traffic pollution, known to be a highly heterogeneous mixture. The observed metabolic perturbations, thus, do not necessarily indicate a causal associations with that specific modeled indicator. It is possible, and perhaps likely, that changes are associated with multiple, correlated pollutants within a complex traffic mixture. It makes sense, therefore, that 30%-40% of the significant features in the MWAS models were associated with at least two or more individual traffic pollutant indicators.

Collectively, our study design and approach resolved statistically robust metabolic differences with changes in TRAP exposures. Despite this, several possible caveats, inherent in many omics-based analyses and small panel designs, deserve specific attention. Although we designed this study to recruit panels of students from both dorms that were demographically balanced, this was largely a convenience sample with some notable discrepancies between students in the two locations (Table 2.1). Students in the Near Dorm, on average, moved into their dorm rooms earlier than students in the Far Dorm, potentially contributing to differences in exposure and, perhaps, corresponding metabolomic expression. Similarly, the Far Dorm panel included a greater fraction of second-, as compared to first-year students. These differences in the two panels, where differences in time spent on campus and exposure to either traffic or other unspecified environmental factors (e.g., diet, indoor pollutants), may have truly been the factors responsible for the observed metabolomic differences in these profiles. To account for this, the MWAS regression models included terms to address these potential between participant differences, including age, sex, BMI, race, person-days within a dorm location, as well as dorm location itself, as a means of controlling for non-traffic related environmental factors that might differ among these two subpanels(Walker et al. 2016). Results from sensitivity analyses of the MWAS output were consistent and robust to model specification and inclusion of these covariates.

There is also a possibility that findings from small panels may be unduly influenced by individual observations. Most of the 100 to 1000 unique metabolic features significantly associated with at least one or more TRAPs, however, were prevalent in at least 38% of the participants, suggesting that the differences were not driven by extreme response in relatively few participants. Similarly, in highly multidimensional analyses, there is an increased risk of multiple comparisons and Type I errors. To address this, we applied several stringent criteria when conducting mummichog, including excluding model findings with $FDR_{B\text{-}H}$ significance greater 0.05, as well as restricting output to a subset of the six most abundant adducts in each ionization mode. By contrast, previous studies using similar environmental metabolomics methods set significance cut offs at FDR corrected p-values of less than 0.20, and included all 16 ion derivative and

adduct forms when matching the unknown features to the existing metabolic databases (Chandler et al. 2016; Tebani et al. 2017; Vlaanderen et al. 2017), thus increasing the risk of false positive discovery.

CONCLUSIONS

Recent advances in HRM support its use as a highly sensitive platform, capable of identifying thousands of small molecules, produced both endogenously and exogenously. We view the results from this study as providing further evidence of HRM's ability to elucidate biologically-relevant pathways associated with exposures to key environmental pollutants and sources. Our results were broadly consistent with the limited number of similar studies, which have examined perturbations in the human metabolome and ambient air pollution, in showing broad metabolomic perturbation associated with several oxidative stress and inflammatory pathways (Li et al. 2017; Surowiec et al. 2016; Vlaanderen et al. 2017). Most intriguingly, however, were results from our MWAS models, which point to the potential of HRM as tool for biomarker discovery. Here, we identified and validated several metabolites in plasma and saliva that were directly associated with external traffic pollution measurements in our panel. Collectively, the current findings support the use of environmental metabolomics, as a sensitive means for conducting air pollution exposure and epidemiologic analyses, in panel-based designs.

ACKNOWLEDGEMENT

Support for this project were provided through a contract with the Health Effects Institute (RFA #4942-RFA13-1/14-3). The field study conducted as part of this study benefitted greatly from the assistance of many students, staff, and faculty at both Georgia Tech and Emory. Specific thanks go to C. Cornwell, K. Parada, S. Shim, K. Johnson and E. Yang for their tremendous help in conducting the field study. We want to thank Dr. R. Weber, Dr. V. Verma, and Ms. D. Gao for their measurements of oxidative potential of ambient fine particles via DTT assay. We are indebted to Dr. J. Schauer (U. Wisconsin) for loaning us several instruments to supplement our sampling network. We would also like to thank Dr. Seung-Hyun Cho from RTI, Inc. for her collaboration on this project. The Georgia EPD allowed us access to their roadside monitoring site and helped provide data from those monitors, and we particularly thank Ken Buckley for his assistance with this. The study used on the instrumentation assembled for field studies conducted as part of the Southeastern Center for Air Pollution and Epidemiology (SCAPE), which was funded by a US Environmental Protection Agency STAR grant R834799. The information in this document may not necessarily reflect the views of the Agency and no official endorsement should be inferred. We also like to thank Ms. V. Tran for conducting the LC/MS on the DRIVE biosamples. Dr. Golan gratefully acknowledges support by a post-doctoral fellowship from the Environment and Health Fund, Jerusalem, Israel. We acknowledge NSF for providing a fellowship to JM (DGE-1650044), and Dr. Russell made use of funds provided by a generous gift from Howard T. Tellepson. Dr. Walker gratefully acknowledges the following grants supported by NIH (NIMH R01MH107205, NIEHS T32ES012870, and NIH S10OD018006). We acknowledge the support from the HERCULES exposome research center, supported by the National Institute of Environmental Health Sciences of the National Institutes of Health (P30ES019776). The content is solely the responsibility of the authors and does not necessarily represent the official views of the National Institutes of Health. We owe a debt of gratitude to the administrators at Georgia Tech for allowing us to conduct this study on campus and in their residence hall facilities.

REFERENCE

1. Alfaro MF, Walby WF, Adams WC, Schelegle ES. 2007. Breath condensate levels of 8-isoprostane and leukotriene b4 after ozone inhalation are greater in sensitive versus nonsensitive subjects. Experimental lung research 33:115-133.
2. Amorim JH, Rodrigues V, Tavares R, Valente J, Borrego C. 2013. Cfd modelling of the aerodynamic effect of trees on urban air pollution dispersion. Science of the Total Environment 461:541-551.
3. Baccarelli A, Wright RO, Bollati V, Tarantini L, Litonjua AA, Suh HH, et al. 2009. Rapid DNA methylation changes after exposure to traffic particles. American journal of respiratory and critical care medicine 179:572-578.
4. Baja ES, Schwartz JD, Wellenius GA, Coull BA, Zanobetti A, Vokonas PS, et al. 2010. Traffic-related air pollution and qt interval: Modification by diabetes, obesity, and oxidative stress gene polymorphisms in the normative aging study. Environmental health perspectives 118:840.
5. Biselli R, Farrace S, de Simone C, Fattorossi A. 1996. Potentiation of human polymorphonuclear leukocyte activation by atrial natriuretic peptide. Inhibitory effect of carnitine congeners. Inflammation 20:33-42.
6. Bo L, Jiang S, Xie Y, Kan H, Song W, Zhao J. 2016. Effect of vitamin e and omega-3 fatty acids on protecting ambient pm2. 5-induced inflammatory response and oxidative stress in vascular endothelial cells. PloS one 11:e0152216.
7. Bräuner EV, Forchhammer L, Møller P, Simonsen J, Glasius M, Wåhlin P, et al. 2007. Exposure to ultrafine particles from ambient air and oxidative stress–induced DNA damage. Environmental health perspectives 115:1177.
8. Breitner S, Schneider A, Devlin RB, Ward-Caviness CK, Diaz-Sanchez D, Neas LM, et al. 2016. Associations among plasma metabolite levels and short-term exposure to pm 2.5 and ozone in a cardiac catheterization cohort. Environment international 97:76-84.
9. Brigelius-Flohe R, Traber MG. 1999. Vitamin e: Function and metabolism. The FASEB Journal 13:1145-1155.
10. Bundy JG, Davey MP, Viant MR. 2009. Environmental metabolomics: A critical review and future perspectives. Metabolomics 5:3-21.
11. Carpagnano G, Kharitonov S, Foschino-Barbaro M, Resta O, Gramiccioni E, Barnes P. 2003. Increased inflammatory markers in the exhaled breath condensate of cigarette smokers. European Respiratory Journal 21:589-593.
12. Cerecetto H, Lopez G. 2007. Antioxidants derived from vitamin e: An overview. Mini reviews in medicinal chemistry 7:315-338.
13. Chandler JD, Hu X, Ko E-J, Park S, Lee Y-T, Orr M, et al. 2016. Metabolic pathways of lung inflammation revealed by high-resolution metabolomics (hrm) of h1n1 influenza virus infection in mice. American Journal of Physiology-Regulatory, Integrative and Comparative Physiology 311:R906-R916.
14. Choe E, Min DB. 2009. Mechanisms of antioxidants in the oxidation of foods. Comprehensive Reviews in Food Science and Food Safety 8:345-358.

15. Chow CK. 1991. Vitamin e and oxidative stress. Free Radical Biology and Medicine 11:215-232.

16. Chuang K-J, Chan C-C, Su T-C, Lee C-T, Tang C-S. 2007. The effect of urban air pollution on inflammation, oxidative stress, coagulation, and autonomic dysfunction in young adults. American journal of respiratory and critical care medicine 176:370-376.

17. Cotran S, Kumar C, Collins T, Robbins W. 1999. Pathologic basis of disease. Ed. Philadelphia: Saunders Co.

18. Dahlén S-E, Björk J, Hedqvist P, Arfors K-E, Hammarström S, Lindgren JA, et al. 1981. Leukotrienes promote plasma leakage and leukocyte adhesion in postcapillary venules: In vivo effects with relevance to the acute inflammatory response. Proceedings of the National Academy of Sciences 78:3887-3891.

19. Delfino RJ, Staimer N, Gillen D, Tjoa T, Sioutas C, Fung K, et al. 2006. Personal and ambient air pollution is associated with increased exhaled nitric oxide in children with asthma. Environ Health Perspect 114:1736-1743.

20. Delfino RJ, Staimer N, Tjoa T, Gillen D, Kleinman MT, Sioutas C, et al. 2008. Personal and ambient air pollution exposures and lung function decrements in children with asthma. Environ Health Perspect 116:550-558.

21. Devchand PR, Keller H, Peters JM, Vazquez M, Gonzalez FJ, Wahli W. 1996. The pparα–leukotriene b4 pathway to inflammation control. Nature 384:39-43.

22. Durkacz BW, Omidiji O, Gray DA, Shall S. 1980. (adp-ribose) n participates in DNA excision repair. Nature 283:593.

23. Faber J, Brodzik K, Gołda-Kopek A, Łomankiewicz D. 2013. Air pollution in new vehicles as a result of voc emissions from interior materials. Polish Journal of Environmental Studies 22.

24. Ford-Hutchinson A, Bray M, Doig MV, Shipley M, Smith M. 1980. Leukotriene b, a potent chemokinetic and aggregating substance released from polymorphonuclear leukocytes. Nature 286:264-265.

25. Gonzalez FJ. 2005. Role of cytochromes p450 in chemical toxicity and oxidative stress: Studies with cyp2e1. Mutation Research/Fundamental and Molecular Mechanisms of Mutagenesis 569:101-110.

26. Greenbaum D, Shaikh R. 2010. First steps toward multipollutant science for air quality decisions. Epidemiology 21:195-197.

27. Hammarström S. 1983. Leukotrienes. Annual review of biochemistry 52:355-377.

28. Health Effects Institute PotHEoT-RAP. 2010. Traffic-related air pollution: A critical review of the literature on emissions, exposure, and health effects:Health Effects Institute.

29. Henderson WR. 1994. The role of leukotrienes in inflammation. Annals of internal medicine 121:684-697.

30. Hines A, Oladiran GS, Bignell JP, Stentiford GD, Viant MR. 2007. Direct sampling of organisms from the field and knowledge of their phenotype: Key recommendations for environmental metabolomics. Environmental Science & Technology 41:3375-3381.

31. Holguin F, Flores S, Ross Z, Cortez M, Molina M, Molina L, et al. 2007. Traffic-related exposures, airway function, inflammation, and respiratory symptoms in children. American journal of respiratory and critical care medicine 176:1236-1242.

32. Horrobin D. 1992. Nutritional and medical importance of gamma-linolenic acid. Progress in lipid research 31:163-194.

33. Hospers JJ, Postma DS, Rijcken B, Weiss ST, Schouten JP. 2000. Histamine airway hyper-responsiveness and mortality from chronic obstructive pulmonary disease: A cohort study. The Lancet 356:1313-1317.

34. Hüls A, Krämer U, Herder C, Fehsel K, Luckhaus C, Stolz S, et al. 2017. Genetic susceptibility for air pollution-induced airway inflammation in the salia study. Environmental research 152:43-50.

35. Johns DO, Stanek LW, Walker K, Benromdhane S, Hubbell B, Ross M, et al. 2012. Practical advancement of multipollutant scientific and risk assessment approaches for ambient air pollution. Environmental Health Perspectives 120:1238-1242.

36. Johnson CH, Ivanisevic J, Siuzdak G. 2016. Metabolomics: Beyond biomarkers and towards mechanisms. Nature Reviews Molecular Cell Biology 17:451-459.

37. Kelly FJ. 2003. Oxidative stress: Its role in air pollution and adverse health effects. Occupational and environmental medicine 60:612-616.

38. Kim JJ, Smorodinsky S, Lipsett M, Singer BC, Hodgson AT, Ostro B. 2004. Traffic-related air pollution near busy roads: The east bay children's respiratory health study. American journal of respiratory and critical care medicine 170:520-526.

39. Künzli N, Kaiser R, Medina S, Studnicka M, Chanel O, Filliger P, et al. 2000. Public-health impact of outdoor and traffic-related air pollution: A european assessment. The Lancet 356:795-801.

40. Ladva CN, Golan R, Greenwald R, Yu T, Sarnat SE, Flanders WD, et al. 2017. Metabolomic profiles of plasma, exhaled breath condensate, and saliva are correlated with potential for air toxics detection. Journal of breath research 12:016008.

41. Lankadurai BP, Nagato EG, Simpson MJ. 2013. Environmental metabolomics: An emerging approach to study organism responses to environmental stressors. Environmental Reviews 21:180-205.

42. Laumbach RJ, Kipen HM. 2012. Respiratory health effects of air pollution: Update on biomass smoke and traffic pollution. Journal of allergy and clinical immunology 129:3-11.

43. Lee C, Lewis R, Corey E, Austen K. 1983. Conversion of leukotriene d4 to leukotriene e4 by a dipeptidase released from the specific granule of human polymorphonuclear leucocytes. Immunology 48:27.

44. Li H, Cai J, Chen R, Zhao Z, Ying Z, Wang L, et al. 2017. Particulate matter exposure and stress hormone levels: A randomized, double-blind, crossover trial of air purification. Circulation 136:618-627.

45. Li S, Park Y, Duraisingham S, Strobel FH, Khan N, Soltow QA, et al. 2013. Predicting network activity from high throughput metabolomics. PLoS Comput Biol 9:e1003123.

46. Liu MC, Bleecker ER, Lichtenstein LM, Kagey-Sobotka A, Niv Y, McLemore TL, et al. 1990. Evidence for elevated levels of histamine, prostaglandin d2, and other bronchoconstricting prostaglandins in the airways of subjects with mild asthma. American Review of Respiratory Disease 142:126-132.

47. Lodovici M, Bigagli E. 2011. Oxidative stress and air pollution exposure. Journal of toxicology 2011.

48. Mahieu NG, Patti GJ. 2017. Systems-level annotation of a metabolomics data set reduces 25 000 features to fewer than 1000 unique metabolites. Analytical chemistry 89:10397-10406.

49. Mancuso P, Whelan J, DeMichele SJ, Snider CC, Guszcza JA, Claycombe KJ, et al. 1997. Effects of eicosapentaenoic and gamma-linolenic acid on lung permeability and alveolar macrophage eicosanoid synthesis in endotoxic rats. Critical care medicine 25:523-532.

50. Martens DS, Gouveia S, Madhloum N, Janssen BG, Plusquin M, Vanpoucke C, et al. 2017. Neonatal cord blood oxylipins and exposure to particulate matter in the early-life environment: An environage birth cohort study. Environmental health perspectives 125:691.

51. Mauderly JL, Burnett RT, Castillejos M, Ozkaynak H, Samet JM, Stieb DM, et al. 2010. Is the air pollution health research community prepared to support a multipollutant air quality management framework? Inhal Toxicol 22:1-19.

52. McCreanor J, Cullinan P, Nieuwenhuijsen MJ, Stewart-Evans J, Malliarou E, Jarup L, et al. 2007. Respiratory effects of exposure to diesel traffic in persons with asthma. New England Journal of Medicine 357:2348-2358.

53. Menni C, Metrustry SJ, Mohney RP, Beevers S, Barratt B, Spector TD, et al. 2015. Circulating levels of antioxidant vitamins correlate with better lung function and reduced exposure to ambient pollution. American journal of respiratory and critical care medicine 191:1203-1207.

54. Menzel D. 1979. Nutritional needs in environmental intoxication: Vitamin e and air pollution, an example. Environmental health perspectives 29:105.

55. Miller GW, Jones DP. 2014. The nature of nurture: Refining the definition of the exposome. toxicological sciences 137:1-2.

56. Mordukhovich I, Wilker E, Suh H, Wright R, Sparrow D, Vokonas PS, et al. 2009. Black carbon exposure, oxidative stress genes, and blood pressure in a repeated-measures study. Environmental health perspectives 117:1767.

57. Morgan ET. 1997. Regulation of cytochromes p450 during inflammation and infection. Drug metabolism reviews 29:1129-1188.

58. Morrison N, Bearden D, Bundy JG, Collette T, Currie F, Davey MP, et al. 2007. Standard reporting requirements for biological samples in metabolomics experiments: Environmental context. Metabolomics 3:203-210.

59. Nel AE, Diaz-Sanchez D, Li N. 2001. The role of particulate pollutants in pulmonary inflammation and asthma: Evidence for the involvement of organic chemicals and oxidative stress. Current opinion in pulmonary medicine 7:20-26.

60. Nelson DL, Lehninger AL, Cox MM. 2008. Lehninger principles of biochemistry:Macmillan.

61. Niu Y-C, Feng R-N, Hou Y, Li K, Kang Z, Wang J, et al. 2012. Histidine and arginine are associated with inflammation and oxidative stress in obese women. British Journal of Nutrition 108:57-61.

62. North ML, Amatullah H, Khanna N, Urch B, Grasemann H, Silverman F, et al. 2011. Augmentation of arginase 1 expression by exposure to air pollution exacerbates the airways hyperresponsiveness in murine models of asthma. Respiratory research 12:19.

63. Omar NYM, Abas MRB, Rahman NA, Tahir NM, Rushdi AI, Simoneit BR. 2007. Levels and distributions of organic source tracers in air and roadside dust particles of kuala lumpur, malaysia. Environmental Geology 52:1485-1500.

64. Packer L. 1991. Protective role of vitamin e in biological systems. The American journal of clinical nutrition 53:1050S-1055S.

65. Peters A, Von Klot S, Heier M, Trentinaglia I, Hörmann A, Wichmann HE, et al. 2004. Exposure to traffic and the onset of myocardial infarction. New England Journal of Medicine 351:1721-1730.

66. Rabinovitch N, Strand M, Gelfand EW. 2006. Particulate levels are associated with early asthma worsening in children with persistent disease. American journal of respiratory and critical care medicine 173:1098-1105.

67. Rigotti A. 2007. Absorption, transport, and tissue delivery of vitamin e. Molecular aspects of medicine 28:423-436.

68. Sala A, Voelkel N, Maclouf J, Murphy RC. 1990. Leukotriene e4 elimination and metabolism in normal human subjects. Journal of Biological Chemistry 265:21771-21778.

69. Salas A, Panes J, Elizalde J, Granger D, Pique J. 1999. Reperfusion-induced oxidative stress in diabetes: Cellular and enzymatic sources. Journal of leukocyte biology 66:59-66.

70. Salmon JA, Higgs GA. 1987. Prostaglandins and leukotrienes as inflammatory mediators. British medical bulletin 43:285-296.

71. Salvi S. 2007. Health effects of ambient air pollution in children. Paediatric Respiratory Reviews 8:275-280.

72. Sarnat SE, Raysoni AU, Li WW, Holguin F, Johnson BA, Luevano SF, et al. 2012. Air pollution and acute respiratory response in a panel of asthmatic children along the u.S.-mexico border. Environmental Health Perspectives 120:437-444.

73. Silkoff PE, Robbins RA, Gaston B, Lundberg JO, Townley RG. 2000. Endogenous nitric oxide in allergic airway disease. Journal of allergy and clinical immunology 105:438-448.

74. Simon-Manso Y, Lowenthal MS, Kilpatrick LE, Sampson ML, Telu KH, Rudnick PA, et al. 2013. Metabolite profiling of a nist standard reference material for human plasma (srm 1950): Gc-ms, lc-ms, nmr, and clinical laboratory analyses, libraries, and web-based resources. Analytical chemistry 85:11725-11731.

75. Simpson MJ, McKelvie JR. 2009. Environmental metabolomics: New insights into earthworm ecotoxicity and contaminant bioavailability in soil. Analytical and bioanalytical chemistry 394:137-149.

76. Singh U, Devaraj S, Jialal I. 2005. Vitamin e, oxidative stress, and inflammation. Annu Rev Nutr 25:151-174.

77. Solomon PA, Costantini M, Grahame TJ, Gerlofs-Nijland ME, Cassee FR, Russell AG, et al. 2012. Air pollution and health: Bridging the gap from sources to health outcomes: Conference summary. Air Quality Atmosphere and Health 5:9-62.

78. Steiner DR, Gonzalez NC, Wood JG. 2001. Leukotriene b 4 promotes reactive oxidant generation and leukocyte adherence during acute hypoxia. Journal of applied physiology 91:1160-1167.

79. Surowiec I, Karimpour M, Gouveia-Figueira S, Wu J, Unosson J, Bosson JA, et al. 2016. Multi-platform metabolomics assays for human lung lavage fluids in an air pollution exposure study. Analytical and bioanalytical chemistry 408:4751-4764.

80. Szabó C. 1998. Role of poly (adp-ribose) synthetase in inflammation. European journal of pharmacology 350:1-19.

81. Szabó C, Dawson VL. 1998. Role of poly (adp-ribose) synthetase in inflammation and ischaemia–reperfusion. Trends in Pharmacological Sciences 19:287-298.

82. TABOR H. 1954. Metabolic studies on histidine, histamine, and related imidazoles. Pharmacological reviews 6:299-343.

83. Tebani A, Schmitz-Afonso I, Abily-Donval L, Héron B, Piraud M, Ausseil J, et al. 2017. Urinary metabolic phenotyping of mucopolysaccharidosis type i combining untargeted and targeted strategies with data modeling. Clin Chim Acta 475:7-14.

84. Traber MG, Stevens JF. 2011. Vitamins c and e: Beneficial effects from a mechanistic perspective. Free Radical Biology and Medicine 51:1000-1013.

85. Uppal K, Soltow QA, Strobel FH, Pittard WS, Gernert KM, Yu TW, et al. 2013. Xmsanalyzer: Automated pipeline for improved feature detection and downstream analysis of large-scale, non-targeted metabolomics data. Bmc Bioinformatics 14.

86. Vedal S, Kaufman JD. 2011. What does multi-pollutant air pollution research mean? American Journal of Respiratory and Critical Care Medicine 183:4-6.

87. Viant MR. 2008. Recent developments in environmental metabolomics. Mol BioSyst 4:980-986.

88. Vlaanderen J, Janssen N, Hoek G, Keski-Rahkonen P, Barupal D, Cassee F, et al. 2017. The impact of ambient air pollution on the human blood metabolome. Environmental Research 156:341-348.

89. Vossoughi M, Schikowski T, Vierkötter A, Sugiri D, Hoffmann B, Teichert T, et al. 2014. Air pollution and subclinical airway inflammation in the salia cohort study. Immunity & ageing 11:5.

90. Walker D, Go Y, Liu K, Pennell K, Jones D. 2016. Population screening for biological and environmental properties of the human metabolic phenotype: Implications for personalized medicine. Metabolic Phenotyping in Personalized and Public Healthcare Elservier.

91. Wang W, Wu F-Y, Huang M-J, Kang Y, Cheung KC, Wong MH. 2013. Size fraction effect on phthalate esters accumulation, bioaccessibility and in vitro cytotoxicity of indoor/outdoor dust, and risk assessment of human exposure. Journal of hazardous materials 261:753-762.

92. Whitney E, Rolfes SR. 2012. Understanding nutrition:Nelson Education.

93. Yu T, Park Y, Johnson JM, Jones DP. 2009. Aplcms—adaptive processing of high-resolution lc/ms data. Bioinformatics 25:1930-1936.

94. Zmirou D, Gauvin S, Pin I, Momas I, Sahraoui F, Just J, et al. 2004. Traffic related air pollution and incidence of childhood asthma: Results of the vesta case-control study. Journal of Epidemiology and Community Health 58:18-23.

95. Zuurbier M, Hoek G, Oldenwening M, Meliefste K, Krop E, van den Hazel P, et al. 2011. In-traffic air pollution exposure and cc16, blood coagulation, and inflammation markers in healthy adults. Environmental health perspectives 119:1384.

CHAPTER 2 TABLES AND FIGURES

Table 2.1. Traffic pollutant levels and baseline demographic information of the participants in the personal exposure sampling session over the data collection period.

Variable	Overall	Near Dorm	Far Dorm
Traffic Pollutant levels[#]			
BC ($\mu g/m^3$), Mean (SD)	--	0.88 (0.90)	0.78 (0.60)
CO (ppb), Mean (SD)	--	343 (122)	209 (132)
NO (ppb), Mean (SD)	--	15.9 (14.9)	12.2 (16.0)
NO_2 (ppb), Mean (SD)	--	23.3 (9.6)	21.4 (4.7)
NO_x (ppb), Mean (SD)	--	39.2 (22.4)	33.7 (19.3)
$PM_{2.5}$ ($\mu g/m^3$), Mean (SD)	--	11.1 (5.5)	11.0 (5.9)
Demographic Characteristics	n = 51	n = 23	n = 28
Age, Mean (SD)	19.3 (0.9)	19.2 (0.9)	19.4 (0.8)
BMI (SD)	23.3 (3.0)	22.7 (3.1)	23.9 (2.9)
Gender, n (%)			
Female	24 (47)	11 (48)	13 (46)
Male	27 (53)	12 (52)	15 (54)
Academic Year, n (%)			
Freshman	29 (57)	16 (70)	13 (46)
Sophomore	14 (27)	2 (9)	12 (43)
Junior	7 (14)	4 (17)	3 (11)
Senior	1 (2)	1 (4)	0 (0)
Days in Dorm prior to first plasma collection (SD)	69 (119)	86 (161)	55 (67)
Time Spent Outdoors*, n (%)			
Less than 1 hour	4 (8)	2 (9)	2 (7)
1-2 hours	21 (42)	11 (48)	10 (37)
3-4 hours	18 (36)	8 (35)	10 (37)
5 hours or more	7 (14)	2 (8)	5 (19)
Time Spent in Vehicle*, n (%)			
Less than 1 hour	20 (40)	8 (35)	12 (44)
1-2 hours	27 (54)	14 (61)	13 (48)
3-4 hours	2 (4)	1 (4)	1 (4)
5 hours or more	1 (2)	0 (0)	1 (4)

[#]24-hour average outdoor levels

*Daily self reported average of time-activity patterns prior to DRIVE study.

Table 2.2. Number of significant features (FDR_{B-H}<0.05) associated with TRP in multiple biomatrices-technical columns

Biomatrices & Technical Column	Total number of features extracted	BC		CO		NO		NO_2		NO_X		$PM_{2.5}$		Number of unique features*
		Indoor	Outdoor	Indoor	Outdoor	Indoor	Outdoor	Indoor	Outdoor	Indoor	Outdoor	Indoor	Outdoor	
HILIC-Plasma	13,419	182	174	138	143	198	178	153	168	124	132	214	203	847
C18-Plasma	7,347	90	102	76	77	73	83	101	109	88	88	101	119	444
HILIC-Saliva	21,313	312	336	185	186	237	263	235	234	238	246	371	359	1,320
C18-Saliva	7,700	94	102	67	67	70	90	86	77	68	75	99	105	399

* Number of unique metabolic features that were statistically significantly (FDR_{B-H}<0.05) associated with at least one or more TRPs

Acronym: TRP, traffic-related pollutant; FDR_{B-H} , false discover rate correction using the Benjamini-Hochberg procedure ; BC, black carbon; CO, carbon monoxide; NO, nitric oxide; NO_2, nitrogen dioxide; NO_x, nitrogen oxide; $PM_{2.5}$, fine particulate matter.

Table 2.3. Chemical identity of the metabolic features significantly associated with TRP (FDR_{B-H}<0.05) verified by MS/MS in DRIVE study

m/z	RT (s)	MS/MS Match	Adduct Form	Associated TRP	Biomatrix Column
137.0463	44.2	HYPOXANTHINE	M+H[1+]	Indoor: CO (β= 0.007) Outdoor: CO (β= 0.007)	HILIC-Plasma
279.2324	26.0	GAMMA-LINOLENIC ACID	M+H[1+]	Indoor: $PM_{2.5}$ (β= -0.337)	HILIC-Plasma
348.0709	147.6	ADENOSINE 5'-MONOPHOSPHATE	M+H[1+]	Indoor: CO (β= 0.003) NO (β= 0.022) Outdoor: CO (β= 0.003) NO (β= 0.033)	HILIC-Plasma
391.2848	25.5	BIS(2-ETHYLHEXYL)PHTHALATE	M+H[1+]	Indoor: CO (β= 0.001) NO (β= 0.063) Outdoor: BC (β= 0.599) CO (β= 0.006) NO (β= 0.081)	HILIC-Plasma
112.0511	50.0	CYTOSINE	M+H[1+]	Indoor: NO_2 (β= 0.084)	HILIC-Saliva
116.0711	112	L-PROLINE	M+H[1+]	Outdoor: NO_2 (β= -0.093)	HILIC-Saliva
156.0773	98.3-101.0	L-HISTIDINE	M+H[1+]	Outdoor: $PM_{2.5}$ (β= -0.305)	HILIC-Saliva
89.0239	22.2-22.9	(S)-LACTATE GLYCERALDEHYDE	M-H[1-]	Outdoor: $PM_{2.5}$ (β= -0.093)	C18-Plasma
173.1039	23.3	L-ARGININE	M-H[1-]	Indoor: BC (β= -0.615) NO_X (β= -0.024) Outdoor: NO_X (β= -0.027)	C18-Plasma
223.0719	24.6	3-HYDROXYKYNURENINE	M-H[1-]	Outdoor: BC (β= -1.416)	C18-Saliva

Acronym: m/z, mass to charge ratio; RT, retention time; TRP, traffic-related pollutant; BC, black carbon; CO, carbon monoxide; NO, nitric oxide; NO_2, nitrogen dioxide; NO_x, nitrogen oxide; $PM_{2.5}$, fine particulate matter.

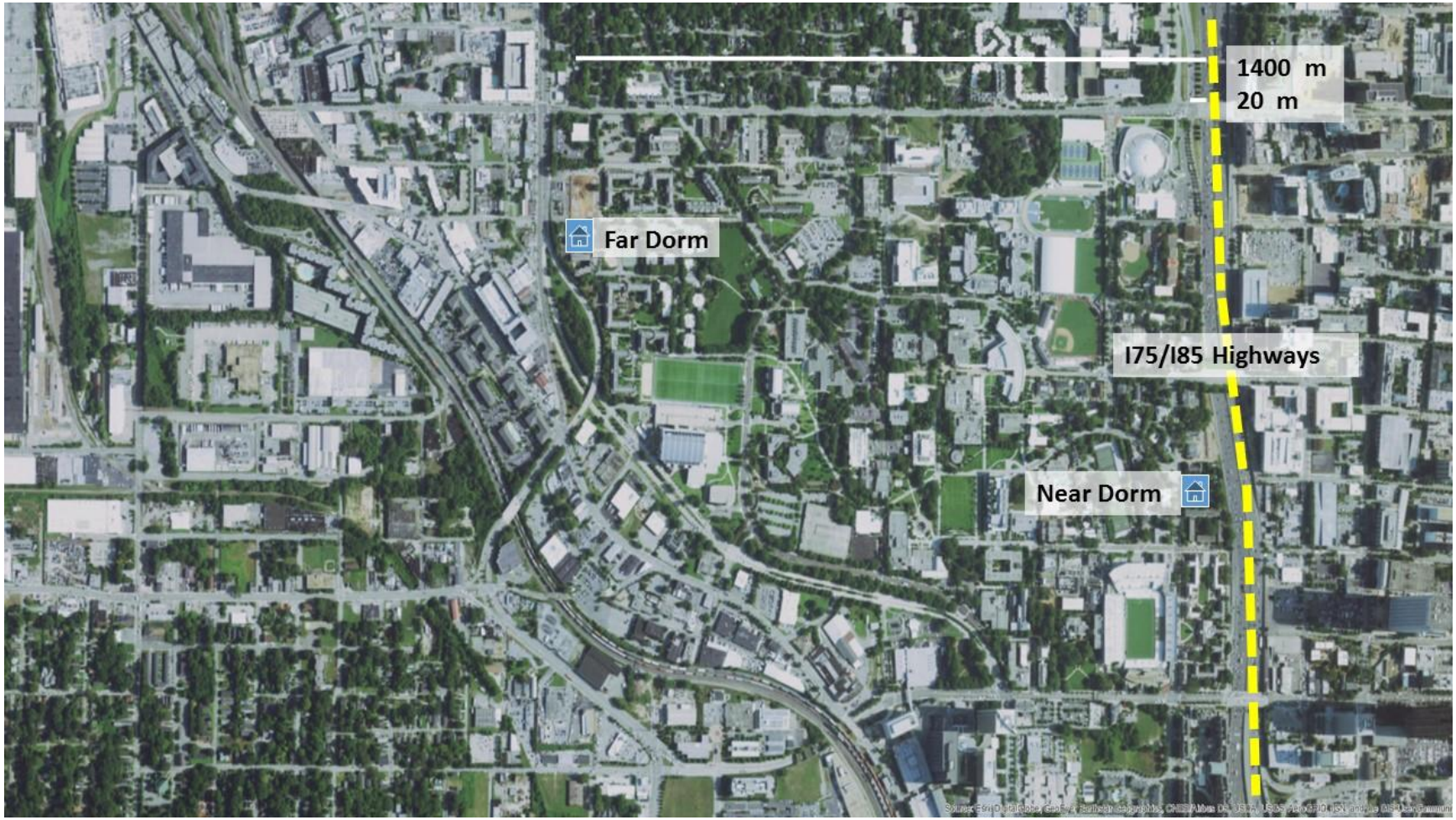

Figure 2.1. DRIVE study location. Yellow dash line denotes the I75/I85 interstate highways. Near Dorm is located only 20 meters away from the highway, while Far Dorm is 1,400 meters away from the highway.

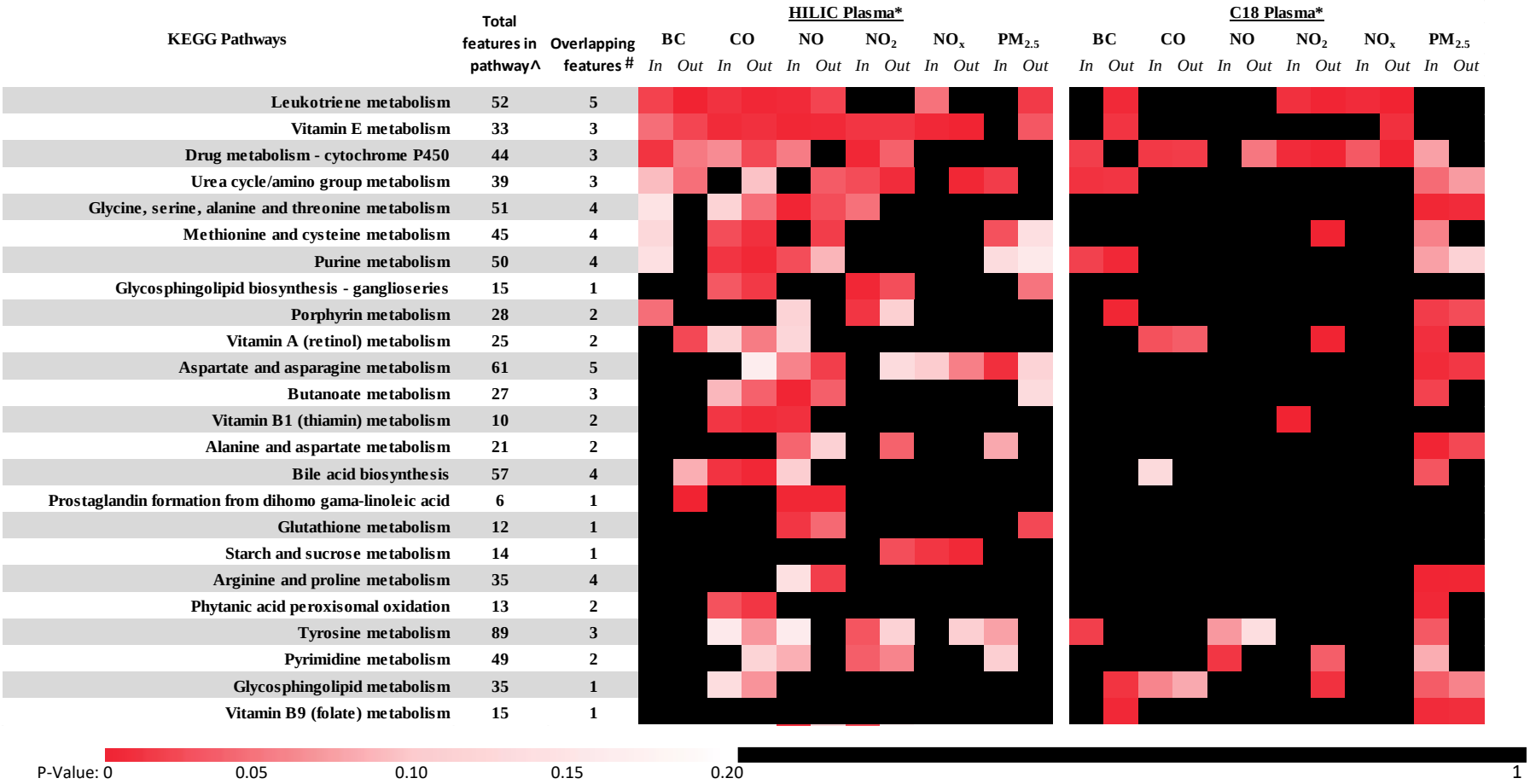

Figure 2.2a. Metabolic pathways associated with ≥ 3 TRP exposure indicators in plasma. Cells were shaded according to the strength (i.e. p-value) of the association between each of metabolic pathways (KEGG) and significant features (FDR_{B-H}<0.05) that were associated with each indoor/outdoor single traffic pollutant indicator. Pathways are ordered according to the total number of the significant pathway-traffic pollutant associations (p<0.05) in the HILIC column (positive ion mode) and the C18 column (negative ion mode).

*For HILIC positive ion mode, only the following adducts were considered: M[1+], M+H[1+], M-H2O+H[1+], M+Na[1+], M+K[1+], M+2H[2+], and M(C13)+2H[2+]
For C18 negative ion mode, only the following adducts were considered: M-H[-], M+Cl[-], M+ACN-H[-], M+HCOO[-], M(C13)-H[-], M-H2O-H[-], and M+Na-2H[-]

^Total number of metabolites within the specific metabolic pathway
#Number of metabolic features in the samples with m/z matched to the metabolites within the specific metabolic pathway

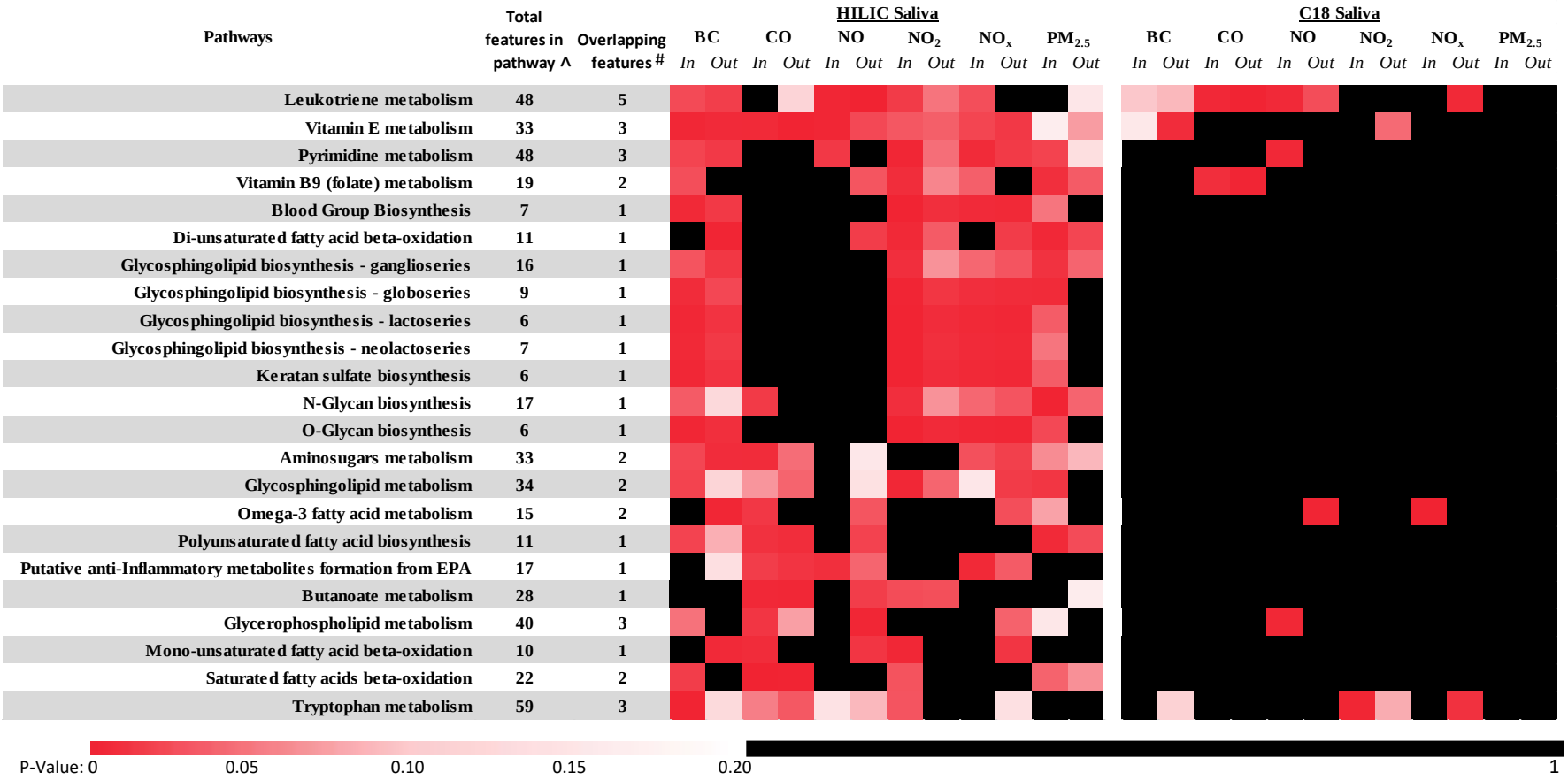

Figure 2.2b. Metabolic pathways associated with ≥ 3 TRP exposure indicators in saliva. Cells were shaded according to the strength (i.e. p-value) of the association between each of metabolic pathways (KEGG) and significant features ($FDR_{B\text{-}H}$<0.05) that were associated with each indoor/outdoor single traffic pollutant indicator. Pathways are ordered according to the total number of the significant pathway-traffic pollutant associations (p<0.05) in the HILIC column (positive ion mode) and the C18 column (negative ion mode).

*For HILIC positive ion mode, only the following adducts were considered: M[1+], M+H[1+], M-H2O+H[1+], M+Na[1+], M+K[1+], M+2H[2+], and M(C13)+2H[2+]
For C18 negative ion mode, only the following adducts were considered: M-H[-], M+Cl[-], M+ACN-H[-], M+HCOO[-], M(C13)-H[-], M-H2O-H[-], and M+Na-2H[-]

^Total number of metabolites within the specific metabolic pathway
#Number of metabolic features in the samples with m/z matched to the metabolites within the specific metabolic pathway

CHAPTER 2 SUPPLEMENTAL MATERIALS

Table S2.1. Mean indoor and outdoor levels of TRPs at Near Dorm and Far Dorm during the study period

Pollutant	Indoor		Outdoor	
	Near Dorm	Far Dorm	Near Dorm	Far Dorm
BC ($\mu g/m^3$)	0.78 ± 0.55	0.61 ± 0.53	0.88 ± 0.90	0.78 ± 0.60
CO (ppb)	321 ± 121	204 ± 128	343 ± 122	209 ± 132
NO (ppb)	7.4 ± 7.9	4.1 ± 11.3	15.9 ± 14.9	12.2 ± 16.0
NO_2 (ppb)	26.8 ± 14.8	26.1 ± 8.2	23.3 ± 9.6	21.4 ± 4.7
NO_x (ppb)	34.1 ± 21.4	30.2 ± 17.3	39.2 ± 22.4	33.7 ± 19.3
$PM_{2.5}$ ($\mu g/m^3$)	8.9 ± 4.7	9.9 ± 5.5	11.1 ± 5.5	11.0 ± 5.9

Acronym: TRP, traffic-related pollutant; BC, black carbon; CO, carbon monoxide; NO, nitric oxide; NO_2, nitrogen dioxide; NO_x, nitrogen oxide; $PM_{2.5}$, fine particulate matter.

Table S2.2a. Tentative match of the plasma metabolic features associated with TRP to the metabolites within Leukotriene pathway using HILIC column with positive ion mode

m/z	RT (s)	Tentative Match	Adduct Form	Associated TRP	Also found in
168.1135	51.6	12-oxo-leukotriene B4 5-oxo-6-trans-leukotriene B4 5-oxo-6E-12-epi- leukotriene B4	M(C13)+2H[2+]	Indoor: CO	C18-Plasma HILIC-Saliva C18-Saliva
336.2319	52.6	Leukotriene B4 5(S)-HPETE 6-trans-leukotriene B4 6E-12-epi- leukotriene B4 20-hydroxy-10,11-dihydro-leukotriene B4 6,7-dihydro-5-oxo-leukotriene B4 6,7-dihydro-5-oxo-12-epi- leukotriene B4 10,11-dihydro-12-oxo- leukotriene B4	M[1+] M+H[1+] M-H2O+H[1+] M+H2O+H[1+]	Indoor: CO, NO, $PM_{2.5}$ Outdoor: BC, CO, $PM_{2.5}$	C18-Saliva
358.2129	46.0	6-trans-leukotriene B4 6E-12-epi-leukotriene B4 6,7-dihydro-5-oxo-leukotriene B4 6,7-dihydro-5-oxo-12-epi-leukotriene B4 10,11-dihydro-12-oxo-leukotriene B4	M+Na[1+]	Outdoor: CO	
360.2246	30.0	10,11-dihydro-leukotriene B4 10,11-dihydro-12-epi-leukotriene B4 6,7-dihydro-12-epi-leukotriene B4 6,7-dihydro-leukotriene B4	M+Na[1+]	Indoor: BC, NO, NO_X Outdoor: BC, NO, NO_X	
388.1831	23.1	12-oxo-20-dihydroxy-leukotriene B4	M+Na[1+]	Indoor: CO Outdoor: CO, NO	
450.1929	160.2	20-carboxy-leukotriene E4	M-H2O+H[1+]	Indoor: BC, NO_2, $PM_{2.5}$ Outdoor: BC, NO_2	

Acronym: m/z, mass to charge ratio; RT, retention time; TRP, traffic-related pollutant; BC, black carbon; CO, carbon monoxide; NO, nitric oxide; NO_2, nitrogen dioxide; NO_x, nitrogen oxide; $PM_{2.5}$, fine particulate matter.

Table S2.2b. Tentative match of the plasma metabolic features associated with TRP to the metabolites within Leukotriene pathway using C18 column with negative ion mode

m/z	RT (s)	Tentative Match	Adduct Form	Associated TRPs	Also found in
336.1519	182.4	omega-carboxy-trinor-leukotriene B4	M(C13)-H[-]	Indoor: CO, NO_2, NO_X Outdoor: CO, NO, NO_2, NO_X	
373.2254	199.6	12-oxo-leukotriene B4 5-oxo-6-trans-leukotriene B4 5-oxo-6E-12-epi-leukotriene B4	M+ACN-H[-]	Outdoor: NO_X ,$PM_{2.5}$	HILIC-Plasma HILIC-Saliva C18-Saliva
382.1413	216.7	12-oxo-20-carboxy-leukotriene B4	M+Na-2H[-]	Outdoor: BC	C18-Saliva
622.2786	195.4	10,11-dihydro-12R-hydroxy-leukotriene C4	M-H2O-H[-]	Indoor: NO_2, NO_X Outdoor: NO_2, NO_X	C18-Saliva
638.2741	204.0	12-oxo-c-leukotriene B3	M-H[-]	Indoor: NO, NO_2, NO_X Outdoor: BC, NO_2, NO_X	HILIC-Saliva

Acronym: m/z, mass to charge ratio; RT, retention time; TRP, traffic-related pollutant; BC, black carbon; CO, carbon monoxide; NO, nitric oxide; NO_2, nitrogen dioxide; NO_x, nitrogen oxide; $PM_{2.5}$, fine particulate matter.

Table S2.2c. Tentative match of the saliva metabolic features associated with TRP to the metabolites within Leukotriene pathway using HILIC column with positive ion mode

m/z	RT (s)	Tentative Match	Adduct Form	Associated TRPs	Also found in
249.1349	95.4	Leukotriene D4	M+2H[2+]	Indoor: BC	
349.2020	172.4	20-oxo-leukotriene B4 12-oxo-20-hydroxy-leukotriene B4 20-carboxy-10,11-dihydro- leukotriene B4	M[1+] M-H2O+H[1+]	Indoor: NO	HILIC-Plasma C18-Plasma C18-Saliva
376.0926	136.7	18,20-dioxo-20-CoA-leukotriene B4	M(C13)+3H[3+]	Indoor: NO, NO_2 Outdoor: NO, NO_2	
440.1751	116.8	18-carboxy-dinor- leukotriene E4	M+H[1+]	Indoor: $PM_{2.5}$	
452.2124	172.9	20-oxo-leukotriene E4	M[1+]	Outdoor: $PM_{2.5}$	
478.2059	137.7	Leukotriene E4	M+K[1+]	Outdoor: NO	
602.1245	198.2	16,18-oxo-18-CoA-dinor- leukotriene E4	M(C13)+2H[2+]	Outdoor: $PM_{2.5}$	
639.2783	23.8	12-oxo-c- leukotriene B3	M[1+]	Indoor: $PM_{2.5}$	C18-Plasma
1229.2781	207.6	CoA-20-carboxy-18-oxo- leukotriene E4 18(R)-hydroxy-20-oxo-20-CoA- leukotriene E4	M(C13)+H[1+] M[1+]	Indoor: NO_X	

Acronym: m/z, mass to charge ratio; RT, retention time; TRP, traffic-related pollutant; BC, black carbon; CO, carbon monoxide; NO, nitric oxide; NO_2, nitrogen dioxide; NO_x, nitrogen oxide; $PM_{2.5}$, fine particulate matter.

Table S2.2d. Tentative match of the saliva metabolic features associated with TRP to the metabolites within Leukotriene pathway using C18 column with negative ion mode

m/z	RT (s)	Tentative Match	Adduct Form	Associated TRPs	Also found in
371.2005	195.0	Leukotriene B4 5(S)-HPETE	M+Cl[-]	Indoor: CO, $PM_{2.5}$ Outdoor: CO	HILIC-Plasma
373.2248	211.3	12-oxo-leukotriene B4 5-oxo-6-trans-leukotriene B4 5-oxo-6E-12-epi-leukotriene B4	M+ACN-H[-]	Indoor: CO Outdoor: CO	HILIC-Plasma C18-Plasma HILIC-Saliva
387.1951	193.3	20-hydroxy-leukotriene B4	M+Cl[-]	Indoor: BC Outdoor: BC	
407.1714	196.7	12-oxo-20-carboxy-leukotriene B4	M+HCOO[-]	Outdoor: $PM_{2.5}$	HILIC-Plasma
661.2647	182.5	10,11-dihydro-12R-hydroxy-leukotriene C4	M+Na-2H[-]	Indoor: BC	C18-Plasma

Acronym: m/z, mass to charge ratio; RT, retention time; TRP, traffic-related pollutant; BC, black carbon; CO, carbon monoxide; NO, nitric oxide; NO_2, nitrogen dioxide; NO_x, nitrogen oxide; $PM_{2.5}$, fine particulate matter.

Table S2.3a. Tentative match of the plasma metabolic features associated with TRP to the metabolites within Vitamin E metabolism using HILIC column with positive ion mode

m/z	RT (s)	Tentative Match	Adduct Form	Associated TRP	Also found in
168.1135	51.6	7'-carboxy-gama-chromanol	M(C13)+2H[2+]	Indoor: CO	C18 Plasma C18 Saliva
348.2264	26.6	7'-carboxy-alpha-chromanol	M+H[1+]	Indoor: CO, NO Outdoor: CO, NO	
413.2673	28.1	11'-carboxy-alpha-tocotrienol	M[1+]	Indoor: NO Outdoor: BC	HILIC Saliva
476.2879	26.0	13'-carboxy-alpha-tocotrienol	M+Na[1+]	Indoor: NO, NO_2, NO_X Outdoor: NO, NO_2, NO_X	

Acronym: m/z, mass to charge ratio; RT, retention time; TRP, traffic-related pollutant; BC, black carbon; CO, carbon monoxide; NO, nitric oxide; NO_2, nitrogen dioxide; NO_x, nitrogen oxide; $PM_{2.5}$, fine particulate matter.

Table S2.3b. Tentative match of the plasma metabolic features significantly associated with TRP (FDR_{B-H}<0.05) to the metabolites within Vitamin E metabolism using C18 column with negative ion mode

m/z	RT (s)	Tentative Match	Adduct Form	Associated TRP	Also found in
373.2254	199.6	7'-carboxy-gama-chromanol	M+ACN-H[-]	Outdoor: NO_X, $PM_{2.5}$	HILIC Plasma C18 Saliva
409.2381	184.9	9'-carboxy-alpha-chromanol	M+Na-2H[-]	Outdoor: BC	C18 Saliva
439.2759	202.1	11'-carboxy-gama-tocotrienol	M+ACN-H[-]	Indoor: NO_X Outdoor: NO_X	

Acronym: m/z, mass to charge ratio; RT, retention time; TRP, traffic-related pollutant; BC, black carbon; CO, carbon monoxide; NO, nitric oxide; NO_2, nitrogen dioxide; NO_x, nitrogen oxide; $PM_{2.5}$, fine particulate matter.

Table S2.3c. Tentative match of the saliva metabolic features significantly associated with TRP (FDR_{B-H}<0.05) to the metabolites within Vitamin E metabolism using HILIC column with positive ion mode

m/z	RT (s)	Tentative Match	Adduct Form	Associated TRP	Also found in
384.1730	50.0	7'-carboxy-alpha-tocotrienol	M+K[1+]	Indoor: BC, $PM_{2.5}$ Outdoor: BC, $PM_{2.5}$	
390.1552	186.5	7'-carboxy-gama-tocotrienol	M+NaCl[1+]	Indoor: $PM_{2.5}$ Outdoor: $PM_{2.5}$	
415.2824	72.4	11'-carboxy-alpha-tocotrienol	M(C13)+H[1+]	Indoor: BC, CO,$PM_{2.5}$ Outdoor: BC, CO, NO, $PM_{2.5}$	HILIC Plasma
462.2761	33.1	13'-carboxy-gama-tocotrienol	M+Na[1+]	Outdoor: $PM_{2.5}$	C18 Saliva

Acronym: m/z, mass to charge ratio; RT, retention time; TRP, traffic-related pollutant; BC, black carbon; CO, carbon monoxide; NO, nitric oxide; NO_2, nitrogen dioxide; NO_x, nitrogen oxide; $PM_{2.5}$, fine particulate matter.

Table S2.3d. Tentative match of the saliva metabolic features significantly associated with TRP (FDR_{B-H}<0.05) to the metabolites within Vitamin E metabolism using C18 column with negative ion mode

m/z	RT (s)	Tentative Match	Adduct Form	Associated TRP	Also found in
373.2248	211.3	7'-carboxy-gama-chromanol	M+ACN-H[-]	Indoor: CO Outdoor: CO	HILIC Plasma C18 Plasma
409.2374	174.5	9'-carboxy-alpha-chromanol	M+Na-2H[-]	Indoor: BC Outdoor: BC	HILIC Plasma
439.3194	250.2	13'-hydroxy-alpha-tocotrienol	M-H[-]	Indoor: BC Outdoor: BC, NO_2	
454.2750	198.6	13'-carboxy-gama-tocotrienol	M-H+O[-]	Indoor: NO, NO_2, NO_X Outdoor: NO, NO_2, NO_X	C18 Plasma
460.2970	203.1	13'-hydroxy-alpha-tocotrienol	M+Na-2H[-]	Outdoor: $PM_{2.5}$	

Acronym: m/z, mass to charge ratio; RT, retention time; TRP, traffic-related pollutant; BC, black carbon; CO, carbon monoxide; NO, nitric oxide; NO_2, nitrogen dioxide; NO_x, nitrogen oxide; $PM_{2.5}$, fine particulate matter.

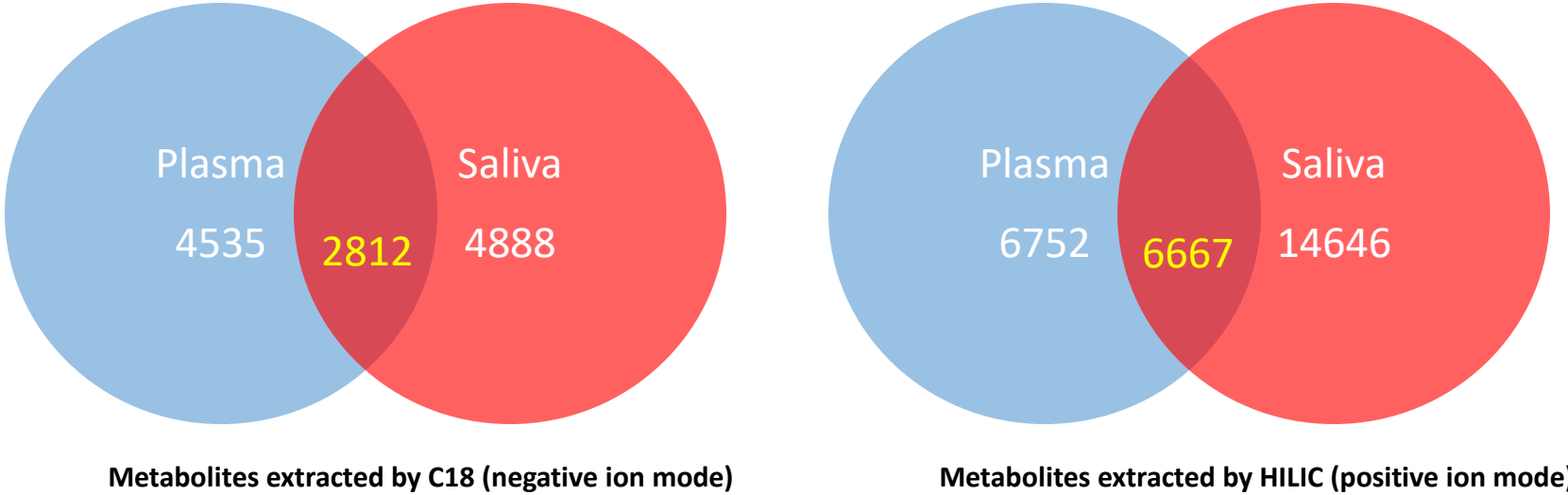

Figure S2.1 Number of features extracted in saliva and plasma samples. 7,347 and 7,700 metabolic features were reliably extracted in plasma and saliva samples respectively using C18 column with negative ion mode, where 2,812 features were detected in both plasma and saliva samples. In HILIC column with positive ion mode, 13,419 and 21,313 metabolic features were reliably extracted, among which 6,667 features were detected in both plasma and saliva samples.

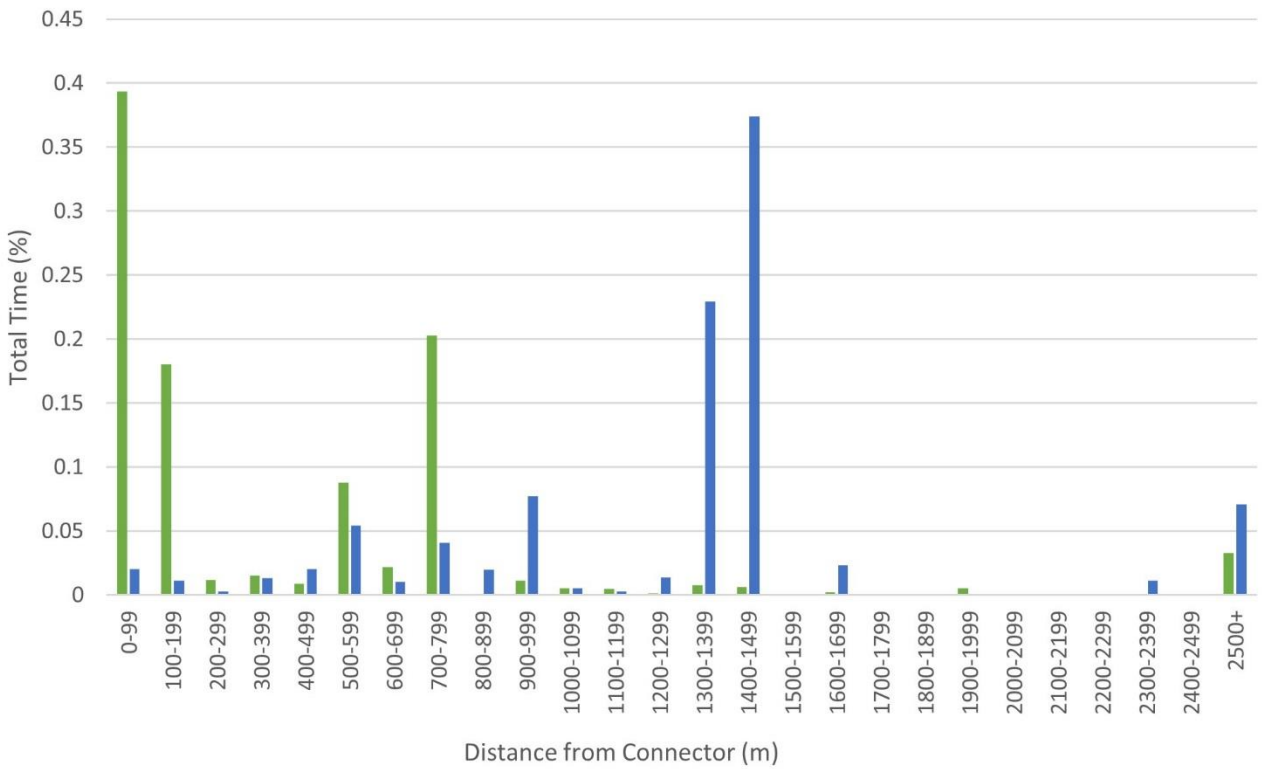

Figure S2.2. Percentage of time spent by linear distance to the highway, by dorm participants. Green bars represent distribution of time among students living in the Near Dorm (20m from the highway); blue bars represent distribution of time among students living in the Far Dorm (1.4 km from the highway).

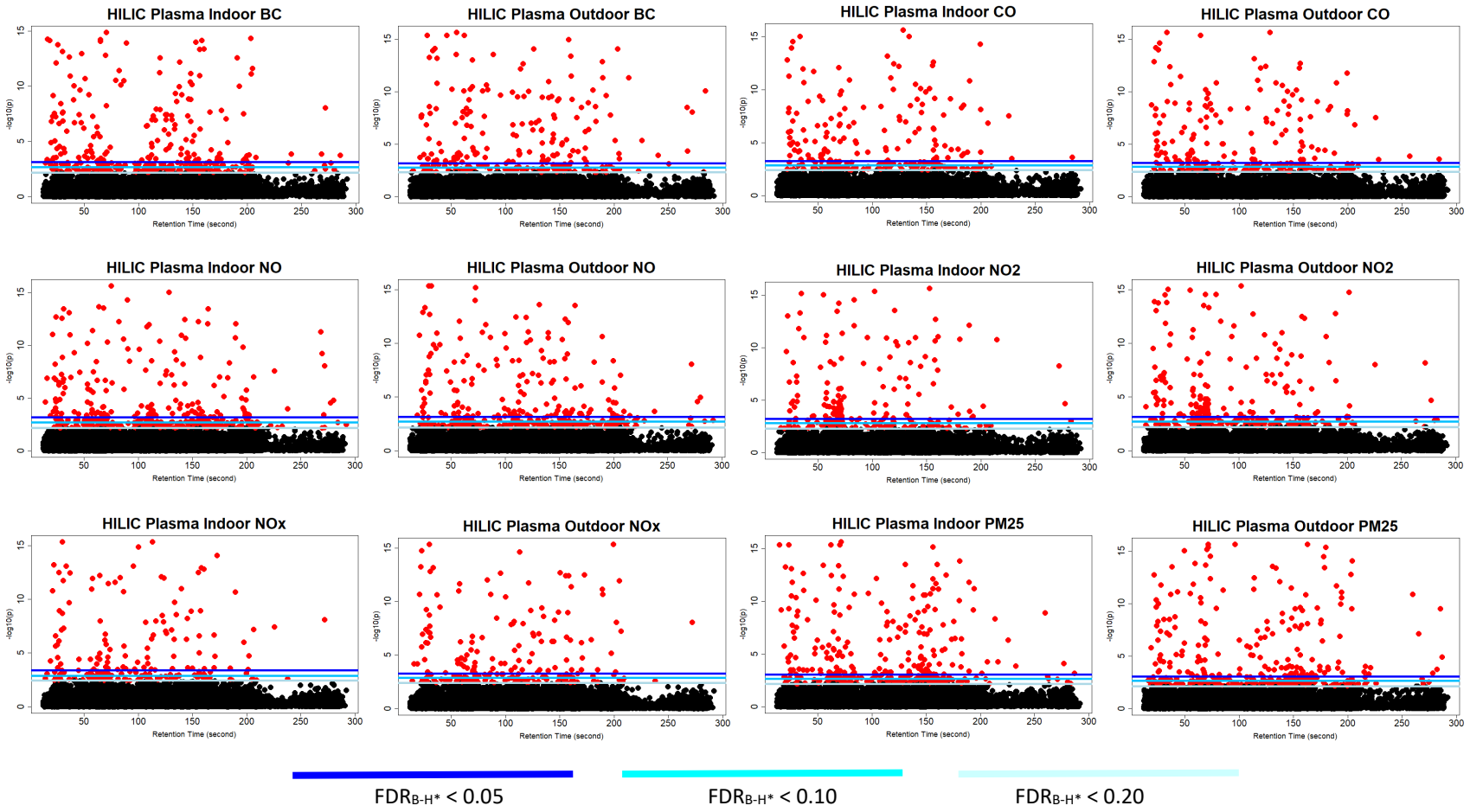

Figure S2.3a. Manhattan plots of associations between changes in plasma feature intensities with level of traffic-related pollutants using the HILIC column with positive ion mode. X-axis denotes the retention time of the metabolic features (in seconds). Y-axis denotes the negative log-10 value of the p-value from the association between intensity of each metabolic feature and level of traffic related air pollutant using the mixed effect model. 847 unique metabolic features were statistically significantly (FDR_{B-H} <0.05) associated with at least one or more TRPs in the plasma samples using the HILIC column with positive ion mode.

* FDR_{B-H}, false discover rate correction using the Benjamini-Hochberg procedure

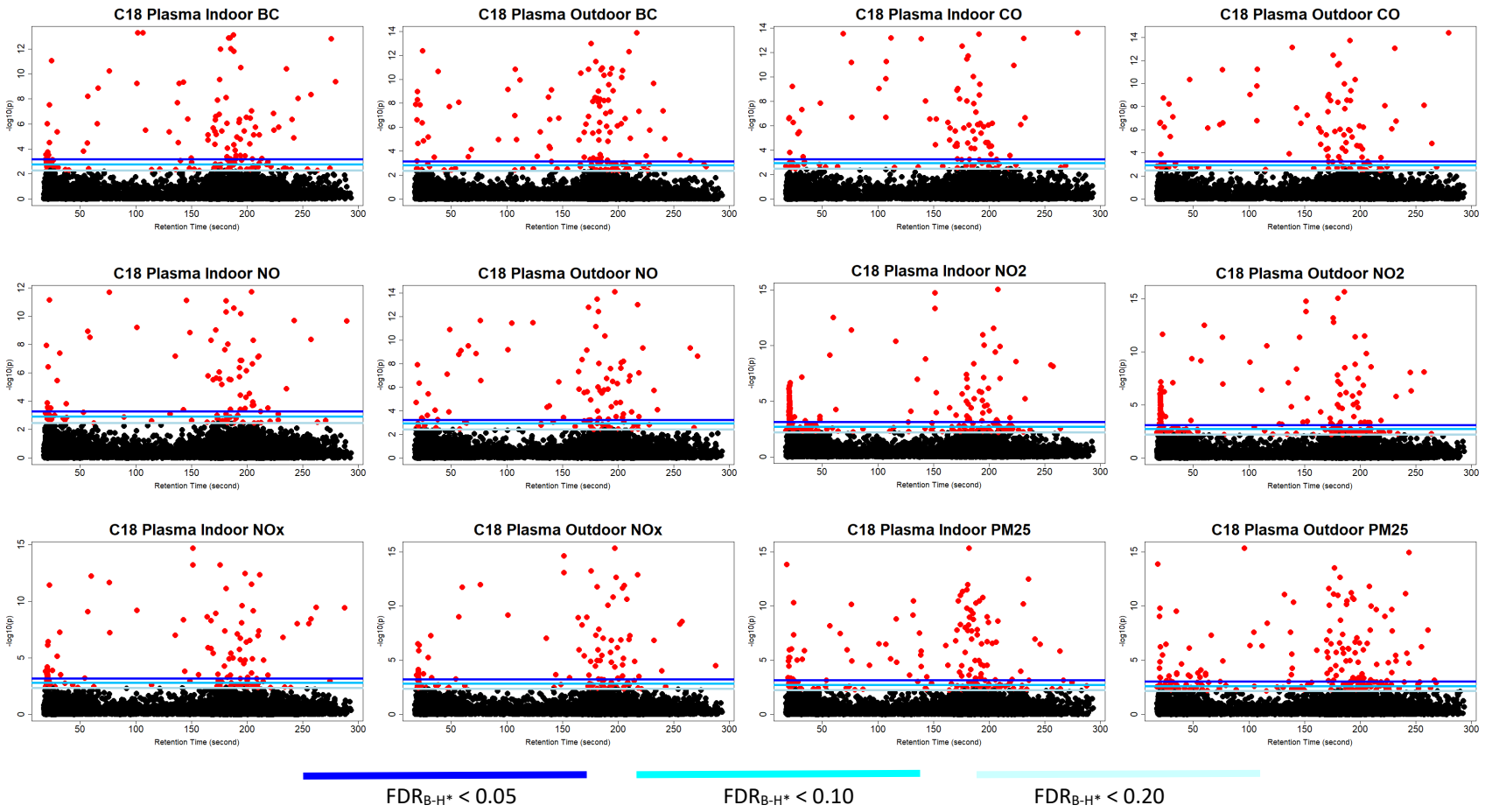

Figure S2.3b. Manhattan plots of associations between changes in plasma feature intensities with level of traffic-related pollutants using the C18 column with negative ion mode. X-axis denotes the retention time of the metabolic features (in seconds). Y-axis denotes the negative log-10 value of the p-value from the association between intensity of each metabolic feature and level of traffic related air pollutant using the mixed effect model. 444 unique metabolic features were statistically significantly (FDR_{B-H} <0.05) associated with at least one or more TRPs in the plasma samples using theC18 column with negative ion mode.

* FDR_{B-H}, false discover rate correction using the Benjamini-Hochberg procedure

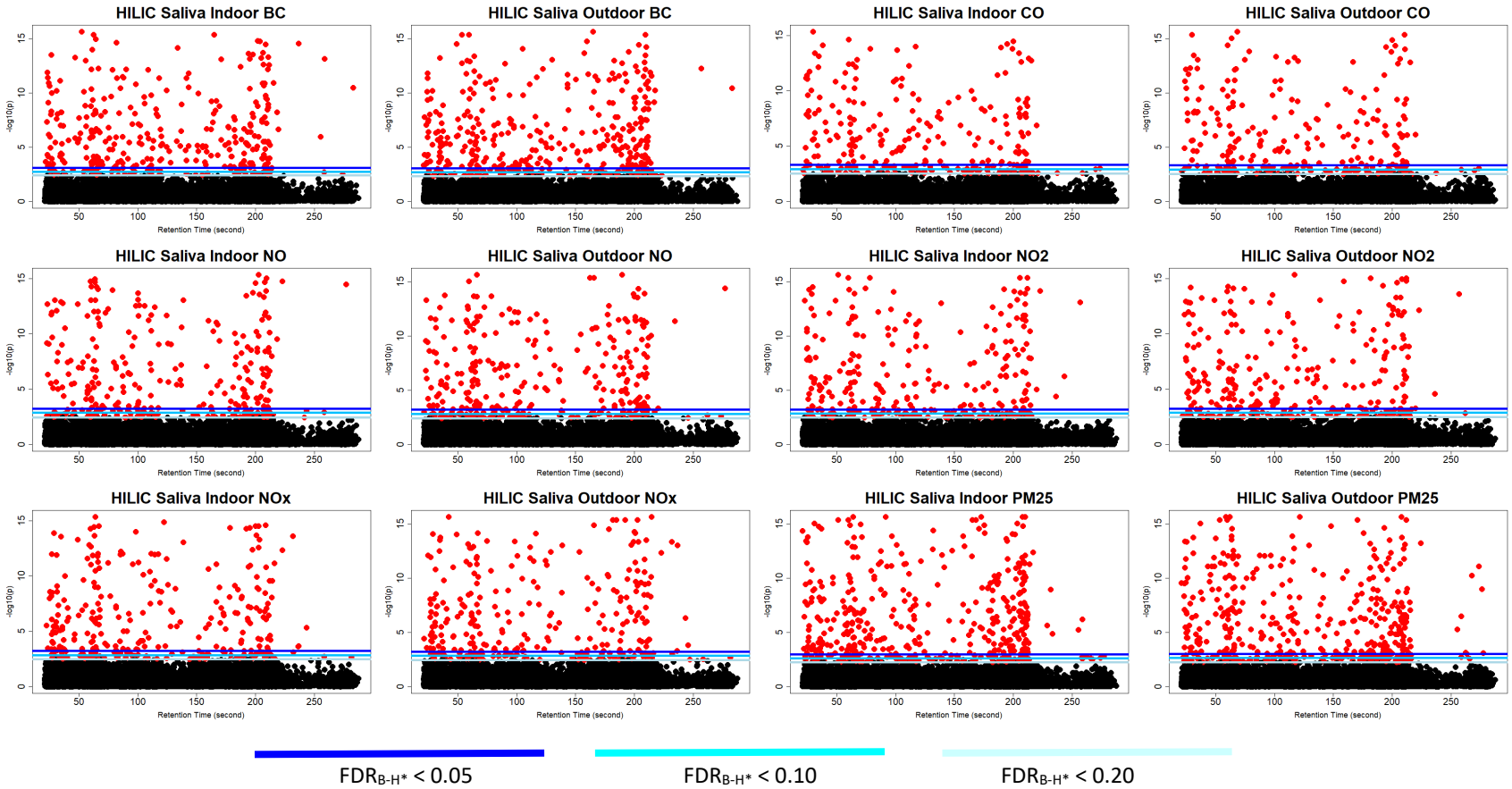

Figure S2.3c. Manhattan plots of associations between changes in saliva feature intensities with level of traffic-related pollutants using the HILIC column with positive ion mode. X-axis denotes the retention time of the metabolic features (in seconds). Y-axis denotes the negative log-10 value of the p-value from the association between intensity of each metabolic feature and level of traffic related air pollutant using the mixed effect model. 1,320 unique metabolic features were statistically ($FDR_{B\text{-}H}$ <0.05) significantly associated with at least one or more TRPs in the saliva samples using the HILIC column with positive ion mode.

* $FDR_{B\text{-}H}$, false discover rate correction using the Benjamini-Hochberg procedure

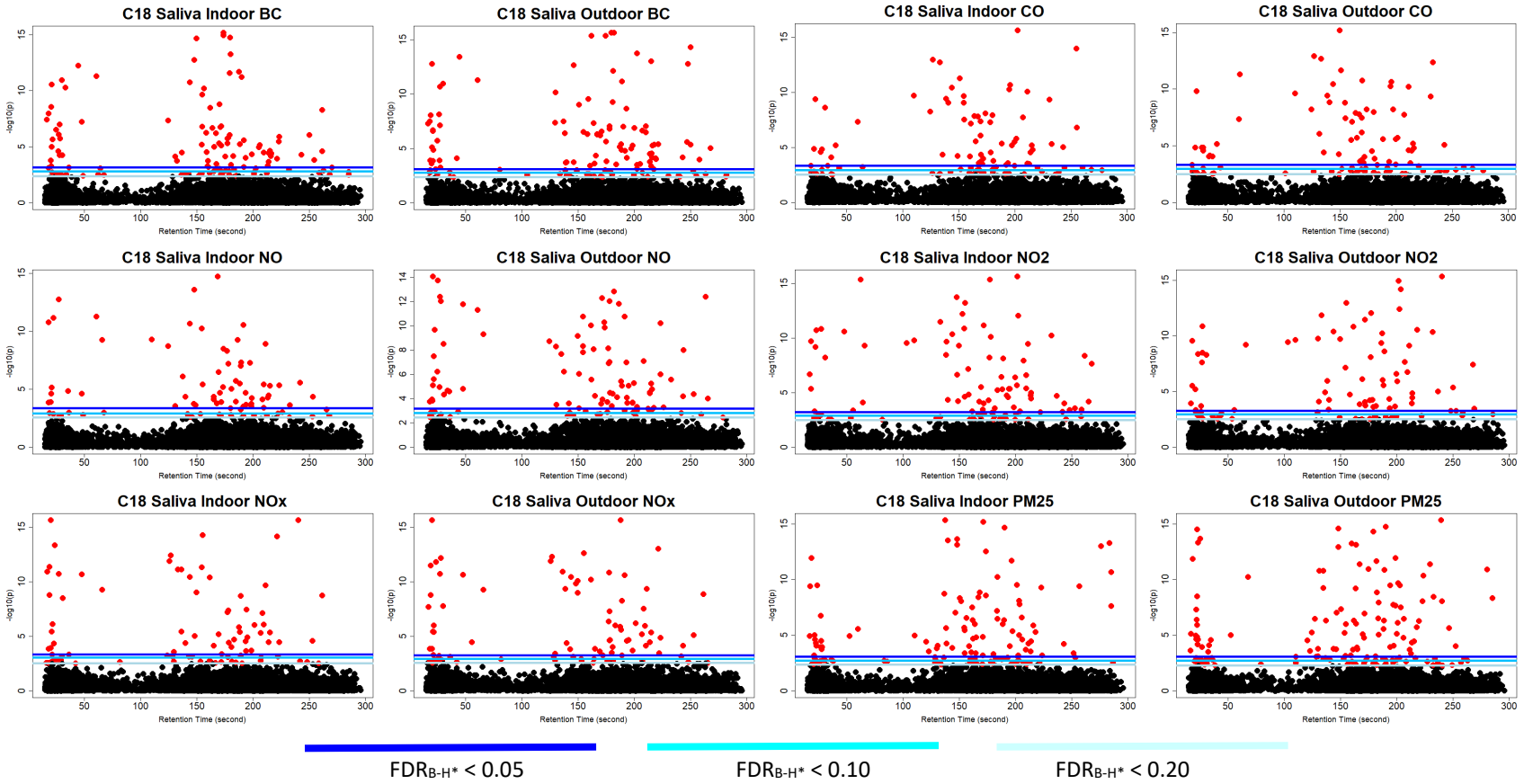

Figure S2.3d. Manhattan plots of associations between changes in saliva feature intensities with level of traffic-related pollutants using the C18 column with negative ion mode. X-axis denotes the retention time of the metabolic features (in seconds). Y-axis denotes the negative log-10 value of the p-value from the association between intensity of each metabolic feature and level of traffic related air pollutant using the mixed effect model. 399 unique metabolic features were statistically (FDR_{B-H} <0.05) significantly associated with at least one or more TRPs in the saliva samples using the C18 column with negative ion mode.

* FDR_{B-H}, false discover rate correction using the Benjamini-Hochberg procedure

CHAPTER 3

Differential Oxidative Stress and Inflammatory Related Acute Metabolic Responses to Traffic-Related Air Pollution in a Panel of Commuters with and without Asthma

Donghai Liang, Chandresh Ladva, Rachel Golan, Tianwei Yu, Stefanie Ebelt Sarnat, Roby Greenwald, Karan Uppal, ViLinh Tran, Che-Jung Chang, Dean Jones, Armistead Russell, Jeremy A. Sarnat

ABSTRACT

Improving exposure assessment to traffic-related air pollution (TRAP) is particularly critical for developing more targeted regulations to better protect public health. Environmental metabolomics has emerged as a promising tool for estimating internal exposure to complex TRAP mixtures. However, considerable questions remain concerning specific metabolites most associated with TRAP, as well as the potential modification of the metabolic responses to TRAP exposure by pre-existing health conditions.

To address these knowledge gaps, we conducted the Atlanta Commuters Exposure (ACE-2) study, a randomized, crossover panel study of asthmatic and healthy commuters, where each participant conducted a scripted highway commute and was randomized to either a scripted side-street commute or clinic exposure session. We measured a suite of 27 pollutants during each exposure session and conducted high-resolution metabolomics profiling on blood samples from the commuters prior to and after each exposure session. We evaluated metabolite and metabolic pathway alternations using an untargeted metabolome-wide association study (MWAS) framework with pathway analyses and chemical annotation.

Most of the measured pollutants were higher during the highway commute compared to the side street commute and clinical session ($p < 0.05$). In total, 17,586 and 9,087 metabolic features were extracted from the plasma samples, in both the negative and positive ionization modes, respectively. 494 and 220 unique metabolic features were associated with at least 3 or more of the 27 pollutants in the negative and positive ionization modes, respectively ($p<0.05$), when controlling for potentially confounding and false discovery. Pathway analysis indicated elicitation of several inflammatory and oxidative stress related metabolic pathways, including leukotriene, vitamin E, cytochrome P450, and tryptophan metabolism. We confirmed the chemical identity of 45 unique metabolites enriched in these metabolic pathways, including inflammatory amino acids such as arginine, histidine, and methionine. Many of these molecules were not only associated with multiple pollutants, but also differentially expressed between asthmatic and healthy participants.

Using a high-resolution environmental metabolomics platform, we observed significant and robust metabolic perturbations associated with numerous TRAP pollutants. We identified xenobiotic-mediated oxidative stress and acute inflammatory response related pathways and metabolites. These results motivate future studies geared towards development of metabolic markers for reflecting TRAP exposures, their corresponding effects, and the asthma etiology.

INTRODUCTION

Traffic related air pollution (TRAP) comprises over 25% of urban fine particulate matter ($PM_{2.5}$) and has been linked to numerous adverse health outcomes, including excess cardiorespiratory mortality, and hospitalizations (Brook et al. 2010; Chen et al. 2008; Health Effects Institute 2010). Although many epidemiologic studies report positive associations between traffic exposures and adverse response, less is known about the specific components of traffic that may be causally responsible for these observations. Thus, improving exposure assessment to TRAP is particularly critical for developing more targeted regulations aimed at reducing the health burden associated with this pollutant source (Health Effects Institute 2010). For primary traffic emission exposures, in particular, an added challenge lies in its chemical and physical heterogeneity, consisting of hundreds of different organic and inorganic components. Moreover, measuring internal, biologically-relevant exposures and corresponding responses is also challenging, due to the lack of sensitive and specific TRAP biomarkers, inter-individual heterogeneity in pharmacokinetics, and the complexity of numerous endogenous pathways that may mediate response.

High-resolution metabolomics, involving the quantitation and identification of thousands of metabolic features associated with exogenous exposure and endogenous processes, has emerged as a powerful tool to improve internal exposure estimation to complex environmental mixtures (Bundy et al. 2009; Lankadurai et al. 2013; Miller and Jones 2014; Simpson and McKelvie 2009; Viant 2008). Previously, we and other groups have demonstrated the capability of environmental metabolomics to capture internal metabolic signals upon exposures to ambient air pollutants (Breitner et al. 2016; Ladva et al. 2017; Martens et al. 2017; Menni et al. 2015; Surowiec et al. 2016; Vlaanderen et al. 2017). Despite this, considerable questions remain concerning specific metabolites and pathways most influenced by TRAP exposures and the adverse responses, as well as the potential modification of metabolic responses to TRAP exposures by pre-existing health conditions.

To address these issues, we leveraged data from an analysis of TRAP exposure and metabolic response from the Atlanta Commuters Exposure (ACE-2) study, a randomized, crossover panel study of asthmatic and healthy commuters. Given their ability to provide accurate assessment of both external exposure and internal response, panel-based studies have proven to be an effective platform to investigate TRAP health effects (Delfino et al. 2006; Delfino et al. 2008; McCreanor et al. 2007; Sarnat et al. 2012). Nevertheless, results from previous targeted, panel-based studies have been inconsistent in identifying specific components of traffic that may be causally responsible for these observations. (Riediker et al. 2004; Zuurbier et al. 2010) and null responses in others (Chiu et al. 2016; Wu et al. 2014). These inconsistencies are perhaps largely due to the lack of robust and specific biomarkers that accurately reflect TRAP exposure or the corresponding effects (Rylance et al. 2013). In previous ACE-2 findings (Ladva et al., 2018), we observed a modest, transient systemic inflammatory and acute respiratory response (using several known traditional biomarkers) following on-road commutes and in association with several common traffic pollutant components. In addition, perturbations of the metabolome were found to be associated with in-vehicle particulate exposure and traditional markers of inflammation. For this analysis, we build on the initial metabolomics analyses of the ACE-2 panel and conducted comprehensive biological pathway analysis and chemical identification, to further understand the metabolic signals most influenced by TRAP. In addition, here we also examine potential modification of metabolic responses to TRAP exposures by asthma status.

METHODS

We conducted the Atlanta Commute Exposure study phase 2 (ACE-2), a randomized, crossover panel study of 60 adults (18-39), asthmatic and healthy, with extensive assessment of in-vehicle environmental exposure and repeated measurements on numerous health endpoints from 2011 to 2013 in Atlanta, GA. The study design, participant demographic characteristics, recruitment and exclusion criteria has been previously detailed (Golan et al. 2017; Krall et al. 2018; Vreeland et al. 2017). Briefly, we randomly

assigned 59 ACE-2 participants to participate in two exposure sessions, exactly 7 days apart, including a highway commute and either a surface street commute or a clinic visit. We conducted each exposure session during the morning rush hour (7 am to 9 am). Specifically, highway commutes took place on Interstate 285 (I-285), a relatively congested highway encircling Atlanta (2016 annual average daily traffic (AADT): 203,000). We conducted the surface street exposure session on side streets within close proximity to Emory University (2016 AADT: 10,400-25,800). The clinic visit sessions was conducted in a dedicated, internal patient examination room within the Emory Environmental Health Laboratory. The highway and surface street commute sessions spanned driving distances of approximately 50 km and 30 km, respectively, with participants driving their personal vehicles, and study staff as passengers. During the clinic visit, participants were seated in the clinic for the duration of the session. The study protocol and all aspects of human subjects' participation were approved and supervised by the Emory University Institutional Review Board.

Exposure Assessment

A detailed description of the ACE-2 sampling methods can be found elsewhere (Golan et al. 2017; Krall et al. 2018; Vreeland et al. 2017). For the current analysis, we selected three groups of source-specific traffic-related air pollutants (TRAPs) a priori based on the source apportionment analyses conducted in a previous publication (Krall et al. 2018), including crustal, primary tailpipe traffic, and non-tailpipe traffic. These souce-specific pollution factors consisted of particle-bound polycyclic aromatic hydrocarbons (pb-PAH), particle number concentration (PNC), fine particulate matter ($PM_{2.5}$), and noise, using both time-integrated and continuous instrumentation. Although noise is not a traditional air pollution indicator, we chose to include it in the analyses given that it has been previously suggested as an independent risk factor and potential confounder of the health effects attributed to traffic emissions (Babisch 2005; Boogaard et al. 2009). In addition, we examined a range of size- and chemically resolved particulate components, including 19 metals that were detected at least 60% of all collected filter samples, as well as black carbon (BC), elemental carbon (EC), organic carbon (OC), and water soluable organic carbon (WSOC).

Biomonitoring and High-Resolution Metabolomics

Among the 59 adults that participated in the scripted commutes, 45 (21 healthy and 24 asthmatic) contributed venous blood prior to and after each sampling session. In total, we collected and analyzed 140 plasma and cell samples (average of 3.1 repeated samples per participant) using established protocols (Go et al. 2015; Ladva et al. 2017). We treated each sample with two volumes of acetonitrile and analyzed in triplicate using liquid chromatography-high-resolution mass spectrometry (LC-HRMS) techniques (Dionex Ultimate 3000; ThermoScientific QExactive). We used C18 hydrophobic reversed-phase chromatography with positive and negative electrospray ionization (ESI) modes, at 70,000 full width at half maximum resolution over a mass-to-charge ratio (m/z) range of 85 to 1250, to enhance the coverage of metabolic feature detection. We applied two quality control pooled reference plasma samples, which included NIST 1950 (Simon-Manso et al. 2013) and pooled human plasma purchased from Equitech Bio, at the beginning and end of each analytical batch of 20 samples for normalization, control of background noise, batch evaluation, and post hoc quantification. Following instrument analyses of all samples, we converted raw data files into .cdf files using ProteoWizard and extracted metabolic signals using apLCMS with modifications by xMSanalyzer with data quality control assessment and batch effect correction (Uppal et al. 2013; Yu et al. 2009). Detected signals ('metabolic features') were uniquely defined by their mass-to-charge ratio (m/z), retention time and ion intensity. For further analyses, we only included metabolic features detected in >20% of all plasma samples, with median coefficients of variation (CV) among technical replicates <30% and Pearson correlation >0.7. Following quality assessment, replicate samples were averaged and averaged intensities were log2 transformed.

Statistical Analysis

We conducted the primary statistical analysis following an untargeted Metabolome-Wide Association Study (MWAS) workflow, where metabolic features were analyzed without prior knowledge of their chemical identity. We conducted linear mixed effect models to assess associations between post minus pre changes in metabolite feature intensity (i.e., relative concentration) and corresponding pollutant

concentrations during the exposure session. The average concentration of each of the traffic metrics, including pbPAH, PNC, $PM_{2.5}$ mass concentration, noise, and 23 speciated particulate components, from each sampling session, was used as the primary exposure metric in single pollutant models. Models testing the main effect for each metric had the following form:

$$\Delta log_2 Y_{ijt} = \mu + \theta_{ij} + \beta_{1\mathrm{j}} Pollutant_{ikt} + \beta_{2\mathrm{j}} Asthma_i + \beta_{3\mathrm{j}} Week_{it} + \beta_{4\mathrm{j}} Age_i + \beta_{5\mathrm{j}} Gender_i + \beta_{6\mathrm{j}} Race_i + \beta_{7\mathrm{j}} BMI_i + \beta_{8\mathrm{j}} Baseline\ log_2 Y_{ijt} + \varepsilon_{ijkt} \quad \text{(Eq. 3.1)}$$

where $\Delta log_2 Y_{ijt}$ refers to the log post- and pre- exposure changes in intensity for metabolic feature j for participant i on sampling date t. Separate models were conducted for each metabolic feature, from each ionization mode (plasma C18 positive ionization column, and plasma C18 negative ionization column). μ is the fixed-effect intercept and a random effect θ_i is included to control for unspecified between-participant heterogeneity. $Pollutant_{ikt}$ refers to the average concentration of the traffic related pollutant k for participant i during the sampling session on sampling date t. $Asthma_i$ refers to whether participant i had self-reported mild-to-moderate asthma or not. We included other covariates to control for potential between-participant differences, including age (continuous), gender (categorical), body mass index (BMI; continuous), and race (categorical, White, Asian, and Other). We also controlled for $Week_{it}$, whether the exposure session corresponded to the first or second week of the commuter's participating the protocol on sampling date t; and $Baseline\ Log_2 Y_{ijt}$, the baseline intensity for metabolic feature j for participant i prior to the commute on sampling date t. ε_{ijkt} represents residual random Normal error.

To further examine potential effect modification of asthma status on the pollutant-metabolic feature associations, we stratified the study population into 1) participants with asthmatic and 2) participants without asthma. The main effects of each of the traffic exposure metrics on the metabolomic profiles for each subgroup were examined using the following model, run for each asthma status subgroup separately:

$$\Delta log_2 Y_{ijt} = \mu + \theta_i + \beta_{1\mathrm{j}} Pollutant_{ikt} + \beta_{2\mathrm{j}} Week_{it} + \beta_{3\mathrm{j}} Age_i + \beta_{4j} Gender_i + \beta_{5j} Race_i + \beta_{6j} BMI_i + \beta_{7j} Baseline\ log_2 Y_{ijt} + \varepsilon_{ijkt} \quad \text{(Eq. 3.2)}$$

Finally, we tested the effect modification by asthmatic status formally, using the model:

$$\Delta log_2 Y_{ijt} = \mu + \theta_{ij} + \beta_{1j} Pollutant_{ikt} + \beta_{2j} Asthma_i + \beta_{3j} Pollutant_{ikt} * Asthma_i + \beta_{4j} Week_{it} + \beta_{5j} Age_i + \beta_{6j} Gender_i + \beta_{7j} Race_i + \beta_{8j} BMI_i + \beta_{9j} Baseline\ log_2 Y_{ijt} + \varepsilon_{ijkt} \quad \text{(Eq. 3.3)}$$

We corrected hypothesis tests to identify differentially expressed features associated with specific traffic-related pollutant levels (by each ionization mode) for multiple comparisons using the Benjamini-Hochberg false discovery rate ($FDR_{B\text{-}H}$) procedure at a 5% false positive (i.e., Type I error) threshold.

Metabolic Pathway Enrichment Analysis and Metabolite Annotation

We used metabolic features that were statistically associated with traffic pollutants to conduct pathway enrichment and metabolite annotation analyses. Pathway identification and module analysis were performed for metabolic features meeting the 5% FDR threshold using mummichog (v. 1.0.5), a bioinformatics platform that infers and categorizes functional biological activity directly from mass spectrometry output, without prior metabolite validation (Amorim et al. 2013 134; Li et al. 2013). We conducted mummichog analyses separately for each set of significant features ($FDR_{BH} < 0.05$) from each of the 27 TRAP-specific linear mixed models, by each ionization mode (i.e., mummichog analyses up to 54 sets of significant features). We selected pathways with adjusted $p < 0.05$ for at least three of the TRAPs models, and with at least four features from the experimental data matched with pathway metabolites. To further minimize the possibility of false positive discovery, we re-run the candidate pathways using a subset of 6 most common forms out of the 16 standard adduct forms in mummichog (For the C18 positive ionization mode, only the following adducts were considered: $M^{[+]}$, $M+H^{[+]}$, $M\text{-}H_2O+H^{[+]}$, $M+Na^{[+]}$, $M+K^{[+]}$, $M+2H^{[2+]}$, and $M(C13)+2H^{[2+]}$; for the C18 negative ionization mode, only the following adducts were considered: $M\text{-}H^{[-]}$, $M+Cl^{[-]}$, $M+ACN\text{-}H^{[-]}$, $M+HCOO^{[-]}$, $M(C13)\text{-}H^{[-]}$, $M\text{-}H_2O\text{-}H^{[-]}$, and $M+Na\text{-}2H^{[-]}$). We presented results in a metabolic-pathway-TRAPs heat map, with each cell of the heat map representing a statistical association between each of the metabolic pathways and each traffic indicator. We compared the

top TRAP pathways in the asthmatic subgroup with the ones in the non-asthma subgroup using a Venn diagram.

We selected the metabolic features that were significantly associated with a TRAP ($FDR_{B-H}<0.05$) in the whole population or in either subgroup, and also significantly enriched in a relevant pathway ($p<0.05$) using mummichog for chemical annotation. Each metabolic feature were annotated by matching mass m/z value for adducts commonly formed to the METLIN (https://metlin.scripps.edu/index.php), ChemSpider (http://www.chemspider.com/), Human Metabolome Database (HMDB), and Kyoto Encyclopedia of Genes and Genomes (KEGG) (http://www.genome.jp/kegg/pathway.html) databases, using a mass error threshold of 10 ppm. We further screened these tentative matches on their retention time, isotope patterns, and peak quality by manually examining the extracted ion chromatograph (EIC). Finally, we confirmed a select number of annotated metabolites by comparison of accurate mass m/z, retention time and ion dissociation patterns to authentic chemical reference standards analyzed using the identical method and instrument parameters via tandem mass spectrometry.

RESULTS

Among the 59 adults who participated in the ACE-2 study, 21 healthy and 24 asthmatic participants provided venous blood specimens prior to and after each sampling session during the study period. We collected 140 plasma and cell samples throughout the study (average of 3.1 repeated samples per participant). As expected, mean levels of pb-PAH, PNC, $PM_{2.5}$, and noise were significantly higher during highway commute sessions as compared to surface street commutes and clinic visits. With the exception of WSOC, mean levels for all organic components of $PM_{2.5}$, along with several metal components, were significantly higher in the highway, indicative of a substantial contrast in the potential exposure level to particulate exposure among the three exposure scenarios ($p <0.05$, Table 3.1). Baseline information obtained from each participant during the study showed generally similar demographic characteristics

among participants with or without asthma, although those with asthma were generally younger than the non-asthmatic participants ($p < 0.05$, Table 3.2).

In total, we extracted 9,087 metabolic features from the positive ionization mode and 17,586 features from the negative ionization mode. The median CV across the triplicate samples for each feature was 23.5% and 25.4% in positive and negative ionization modes, respectively, indicative of good overall data quality. 42% of the extracted ions were found to have m/z matches (< 10 ppm) with metabolites identified in either the Human Metabolome Database (HMDB) or the USEPA's Mobile Air Toxics database.

To test the main effect of pollutant exposure on corresponding metabolic changes, we ran 54 sets of MWAS models (27 individual pollutants of metabolic features in 2 ionization modes). Significant metabolic features among these models ranged from 45 to 576 features ($FDR_{B\text{-}H} < 0.05$, Table S3.1). Specifically, elemental carbon, a traditional maker of diesel vehicles, and vanadium, a metal specie from primary tailpipe according to the source apportionment analyses in ACE-2 study, had the largest number of metabolic associations. In total, 494 and 220 unique metabolic features were associated with at least 3 or more of the 27 pollutants in the negative and positive ionization modes, respectively ($FDR_{B\text{-}H} < 0.05$). We found a similar number of significant features associated with the pollutants in both the asthmatic subgroup and healthy subgroup, 40.1% of which were shared by both subgroup, while 36.6% were observed only in asthmatic subgroup and 23.3% observed only in healthy subgroup. Numerous metabolic features differed significantly by asthma disease status, indicative of effect measure modification. Among the MWAS models, the number metabolic features that were either higher or lower in participants with asthma ranged from 63 to 861 ($FDR_{B\text{-}H} < 0.05$, Table S3.1).

Using mummichog, we further examined whether these significant features associated with TRAPs co-occurred as enriched metabolites within specific known metabolic pathways. In the main effect model (Eq.1), 13 metabolic pathways in negative ionization mode and 10 metabolic pathways in positive ionization mode were significantly associated with at least 20% of all TRAPs in plasma samples (adjusted $p<0.05$, Figure 3.1). Broadly, five pathways consistently appeared to be significantly perturbed across

varying pollutant models, in both ionization modes. These included pathways predominantly associated with xenobiotic-mediated oxidative stress and acute inflammatory response, such as leukotriene metabolism, vitamin E metabolism, cytochrome P450, pyrimidine metabolism, and tryptophan metabolism (Capuron et al. 2011; Chow 1991; Dahlén et al. 1981; Gonzalez 2005; Henderson 1994; Hotamisligil 2006; Mackay et al. 2006; Morgan 1997; Singh et al. 2005; Stoy et al. 2005). The mummichog pathway results were robust to stratification by asthma status (Figure 3.2). Pathways found to be perturbed in the participants with asthma exclusively (N=11), tended to be those heavily related to acute inflammatory processes, including arginine and proline metabolism, as well as the tyrosine metabolism. Similar results were obtained when examining the effect modification of asthmatic status (Eq. 3.3) in modifying the pollutant-metabolome associations, where these oxidative stress or inflammatory responses related pathways again appeared to be the top significant pathways, especially for the primary tailpipe source (Figure 3.3). Based on the strength and consistency of the mummichog results in showing these pollutant-related associations, we focused on annotating constituent metabolic features within these pathways, with the aim of validating the untargeted metabolomic observations.

We screened each of the pollutant-driven metabolic features for spectrum peak quality and purity by manual examination of their respective extracted ion chromatographs (EICs). To reduce the possibility of false positive discovery, we included only spectra with unambiguous EIC peaks (35% and 32% in negative and positive ionization modes, respectively). Finally, we selected those putatively matched features that were both associated with the measured TRAPs and enriched within TRAP exposure-relevant metabolic pathways for chemical identity validation. We matched metabolic feature peaks by accurate mass and retention time to authentic reference standards in an in-house library tandem mass spectrometry run under identical experimental conditions. In total, we confirmed the chemical identity of 26 metabolic features in the negative ionization mode and 24 in the positive ionization mode via MS/MS matching (Table 3.3a and 3.3b, Figure S3.1a and S3.1b). 92% of these verified metabolites were indicative of endogenous metabolic signals related to oxidative stress, inflammatory responses, and nucleic acid damage and repair. For these

50 validated metabolites, we observed consistent significant and negative associations ($\beta < 0$) between anti-inflammatory molecules and corresponding pollutant levels and significant and positive associations ($\beta > 0$) between oxidative or pro-inflammatory metabolites and corresponding pollutant levels (Table 3.3a and 3.3b). Notably, 25 validated metabolites were found exclusively to be associated with pollutant exposure among participants with asthma, while 7 unique metabolites were found among participants without asthma. Specifically, inflammatory and oxidative stress related amino acids, including arginine, histidine, and methionine, were consistently associated with vanadium, elemental carbon, cobalt, and cerium in both negative and positive ionization mode. Several other amino acids related to inflammation and oxidative stress were also identified, including glutamic acid, serine, proline, valine, leucine, lysine, phenylalanine, and tyrosine, each showing biologically plausible strong associations with numerous TRAPs. In addition, we validated a number of intermediate molecules generated from these essential amino acids, some of which were also verified in our recent TRAP metabolomics analyses. These included 3-hydroxykynurenine, hypoxanthine, 5-oxo-proline, and adenosine 5'-monophosphate. Moreover, the direction and strength of these associations differed substantially by asthma status, indicative of the effect modification of asthmatic status on modifying the impact of pollutant exposures on the inflammatory and oxidative stress related metabolic responses (Figure 3.4). Furthermore, these validated metabolites were closely linked and connected in several inflammatory and redox pathways, elucidating the potential molecular mechanisms on traffic-related air pollution toxicity (Figure 3.5).

DISCUSSION

Globally, commuters on average spend approximately one hour and nine minutes within a vehicle each day (Dalia Research et, al. 2017), when concentrations of TRAP frequently exceed ambient levels and represent a large fraction of total daily exposure levels (Adams et al. 2001; Golan et al. 2018; Patton et al. 2016). We examined whether perturbations in the plasma metabolome were detectable following short-term exposures to elevated in-vehicle pollutant levels. To our knowledge, the current analysis is among the

largest prospective longitudinal assessment examining metabolomic changes related to traffic pollution exposures.

A key finding from the current analyses was the identification of several biological pathways which were consistently associated with elevated pollutant levels. These significant pathways were associated with more than 25% of the 27 pollutants across both negative and positive ionization mode, in both the whole panel and in asthma-stratified analyses (Figure 3.1 and Figure 3.2). Many of the identified pathways, including leukotriene, cytochrome P450, vitamin E, tyrosine, methionine, and tryptophan metabolism, are biologically plausible mediators of TRAP-related acute oxidative stress and inflammatory response, which had been closely linked to acute cardiorespiratory responses.

The identification of these specific pollution-mediated pathways mirror results in our and other previous findings (Ladva et al. 2017; Vlaanderen et al. 2017). In a recent analysis of 54 healthy college students living close to a major urban highway (Liang et al. submitted), we identified several oxidative stress and inflammation-related pathways that were significantly associated with TRAP using high-resolution environmental metabolomics, where leukotriene, vitamin E, and cytochrome P450 metabolic pathways showing the strongest associations with multiple TRAP indicators such as BC, NO, and $PM_{2.5}$. Similarly, in a small panel of 31 healthy volunteers exposed to ambient air pollution for 5h, Vlaanderen et al., reported metabolic perturbations within 8 pathways, including tyrosine and tryptophan metabolisms.

The current findings also point to substantial differences in pollutant-metabolic responses by asthma status. In particular, leukotriene metabolism, an active inflammatory mediatory pathway, was consistently the most prominent pathways found among participants showing strongest associations with the main effect for many of the measured TRAPs, and the magnitude of the perturbations differed substantially among asthmatic and healthy participants. As a family of active eicosanoid mediators synthesized from the oxidation of arachidonic acid endogenously, leukotrienes are considered the major cause of inflammation in asthma and allergic rhinitis (Nelson et al. 2008; Salmon and Higgs 1987). In another panel of healthy participants living in close proximity to a major urban roadway (Liang et al. submitted), we demonstrated

that perturbations in leukotriene related metabolites were linked to cumulative exposure to elevated TRAPs, including BC, CO, NO and $PM_{2.5}$. In the current MWAS models, we also observed consistent and robust associations between features putatively matched with leukotriene metabolism and numerous TRAPs, including those from the primary tailpipe (e.g. PAH, BC, and OC), crustal (e.g. Al, Ca and Mg), and non-tailpipe source (e.g. Co, Fe, and Mn). Moreover, the strength and magnitude of the associations between these features and TRAPs significantly differed among asthmatic and healthy participants, indicative of a biologically plausible role of pre-existing condition in modifying the inflammatory responses to TRAPs exposure. Similar pattern of differentiated responses were also observed among putatively matched features enriched in other inflammatory pathways, including arginine, proline, as well as tyrosine metabolism (Figure 3.2 and Figure 3.3).

In addition to inflammation, oxidative stress-related pathways were also shown to be strongly associated with in-vehicle pollution among the ACE-2 participants. Key oxidative stress mediators within these related metabolic pathways included cytochromes P450, terminal oxidase enzymes in electron transfer chains (Gonzalez 2005); vitamin E, a potent fat-soluble antioxidant that protects cells from oxidative damage (Singh et al. 2005); and tryptophan, an α amino acid and essential precursor to the neurotransmitter serotonin and the hormone melatonin (Stoy et al. 2005). Notably these proteins and amino acids have been linked to exposure to air pollution in *in vivo* or *in vitro* models (Kampa and Castanas 2008), including finding where tyrosine and hypoxanthine were found to be associated with short term exposure to air pollutants among healthy volunteers using a similar untargeted high-resolution metabolomics approach (Vlaanderen et al. 2017). In our results, features putatively matched within the tryptophan and vitamin E metabolic pathways showed substantial difference in responses to TRAP exposure among asthmatic participants compared with healthy participants, highlighting a potential mechanistic basis for asthma as a factor enhancing susceptibility to pollutant-mediated oxidative stress response.

Adding to the coherence of the pathway analysis were feature annotation results. Importantly, most of the metabolites we validated were endogenous molecules involved in acute inflammatory response,

oxidative stress, and DNA damage and repair processes. These validated features were prevalent and detectable in most (i.e,. at least 85%) of the biosamples, had triplicate COVs less than 5%, and exhibited relatively pure EIC peaks. Together, these characteristics support their use as potential, sensitive biomarkers of TRAP exposures.

Several amino acids, in particular, showed robust associations with the same suite of TRAPs, including EC, vanadium, and cerium, in both negative and positive ionization mode, with substantially differential responses among asthmatic and healthy participants. Specifically, arginine, an essential α-amino acid related to endothelial function, inflammation, and airway hyperresponsiveness, has been previously reported to be inversely associated with elevated level of air pollution (Silkoff et al. 2000). Here, we also observed consistent negative associations between arginine intensity and concentrations of EC and vanadium. Furthermore, we observed these strength and magnitude of these associations were substantially different among the asthmatic participants and healthy participants, where over 90% of the asthmatic participants had decreased arginine level to elevated vanadium, while opposite trend was observed among healthy participants.

We found similar trends for histidine, another semi-essential amino acid and precursor to histamine (TABOR 1954). Histidine is a well-known inflammatory agent involved in immune responses, including airway hyperresponsiveness (Hospers et al. 2000; Liu et al. 1990). Previously, decreased levels of histidine were found to be significantly associated with inflammation and oxidative stress among groups with pre-existing conditions, such as obesity (Niu et al. 2012). Consistently in our study, we found negative association between histidine and levels of vanadium, specifically among the asthmatic participants, while the responses in histidine were generally positively associated with pollutant concentrations. We also identified methionine in both ionization modes, with differential responses to TRAPs exhibited between asthmatic and healthy participants. Methionine is an essential amino acid that promotes reactive oxygen species (ROS) production endogenously. A recent study has revealed that increased methionine supplementation in diet increases mitochondrial DNA oxidative damage in animal model, indicative of its

hepatotoxicity (Gomez et al. 2009). In ACE-2 asthmatic participants, we observed increased level of methionine associated with elevated cobalt and cerium concentrations during commute.

Aside from these largely endogenous metabolites, we also identified alpha-hydroxyisobutyric acid, a metabolite of exogenous chemical methyl tert-butyl ether (MTBE). MTBE is a gasoline additive commonly used as an oxygenate to raise the octane number. In a Swedish study where four men were exposed to MTBE for 2 hours, metabolites of MTBE were characterized in humans for the first time where analysis of blood and urine samples indicated the presence of MTBE metabolites alpha-hydroxyisobutyric acid (Voelker 1999). In our ACE-2 samples, we observed significant associations between alpha-hydroxyisobutyric acid and five $PM_{2.5}$ metal components, including lead, arsenic, barium, phosphorus, and antimony.

We believe the collective validation of many of these metabolic features using our untargeted metabolomic approach, elucidates a systemic molecular network, of acute traffic-related air pollution toxicity (Figure 3.5). At the center of this network were the perturbations in the arginine metabolism, where in ACE-2 study, elevated TRAP levels may induce augmentation of arginase, leading to increased level of proline and polyamines converted from arginine, resulting in decreased intensities in arginine and its precursors, including citrulline, glutamate, and 5-oxoproline. As reported in numerous *in vitro* and *in vivo* models (Morris et al. 2004; Newaskar et al. 2011; North et al. 2013; Wood et al. 2007), increased levels of proline and polyamines may eventually lead to airway hyperresponsiveness and remodeling, as well as asthma. Meanwhile, we observed increased pollutants associated with decreased intensities of norvaline, a key inhibitor of arginase to correct endothelial dysfunction (Pokrovskiy et al. 2011). Moreover, it is possible that enhanced arginase activity would compete with nitric oxide synthase (NOS) in arginine metabolism (Kim et al. 2009; Xu et al. 2004), leading to reduced bioavailability of endogenously produced nitric oxide. Correspondingly, the amount of creatine produced from arginine, a widely studied anti-oxidant (Guoyao and Morris 1998; Lawler et al. 2002), also decreased.

We believe that a concurrent mechanism, possibly identifiable in our findings, may be that increased ROS and inflammatory mediators (i.e. leukotrienes) induced by TRAP exposure lead to the imbalance of the equilibrated redox environment, contributing to NOS uncoupling and inhibition. The oxidative inactivation on NOS could result in increased bioavailability of nitric oxide and NOS-NO signaling dysregulation (Farah et al. 2018), leading ultimately to multiple adverse health effects including myocardial remodeling (Burger et al. 2009; Saraiva et al. 2005; Yasmin et al. 1997), endothelial dysfunction (Davignon and Ganz 2004; Förstermann et al. 2017), and chronic lung diseases (Grasemann et al. 2011; Holguin 2013; Pifferi et al. 2007). Throughout this process, in-vehicle pollutant exposure might also diminish the antioxidant effect of NOS on xanthine oxidoreductase (XOR) inhibition. XOR catalyzes the oxidation of hypoxanthine to xanthine and the oxidation of xanthine to uric acid, generating potent ROS such as superoxide (Kelley et al. 2010; Vorbach et al. 2003). In homeostatic conditions without abnormal environmental stress, neuronal NOS (nNOS) inhibits XOR to maintain NOS activity (Farah et al. 2018), while the loss of nNOS inhibition of XOR-derived ROS would lead to oxidative-stress-mediated uncoupling of the residual endothelial NOS (eNOS) (Idigo et al. 2012). In our results, we consistently observed elevated TRAP exposure associated with decreased intensities of key components in the XOR pathways, including AMP, hypoxanthine and xanthine. In addition, several precursors of glutathione, an essential antioxidant of preventing damage to important cellular components caused by reactive oxygen species (Ceballos-Picot et al. 1996), were found to decrease as TRAP levels increased in ACE-2 study, including choline, cystine, 5-oxoproline, and glutamate.

Despite these biologically plausible and statistically robust results, specific attention should be given to possible caveats inherent in many omics-based analyses and small panel designs, including our own. In conducting our MWAS modeling, we used each of the 27 TRAP single-pollutant indicators, independently, as surrogates of exposure to primary traffic pollution, a highly heterogeneous mixture. Thus, an observed metabolic perturbation associated with a particular TRAP indicator may not necessarily indicate a causal association between the metabolic feature with that specific modeled indicator. Instead, such change may

be more likely associated with multiple, correlated pollutants within a complex traffic mixture, which is demonstrated by the fact that over 60% of the significant features in the MWAS models were associated with at least three or more individual TRAP indicators. Nevertheless, we did observe that some pollutant were more strongly predictive of metabolic perturbations than the others. Among the validated metabolites, primary tailpipe related TRAP indicators, including EC, particle-bound polycyclic aromatic hydrocarbons, and vanadium. In particular, vanadium, a metal component of $PM_{2.5}$, emitted from fossil fuel combustion and has unknown but potentially adverse health impacts, as well as elemental carbon, a traditional marker of diesel vehicles. Here, we found over 10 inflammatory related amino acids and molecules, including histidine, arginine, and cysteine, showing significant and robust associations with vanadium and elemental carbon among asthmatic participants, indicative the potential role of primary tailpipe exposure in triggering the inflammatory reactions and etiology of asthma.

Additionally, although the demographic characteristics among participants with or without asthma were generally similar, the asthmatic participants were on average 4 years younger than the non-asthmatic participants (Table 3.2), which may contribute to differences in corresponding metabolomic expression, and may have been contributed to some of the observed metabolomic differences in these profiles. To account for these between participant differences, we added terms in the MWAS regression models, including age, gender, BMI, race, and the baseline intensity of each metabolic feature for each participant. In addition, we conducted sensitivity analyses on model specification and inclusion of these covariates, and the results were consistent and robust to model specification and inclusion of these covariates.

It is worth noting that most of the validated metabolites were ubiquitous signals present in at least 85% of the samples, indicating that the observed significant perturbations to TRAP exposure were not necessarily driven by idiosyncratic response among a few individuals. Moreover, these results were generally consistent with the results observed between ACE-2 and another panel TRAP-metabolomics study (Liang et al., submitted) we recently conducted with a similar sample size. Given the highly multidimensional nature of this analysis, there is an inevitable increased risk of false positive discovery (i.e.

Type 1 error) due to the multiple comparisons. Along with using the Benjamini-Hochberg procedure to minimize false positive results, we screened each of the candidate significant features based on the quality and purity of their spectrum peak by manual examination of their respective EICs. For the mummichog pathway analyses, previous studies tend to set significance cut offs at FDR corrected p-values of less than 0.20, and included all 16 ion derivative and adduct forms when matching the unknown features to the existing metabolic databases, thus increasing the risk of false positive discovery (Chandler et al. 2016; Tebani et al. 2017). In contrast, we applied several stringent criteria when conducting mummichog, including excluding model findings with $FDR_{B\text{-}H}$ significance greater 0.05, as well as restricting output to a subset of the six most abundant adducts in each ionization mode.

CONCLUSIONS

Using a high-resolution environmental metabolomics platform, we detected numerous significant metabolic perturbations associated with in-vehicle exposures during commuting. Pathway analyses further elucidated a number of pathways predominantly associated with xenobiotic-mediated oxidative stress and acute inflammatory response, including leukotriene metabolism, vitamin E metabolism, cytochrome P450, pyrimidine metabolism, and tryptophan metabolism. In addition, the features enriched in these pathways responded differentially among asthmatic and healthy participants, indicative of their potential roles in asthma etiology. Our results were broadly consistent with the limited number of similar environmental metabolomics studies. Most interestingly, we were able to identify and validated 45 unique metabolites, many of which were not only significantly associated with multiple TRAP indicators, but also responded differently among participants with and without asthma. These confirmed metabolites were closely linked and connected in several inflammatory and redox pathways, elucidating the potential molecular mechanisms on traffic-related air pollution toxicity. Collectively, the current findings support the potential to develop some of these promising metabolic markers for reflecting TRAP exposures, their corresponding effects, and the asthma etiology.

REFERENCE

1. Adams H, Nieuwenhuijsen M, Colvile R, McMullen M, Khandelwal P. 2001. Fine particle (pm2. 5) personal exposure levels in transport microenvironments, london, uk. Science of the Total Environment 279:29-44.
2. Amorim JH, Rodrigues V, Tavares R, Valente J, Borrego C. 2013. Cfd modelling of the aerodynamic effect of trees on urban air pollution dispersion. Science of the Total Environment 461:541-551.
3. Babisch W. 2005. Traffic, noise and health. In: Environmental health impacts of transport and mobility:Springer, 9-24.
4. Boogaard H, Borgman F, Kamminga J, Hoek G. 2009. Exposure to ultrafine and fine particles and noise during cycling and driving in 11 dutch cities. Atmospheric Environment 43:4234-4242.
5. Breitner S, Schneider A, Devlin RB, Ward-Caviness CK, Diaz-Sanchez D, Neas LM, et al. 2016. Associations among plasma metabolite levels and short-term exposure to pm 2.5 and ozone in a cardiac catheterization cohort. Environment international 97:76-84.
6. Brook RD, Rajagopalan S, Pope CA, Brook JR, Bhatnagar A, Diez-Roux AV, et al. 2010. Particulate matter air pollution and cardiovascular disease: An update to the scientific statement from the american heart association. Circulation 121:2331-2378.
7. Bundy JG, Davey MP, Viant MR. 2009. Environmental metabolomics: A critical review and future perspectives. Metabolomics 5:3-21.
8. Burger DE, Lu X, Lei M, Xiang F-L, Hammoud L, Jiang M, et al. 2009. Neuronal nitric oxide synthase protects against myocardial infarction-induced ventricular arrhythmia and mortality in mice. Circulation 120:1345-1354.
9. Capuron L, Schroecksnadel S, Féart C, Aubert A, Higueret D, Barberger-Gateau P, et al. 2011. Chronic low-grade inflammation in elderly persons is associated with altered tryptophan and tyrosine metabolism: Role in neuropsychiatric symptoms. Biological psychiatry 70:175-182.
10. Ceballos-Picot I, Witko-Sarsat V, Merad-Boudia M, Nguyen AT, Thévenin M, Jaudon MC, et al. 1996. Glutathione antioxidant system as a marker of oxidative stress in chronic renal failure. Free Radical Biology and Medicine 21:845-853.
11. Chen E, Schreier HM, Strunk RC, Brauer M. 2008. Chronic traffic-related air pollution and stress interact to predict biologic and clinical outcomes in asthma. Environmental health perspectives 116:970.
12. Chiu Y-HM, Garshick E, Hart JE, Spiegelman D, Dockery DW, Smith TJ, et al. 2016. Occupational vehicle-related particulate exposure and inflammatory markers in trucking industry workers. Environmental research 148:310-317.
13. Chow CK. 1991. Vitamin e and oxidative stress. Free Radical Biology and Medicine 11:215-232.
14. Dahlén S-E, Björk J, Hedqvist P, Arfors K-E, Hammarström S, Lindgren JA, et al. 1981. Leukotrienes promote plasma leakage and leukocyte adhesion in postcapillary venules: In vivo effects with relevance to the acute inflammatory response. Proceedings of the National Academy of Sciences 78:3887-3891.
15. Davignon J, Ganz P. 2004. Role of endothelial dysfunction in atherosclerosis. Circulation 109:III-27-III-32.
16. Delfino RJ, Staimer N, Gillen D, Tjoa T, Sioutas C, Fung K, et al. 2006. Personal and ambient air pollution is associated with increased exhaled nitric oxide in children with asthma. Environ Health Perspect 114:1736-1743.
17. Delfino RJ, Staimer N, Tjoa T, Gillen D, Kleinman MT, Sioutas C, et al. 2008. Personal and ambient air pollution exposures and lung function decrements in children with asthma. Environ Health Perspect 116:550-558.
18. Farah C, Michel LY, Balligand J-L. 2018. Nitric oxide signalling in cardiovascular health and disease. Nature Reviews Cardiology.

19. Förstermann U, Xia N, Li H. 2017. Roles of vascular oxidative stress and nitric oxide in the pathogenesis of atherosclerosis. Circulation research 120:713-735.
20. Golan R, Ladva C, Greenwald R, Krall JR, Raysoni AU, Kewada P, et al. 2017. Acute pulmonary and inflammatory response in young adults following a scripted car commute. Air Quality, Atmosphere & Health:1-14.
21. Golan R, Ladva C, Greenwald R, Krall JR, Raysoni AU, Kewada P, et al. 2018. Acute pulmonary and inflammatory response in young adults following a scripted car commute. Air Quality, Atmosphere & Health 11:123-136.
22. Gomez J, Caro P, Sanchez I, Naudi A, Jove M, Portero-Otin M, et al. 2009. Effect of methionine dietary supplementation on mitochondrial oxygen radical generation and oxidative DNA damage in rat liver and heart. Journal of bioenergetics and biomembranes 41:309-321.
23. Gonzalez FJ. 2005. Role of cytochromes p450 in chemical toxicity and oxidative stress: Studies with cyp2e1. Mutation Research/Fundamental and Molecular Mechanisms of Mutagenesis 569:101-110.
24. Grasemann H, Al-Saleh S, Scott JA, Shehnaz D, Mehl A, Amin R, et al. 2011. Asymmetric dimethylarginine contributes to airway nitric oxide deficiency in patients with cystic fibrosis. American journal of respiratory and critical care medicine 183:1363-1368.
25. Guoyao W, Morris SM. 1998. Arginine metabolism: Nitric oxide and beyond. Biochemical Journal 336:1-17.
26. Health Effects Institute PotHEoT-RAP. 2010. Traffic-related air pollution: A critical review of the literature on emissions, exposure, and health effects:Health Effects Institute.
27. Henderson WR. 1994. The role of leukotrienes in inflammation. Annals of internal medicine 121:684-697.
28. Holguin F. 2013. Arginine and nitric oxide pathways in obesity-associated asthma. Journal of allergy 2013.
29. Hotamisligil GS. 2006. Inflammation and metabolic disorders. Nature 444:860.
30. Idigo WO, Reilly S, Zhang MH, Zhang YH, Jayaram R, Carnicer R, et al. 2012. Regulation of endothelial nitric-oxide synthase (nos) s-glutathionylation by neuronal nos evidence of a functional interaction between myocardial constitutive nos isoforms. Journal of Biological Chemistry 287:43665-43673.
31. Kampa M, Castanas E. 2008. Human health effects of air pollution. Environmental pollution 151:362-367.
32. Kelley EE, Khoo NK, Hundley NJ, Malik UZ, Freeman BA, Tarpey MM. 2010. Hydrogen peroxide is the major oxidant product of xanthine oxidase. Free Radical Biology and Medicine 48:493-498.
33. Kim JH, Bugaj LJ, Oh YJ, Bivalacqua TJ, Ryoo S, Soucy KG, et al. 2009. Arginase inhibition restores nos coupling and reverses endothelial dysfunction and vascular stiffness in old rats. Journal of applied physiology 107:1249-1257.
34. Krall JR, Ladva CN, Russell AG, Golan R, Peng X, Shi G, et al. 2018. Source-specific pollution exposure and associations with pulmonary response in the atlanta commuters exposure studies. Journal of exposure science & environmental epidemiology:1.
35. Ladva CN, Golan R, Greenwald R, Yu T, Sarnat SE, Flanders WD, et al. 2017. Metabolomic profiles of plasma, exhaled breath condensate, and saliva are correlated with potential for air toxics detection. Journal of breath research 12:016008.
36. Lankadurai BP, Nagato EG, Simpson MJ. 2013. Environmental metabolomics: An emerging approach to study organism responses to environmental stressors. Environmental Reviews 21:180-205.
37. Lawler JM, Barnes WS, Wu G, Song W, Demaree S. 2002. Direct antioxidant properties of creatine. Biochemical and biophysical research communications 290:47-52.
38. Li S, Park Y, Duraisingham S, Strobel FH, Khan N, Soltow QA, et al. 2013. Predicting network activity from high throughput metabolomics. PLoS Comput Biol 9:e1003123.

39. Mackay G, Forrest C, Stoy N, Christofides J, Egerton M, Stone T, et al. 2006. Tryptophan metabolism and oxidative stress in patients with chronic brain injury. European journal of neurology 13:30-42.
40. Martens DS, Gouveia S, Madhloum N, Janssen BG, Plusquin M, Vanpoucke C, et al. 2017. Neonatal cord blood oxylipins and exposure to particulate matter in the early-life environment: An environage birth cohort study. Environmental health perspectives 125:691.
41. McCreanor J, Cullinan P, Nieuwenhuijsen MJ, Stewart-Evans J, Malliarou E, Jarup L, et al. 2007. Respiratory effects of exposure to diesel traffic in persons with asthma. New England Journal of Medicine 357:2348-2358.
42. Menni C, Metrustry SJ, Mohney RP, Beevers S, Barratt B, Spector TD, et al. 2015. Circulating levels of antioxidant vitamins correlate with better lung function and reduced exposure to ambient pollution. American journal of respiratory and critical care medicine 191:1203-1207.
43. Miller GW, Jones DP. 2014. The nature of nurture: Refining the definition of the exposome. toxicological sciences 137:1-2.
44. Morgan ET. 1997. Regulation of cytochromes p450 during inflammation and infection. Drug metabolism reviews 29:1129-1188.
45. Morris CR, Poljakovic M, Lavrisha L, Machado L, Kuypers FA, Morris Jr SM. 2004. Decreased arginine bioavailability and increased serum arginase activity in asthma. American journal of respiratory and critical care medicine 170:148-153.
46. Newaskar M, Hardy KA, Morris CR. 2011. Asthma in sickle cell disease. The Scientific World Journal 11:1138-1152.
47. Niu Y-C, Feng R-N, Hou Y, Li K, Kang Z, Wang J, et al. 2012. Histidine and arginine are associated with inflammation and oxidative stress in obese women. British Journal of Nutrition 108:57-61.
48. North ML, Grasemann H, Khanna N, Inman MD, Gauvreau GM, Scott JA. 2013. Increased ornithine-derived polyamines cause airway hyperresponsiveness in a mouse model of asthma. American journal of respiratory cell and molecular biology 48:694-702.
49. Patton AP, Laumbach R, Ohman-Strickland P, Black K, Alimokhtari S, Lioy PJ, et al. 2016. Scripted drives: A robust protocol for generating exposures to traffic-related air pollution. Atmospheric Environment 143:290-299.
50. Pifferi M, Caramella D, Cangiotti AM, Ragazzo V, Macchia P, Boner AL. 2007. Nasal nitric oxide in atypical primary ciliary dyskinesia. Chest 131:870-873.
51. Pokrovskiy MV, Korokin MV, Tsepeleva SA, Pokrovskaya TG, Gureev VV, Konovalova EA, et al. 2011. Arginase inhibitor in the pharmacological correction of endothelial dysfunction. International journal of hypertension 2011.
52. Riediker M, Cascio WE, Griggs TR, Herbst MC, Bromberg PA, Neas L, et al. 2004. Particulate matter exposure in cars is associated with cardiovascular effects in healthy young men. American journal of respiratory and critical care medicine 169:934-940.
53. Rylance J, Gordon SB, Naeher LP, Patel A, Balmes JR, Adetona O, et al. 2013. Household air pollution: A call for studies into biomarkers of exposure and predictors of respiratory disease. American Journal of Physiology-Lung Cellular and Molecular Physiology 304:L571-L578.
54. Saraiva RM, Minhas KM, Raju SV, Barouch LA, Pitz E, Schuleri KH, et al. 2005. Deficiency of neuronal nitric oxide synthase increases mortality and cardiac remodeling after myocardial infarction: Role of nitroso-redox equilibrium. Circulation 112:3415-3422.
55. Sarnat SE, Raysoni AU, Li WW, Holguin F, Johnson BA, Luevano SF, et al. 2012. Air pollution and acute respiratory response in a panel of asthmatic children along the u.S.-mexico border. Environmental Health Perspectives 120:437-444.
56. Silkoff PE, Robbins RA, Gaston B, Lundberg JO, Townley RG. 2000. Endogenous nitric oxide in allergic airway disease. Journal of allergy and clinical immunology 105:438-448.

57. Simpson MJ, McKelvie JR. 2009. Environmental metabolomics: New insights into earthworm ecotoxicity and contaminant bioavailability in soil. Analytical and bioanalytical chemistry 394:137-149.
58. Singh U, Devaraj S, Jialal I. 2005. Vitamin e, oxidative stress, and inflammation. Annu Rev Nutr 25:151-174.
59. Stoy N, Mackay G, Forrest C, Christofides J, Egerton M, Stone T, et al. 2005. Tryptophan metabolism and oxidative stress in patients with huntington's disease. Journal of neurochemistry 93:611-623.
60. Surowiec I, Karimpour M, Gouveia-Figueira S, Wu J, Unosson J, Bosson JA, et al. 2016. Multi-platform metabolomics assays for human lung lavage fluids in an air pollution exposure study. Analytical and bioanalytical chemistry 408:4751-4764.
61. Viant MR. 2008. Recent developments in environmental metabolomics. Mol BioSyst 4:980-986.
62. Vlaanderen J, Janssen N, Hoek G, Keski-Rahkonen P, Barupal D, Cassee F, et al. 2017. The impact of ambient air pollution on the human blood metabolome. Environmental research 156:341-348.
63. Voelker R. 1999. Fuel additive metabolites probed. JAMA 282:1713-1713.
64. Vorbach C, Harrison R, Capecchi MR. 2003. Xanthine oxidoreductase is central to the evolution and function of the innate immune system. Trends in immunology 24:512-517.
65. Vreeland H, Weber R, Bergin M, Greenwald R, Golan R, Russell AG, et al. 2017. Oxidative potential of pm2. 5 during atlanta rush hour: Measurements of in-vehicle dithiothreitol (dtt) activity. Atmospheric Environment 165:169-178.
66. Wood PL, Khan MA, Moskal JR. 2007. The concept of "aldehyde load" in neurodegenerative mechanisms: Cytotoxicity of the polyamine degradation products hydrogen peroxide, acrolein, 3-aminopropanal, 3-acetamidopropanal and 4-aminobutanal in a retinal ganglion cell line. Brain research 1145:150-156.
67. Wu W, Muller R, Berhane K, Fruin S, Liu F, Jaspers I, et al. 2014. Inflammatory response of monocytes to ambient particles varies by highway proximity. American journal of respiratory cell and molecular biology 51:802-809.
68. Xu W, Kaneko FT, Zheng S, Comhair SA, Janocha AJ, Goggans T, et al. 2004. Increased arginase ii and decreased no synthesis in endothelial cells of patients with pulmonary arterial hypertension. The FASEB journal 18:1746-1748.
69. Yasmin W, Strynadka KD, Schulz R. 1997. Generation of peroxynitrite contributes to ischemia-reperfusion injury in isolated rat hearts. Cardiovascular research 33:422-432.
70. Zuurbier M, Hoek G, Oldenwening M, Lenters V, Meliefste K, van den Hazel P, et al. 2010. Commuters' exposure to particulate matter air pollution is affected by mode of transport, fuel type, and route. Environmental health perspectives 118:783.

CHAPTER 3 TABLES AND FIGURES

Table 3.1. In-vehicle traffic related pollutant levels by commute exposure scenarios

Pollutant	% of Missing	Exposure Scenarios		
		Highway (N=35)	Side Street (N=21)	Clinic (N=14)
Particle Number Counts (#/m^3)*	4%	34800 ± 12900	15300 ± 5980	2440 ± 3800
Noise (Dba)*	8%	68.6 ± 2.7	65.6 ± 1.9	48.2 ± 11.4
pb-PAH (µg/m^3)*	25%	114 ± 30.5	89.8 ± 9.3	11.5 ± 17.9
$PM_{2.5}$ (µg/m^3)*	3%	16.7 ± 6.4	15.5 ± 8.1	4.5 ± 1.5
Organic Components of $PM_{2.5}$ (µg/m^3)				
EC *	24%	2.85 ± 1.21	1.09 ± 0.60	0.21 ± 0.14
OC *	28%	7.66 ± 1.98	7.05 ± 1.45	4.55 ± 0.50
WSOC	37%	8.48 ± 3.75	8.49 ± 4.11	7.04 ± 1.55
BC *	8%	5.57 ± 2.34	2.50 ± 1.31	0.32 ± 0.12
Metal Components of $PM_{2.5}$ (ng/m^3)				
Magnesium (Mg)	22%	8.70 ± 8.02	6.96 ± 5.94	11.7 ± 25.2
Aluminum (Al)	10%	29.4 ± 28.7	28.8 ± 19.4	16.2 ± 18.5
Phosphorus (P)*	9%	3.79 ± 2.91	4.09 ± 2.21	1.82 ± 1.92
Potassium (K)	19%	21.8 ± 18.3	21.1 ± 15.5	9.36 ± 8.12
Calcium (Ca)	17%	41.6 ± 32.6	36.1 ± 28.9	34.7 ± 54.7
Titanium (Ti)	24%	8.41 ± 8.15	9.96 ± 9.65	4.95 ± 4.20
Vanadium (V)*	4%	0.34 ± 0.21	0.28 ± 0.20	0.12 ± 0.14
Chromium (Cr)	40%	1.22 ± 1.09	1.15 ± 0.79	1.08 ± 0.90
Manganese (Mn)	11%	1.50 ± 1.40	1.44 ± 1.01	0.66 ± 0.70
Iron (Fe)*	12%	176 ± 171	159 ± 122	57 ± 69
Cobalt (Co)	20%	0.03 ± 0.02	0.02 ± 0.02	0.02 ± 0.02
Nickle (Ni)	40%	0.57 ± 0.60	0.77 ± 0.78	1.28 ± 1.05
Zinc (Zn)	26%	5.89 ± 3.89	6.37 ± 6.15	4.89 ± 6.50
Arsenic (As)*	4%	0.35 ± 0.22	0.46 ± 0.46	0.12 ± 0.07
Cadmium (Cd)	4%	0.02 ± 0.03	0.03 ± 0.03	0.02 ± 0.02
Antimony (Sb)	6%	2.46 ± 3.39	2.30 ± 2.56	0.72 ± 0.94
Barium (Ba)	12%	18.1 ± 18.1	18.7 ± 22.6	6.1 ± 7.9
Cerium (Ce)	22%	0.16 ± 0.36	0.21 ± 0.53	0.04 ± 0.03
Lead (Pb)*	10%	0.45 ± 0.45	1.21 ± 1.98	0.35 ± 0.39

Acronym: pb-PAH, particle-bound polycyclic aromatic hydrocarbons; $PM_{2.5}$, fine particulate matter; EC, elemental carbon; OC, organic carbon; WSOC, water soluble organic carbon; BC, black carbon. * denotes $p < 0.05$ for Analysis of Variance

Table 3.2: Study Population Demographic Characteristics

	Study population by asthma status	
	Asthmatic (N=24)	Non-asthmatic (N=21)
Age*, Mean ± SD	24.2 ± 4.0	28.4 ± 5.4
Gender, n (%)		
Male	10 (41.7%)	11 (52.4%)
Female	14 (58.3%)	10 (47.6%)
BMI, Mean ± SD	23.2 ± 3.3	23.6 ± 3.7
Race, n (%)		
White	14 (58.3%)	15 (75.0%)
Asian	6 (25.0%)	3 (15.0%)
Other	4 (16.7%)	2 (10.0%)

* denotes $p < 0.05$ for Student's t test or Chi-square test

Table 3.3a. Chemical identity of the metabolic features significantly associated with TRAP (FDR_{B-H}<0.05) in negative ionization mode verified by matching MS/MS verified metabolites library in DRIVE study

m/z	RT (s)	MS/MS Match	Population	Pathway	Associated TRP
103.0385	82.8	alpha-hydroxyisobutyric acid	asthmatic	propanoate metabolism	As (β= -1.14); Ba (β= -0.07); P (β= -0.12); Pb (β= -0.91); Sb (β= -0.47)
109.0280	90.8	Catechol	all	PAH degradation; dioxin degradation	EC (β= 0.07); Co (β= 35.5); K (β= 0.06); P (β= 0.12); Zn (β= 0.12)
115.0021	78.7	maleic acid fumarate	all	tyrosine metabolism; arginine biosynthesis; oxidative phosphorylation	OC (β= 0.46); Co (β= 12.3); K (β= 0.01); Zn (β= 0.05)
128.0339	85.6	5-oxo-proline	all	glutathione metabolism; d-glutamine and d-glutamate metabolism	Ni (β= -0.22); As (β= -0.64); Zn (β= -0.13); Ba (β= -0.07); OC (β= -0.15); $PM_{2.5}$ (β= -0.04)
129.0542	105.8	4-methyl-2-oxopentanoic acid 3-methyl-2-oxopentanoic acid	all	valine, leucine and isoleucine degradation; glucosinolate biosynthesis	Ce (β= 0.37); Cr (β= 0.11)
130.0859	94.5	Leucine	asthmatic	valine, leucine and isoleucine degradation	OC (β= -0.24)
131.0448	135.6	3-ureidopropionate	asthmatic	pyrimidine metabolism	EC (β= -0.74); V (β= -0.98)
146.0446	114.1	glutamic acid n-methyl-d-aspartic acid	all	glutathione metabolism; d-glutamine and d-glutamate metabolism	EC (β= -0.51); OC (β= -0.26); CPC (β= -0.05)
148.0425	92.8	Methionine	all	cysteine and methionine metabolism glucosinolate biosynthesis	Ce (β= 0.44); EC (β= 0.08)
151.0250	89.6	Xanthine	asthmatic	purine metabolism	EC (β= -1.26)
153.0180	88.2	dihydroxybenzoic acids	all	benzoate degradation; phenylalanine, tyrosine and tryptophan biosynthesis	EC (β= -0.38); CO (β= -5.18);
154.0609	112.1	Histidine	asthmatic	histidine metabolism	EC (β= -0.73); V (β= -0.65)
155.0105	69.0	Orotate	asthmatic	pyrimidine metabolism	V (β= -1.18)
161.0443	110.0	3-hydroxy-3-methylglutarate	asthmatic	leucine degration	EC (β= -0.71)
165.0546	83.4	3-2-hydroxyphenyl-propanoate	asthmatic	phenylalanine metabolism; polycyclic aromatic hydrocarbon degradation	PAH (β= -0.01)
167.0199	76.2	Urate	asthmatic	purine metabolism	EC (β= -0.22)
173.1031	145.2	Arginine	asthmatic	arginine and proline metabolism	EC (β= -0.91); V (β= -0.81)
175.0237	81.4	ascorbate d-glucuronolactone	healthy	ascorbate and aldarate metabolism; glutathione metabolism	P (β= -0.16)
180.0655	88.0	Tyrosine	asthmatic	tyrosine metabolism	Co (β= 5.60); EC (β= -1.30, 0.27)
187.1329	92.1	10-hydroxydecanoate	healthy	saturated fatty acids metabolism	Ni (β= -0.25)
209.0294	161.3	d-saccharic acid galactarate	asthmatic	ascorbate and aldarate metabolism	PAH (β= -0.01); EC (β= -0.49)
223.0739	78.5	3-hydroxykynurenine	healthy	tryptophan metabolism	Cr (β= 0.41)
327.2331	564.5	docosahexaenoic acid	asthmatic	biosynthesis of unsaturated fatty acids	Zn (β= -0.24)
346.0554	147.2	adenosine 5'-monophosphate	all	purine metabolism	Co (β= -18.0); WSOC (β= -1.39)

391.2849	104.8	chenodeoxycholate deoxycholate	all	bile acid biosynthesis; bile secretion	EC (β= 0.15); Al (β= 0.01); K (β= 0.02)
464.3014	85.2	glycocholate	asthmatic	bile acid biosynthesis; bile secretion	PAH (β= -0.02); Ce (β= -0.85)

Acronym: m/z, mass to charge ratio; RT, retention time; TRAP, traffic-related air pollutant; pb-PAH, particile-bound polycyclic aromatic hydrocarbons; EC, elemental carbon; OC, organic carbon; WSOC, water soluble organic carbon; BC, black carbon; BC, black carbon; Mg, magnesium; Al, aluminium; P, phosphorus; K, potassium; Ca, calcium; Ti, titanium; V, vanadium; Cr, chromium; Mn, manganese; Fe, iron; Co, cobalt; Ni, nickle; Zn, zinc; As, arsenic; Cd, cadmium; Sb, antimony; Ba, barium; Ce, cerium; Pb, lead.

Table 3.3b. Chemical identity of the metabolic features significantly associated with TRAP (FDR_{B-H}<0.05) in positive ionization mode verified by matching MS/MS verified metabolites library in DRIVE study

m/z	RT (s)	MS/MS Match	Population	Pathway	Associated TRP
94.0655	447.4	aniline	all	aminobenzoate degradation	Ce (β= -0.29);
96.0447	427.0	2-hydroxypyridine	all	nicotinate and nicotinamide metabolism	Co (β= 6.96); Zn (β= 0.04)
104.1073	76.4	choline	all	glycine, serine and threonine metabolism glycerophospholipid metabolism	V (β= -0.58); Ce (β= -0.44); EC (β= -0.08); Ni (β= -0.29)
105.0654	71.0	2,3-diaminopropionic acid	healthy	d-glutamine and d-glutamate metabolism	Cr (β= 0.07); WSOC (β= 0.06)
106.0501	118.9	serine	asthmatic	glycine, serine and threonine metabolism	EC (β= -0.88); V (β= -0.74)
114.0664	84.0	creatinine	asthmatic	arginine and proline metabolism	EC (β= 0.32)
116.0708	63.5	proline	asthmatic	arginine and proline metabolism	EC (β= 0.45)
118.0863	95.1	valine norvaline	all	valine, leucine and isoleucine degradation arginine and proline metabolism	Ce (β= -0.32); EC (β= -0.88)
132.0767	104.0	creatine	asthmatic	arginine and proline metabolism	EC (β= -1.10)
132.1018	71.1	leucine	asthmatic	valine, leucine and isoleucine degradation	Ni (β= 0.29)
137.0456	83.6	hypoxanthine	asthmatic	purine metabolism	Ba (β= -0.07); Cd (β= -297.9); Mn (β= -0.51); P (β= -0.19); $PM_{2.5}$ (β= -0.06); Sb (β= -0.55)
142.0264	139.2	ethanolamine phosphate phosphorylcolamine	all	glycerophospholipid metabolism sphingolipid metabolism	CPC (β= 0.03); WSOC (β= -0.37); As (β= -1.05);
144.0807	88.9	naphthylamine	all	xenobiotics by cytochrome p450	OC (β= -0.07); Ce (β= -0.37)
147.1127	78.7	lysine	asthmatic	lysine biosynthesis and degradation	EC (β= -0.73); V (β= -1.14)
148.0603	120.4	glutamic acid methyl-d-aspartic acid	healthy	glutathione metabolism; d-glutamine and d-glutamate metabolism	CPC (β= -0.04)
150.0582	111.2	methionine	asthmatic	cysteine and methionine metabolism	Co (β= 6.11)
154.0498	131.0	3-hydroxyanthranilate 3-amino-4-hydroxybenzoic acid 3-amino-5-hydroxybenzoic acid	all	tryptophan metabolism; aminobenzoate degradation	PAH (β= 0.03); CPC (β= 0.04); $PM_{2.5}$ (β= 0.09); Cr (β= 0.91)
156.0766	111.5	histidine	asthmatic	histidine metabolism	V (β= -1.06)
166.0861	84.5	phenylalanine	healthy	phenylalanine, tyrosine and tryptophan biosynthesis	Al (β= -0.01); Ce (β= -0.38); Co (β= -5.33); Mg (β= -0.02); Mn (β= -0.11)
171.0054	107.9	glyceraldehyde 3-phosphate diethyl acetal	all	fermentation and glycolysis of carbohydrates	EC (β= 0.31); Pb (β= 0.16)
175.1188	130.4	arginine	asthmatic	arginine and proline metabolism	EC (β= -1.13); V (β= -0.97)
176.1028	96.1	citrulline	asthmatic	arginine biosynthesis	EC (β= -1.07)
204.1229	78.4	o-acetyl-l-carnitine	healthy	insulin resistance	Zn (β= -0.02)
241.0309	130.7	gluconic acid cystine	all	pentose phosphate pathway cysteine and methionine metabolism	V (β= -0.57)

Acronym: m/z, mass to charge ratio; RT, retention time; TRAP, traffic-related air pollutant; pb-PAH, particile-bound polycyclic aromatic hydrocarbons; EC, elemental carbon; OC, organic carbon; WSOC, water soluble organic carbon; BC, black carbon; BC, black carbon; Mg, magnesium; Al, aluminium; P, phosphorus; K, potassium; Ca, calcium; Ti, titanium; V, vanadium; Cr, chromium; Mn, manganese; Fe, iron; Co, cobalt; Ni, nickle; Zn, zinc; As, arsenic; Cd, cadmium; Sb, antimony; Ba, barium; Ce, cerium; Pb, lead.

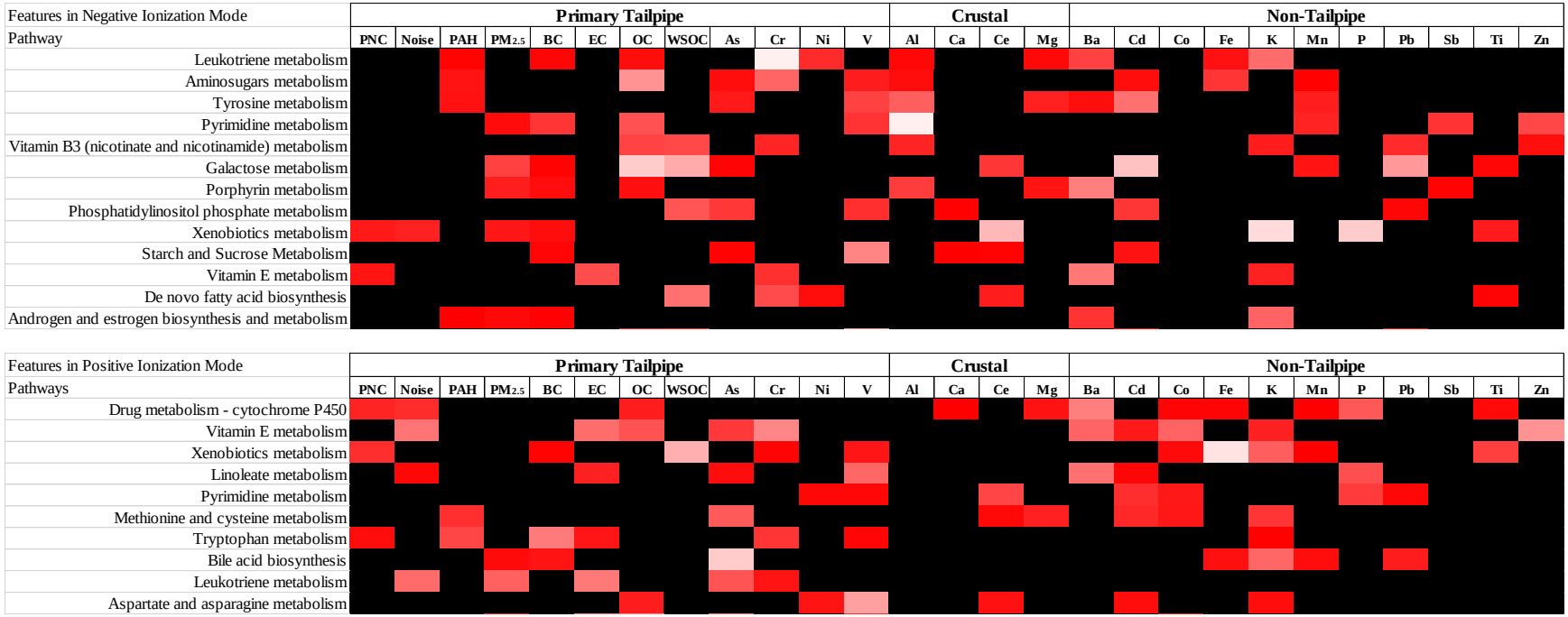

Figure 3.1 Metabolic pathways associated with ≥ 5 TRAP exposure indicators in all ACE-2 participants. Cells were shaded according to the strength (i.e. p-value) of the association between each of metabolic pathways (KEGG) and significant features ($FDR_{B\text{-}H}<0.05$) that were associated with each single traffic pollutant indicator. Pathways are ordered according to the total number of the significant pathway-traffic pollutant associations ($p<0.05$) in the C18 column negative ionization mode and positive ionization mode.

*For HILIC positive ion mode, only the following adducts were considered: M[1+], M+H[1+], M-H2O+H[1+], M+Na[1+], M+K[1+], M+2H[2+], and M(C13)+2H[2+]
For C18 negative ion mode, only the following adducts were considered: M-H[-], M+Cl[-], M+ACN-H[-], M+HCOO[-], M(C13)-H[-], M-H2O-H[-], and M+Na-2H[-]

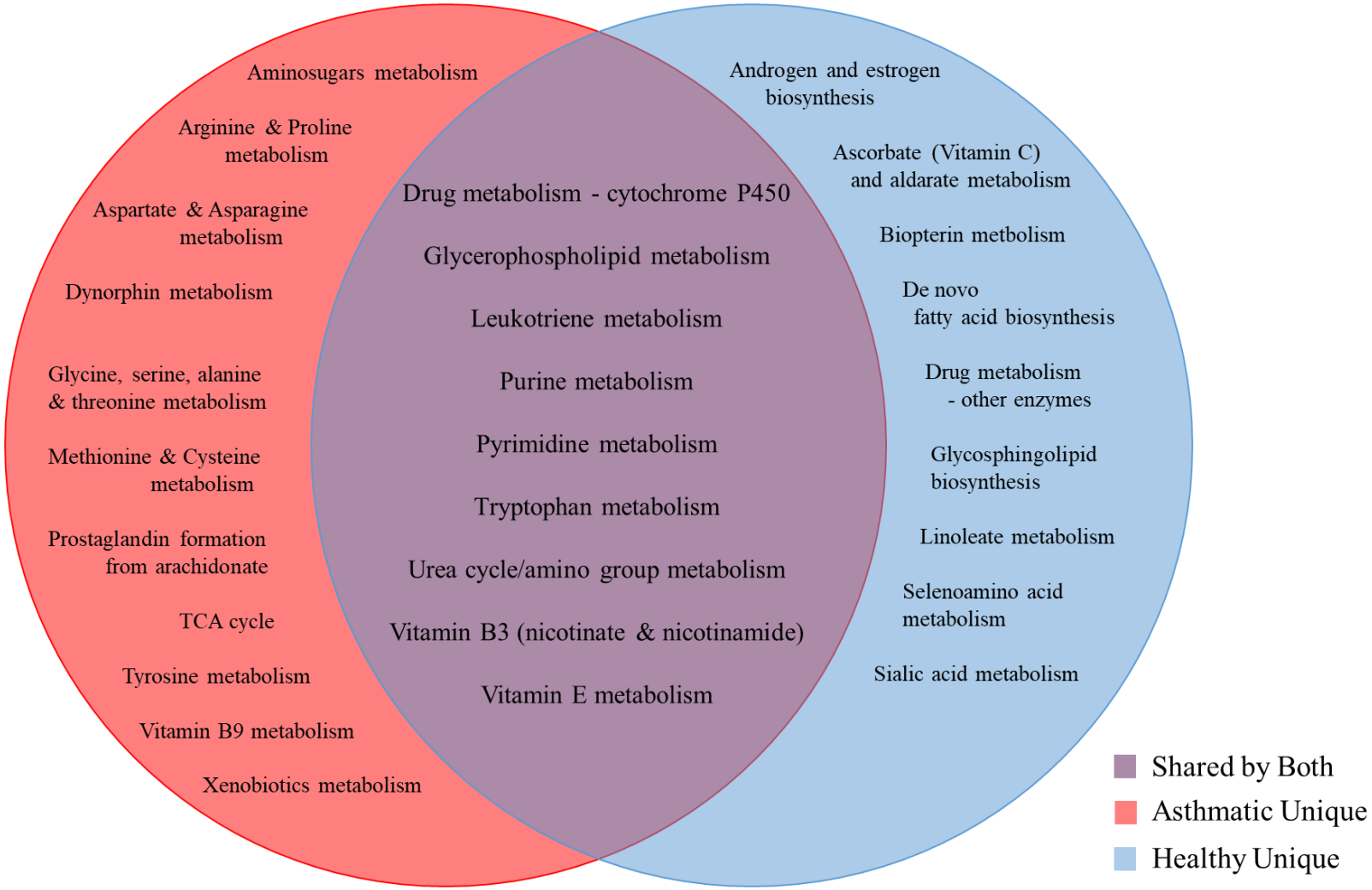

Figure 3.2 Top Metabolic pathways associated with TRAP exposure indicators in asthmatic and healthy participants. The metabolic pathways (KEGG) presented in the Venn diagram were the top significant pathways (associated with at least 25% of the TRAP indicators), where significant features ($FDR_{B\text{-}H}<0.05$) that were associated with single traffic pollutant indicator were enriched. 9 pathways were found in both asthmatic and health participants, while 11 unique pathways were identified only in asthmatic participants and 10 only in healthy participants.

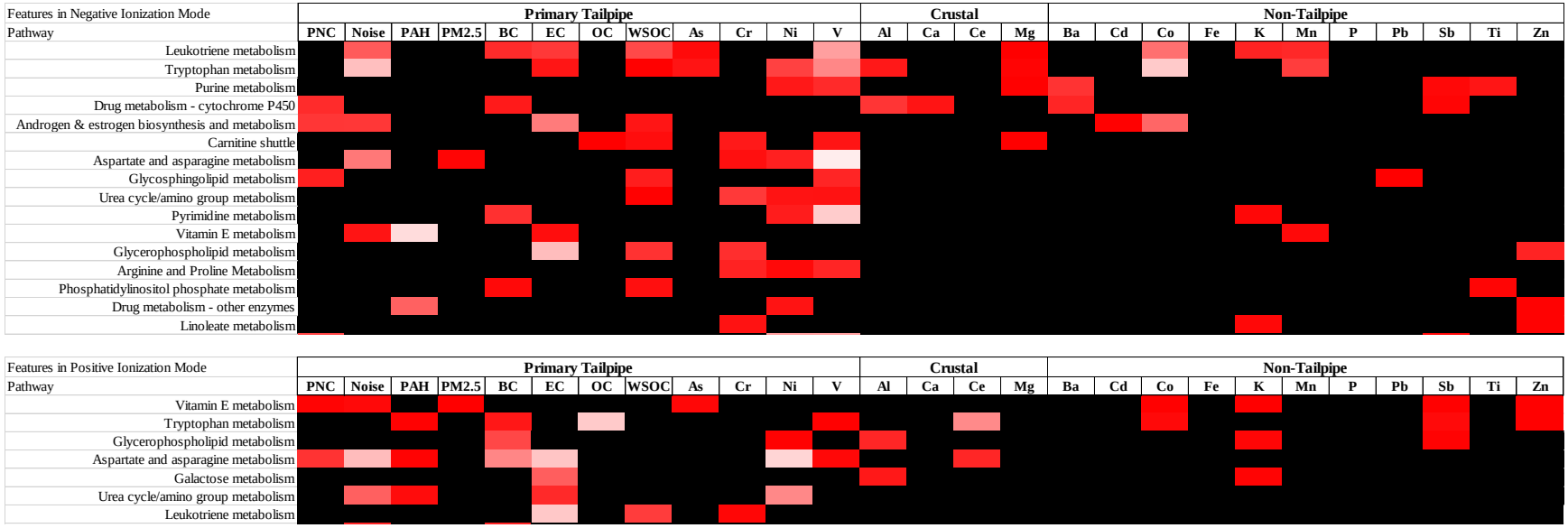

Figure 3.3 Metabolic pathways associated with significant effect modification of asthmatic status on TRAP-metabolic feature association. Cells were shaded according to the strength (i.e. p-value) of the association between each of metabolic pathways (KEGG) and features that were associated with significant effect modification of asthmatic status on the associations between each single traffic pollutant indicator and feature internsity ($FDR_{B\text{-}H}<0.05$). Pathways are ordered according to the total number of the significant pathway-traffic pollutant associations ($p<0.05$) in the C18 column negative ionization mode and positive ionization mode.

*For HILIC positive ion mode, only the following adducts were considered: M[1+], M+H[1+], M-H2O+H[1+], M+Na[1+], M+K[1+], M+2H[2+], and M(C13)+2H[2+]
For C18 negative ion mode, only the following adducts were considered: M-H[-], M+Cl[-], M+ACN-H[-], M+HCOO[-], M(C13)-H[-], M-H2O-H[-], and M+Na-2H[-]

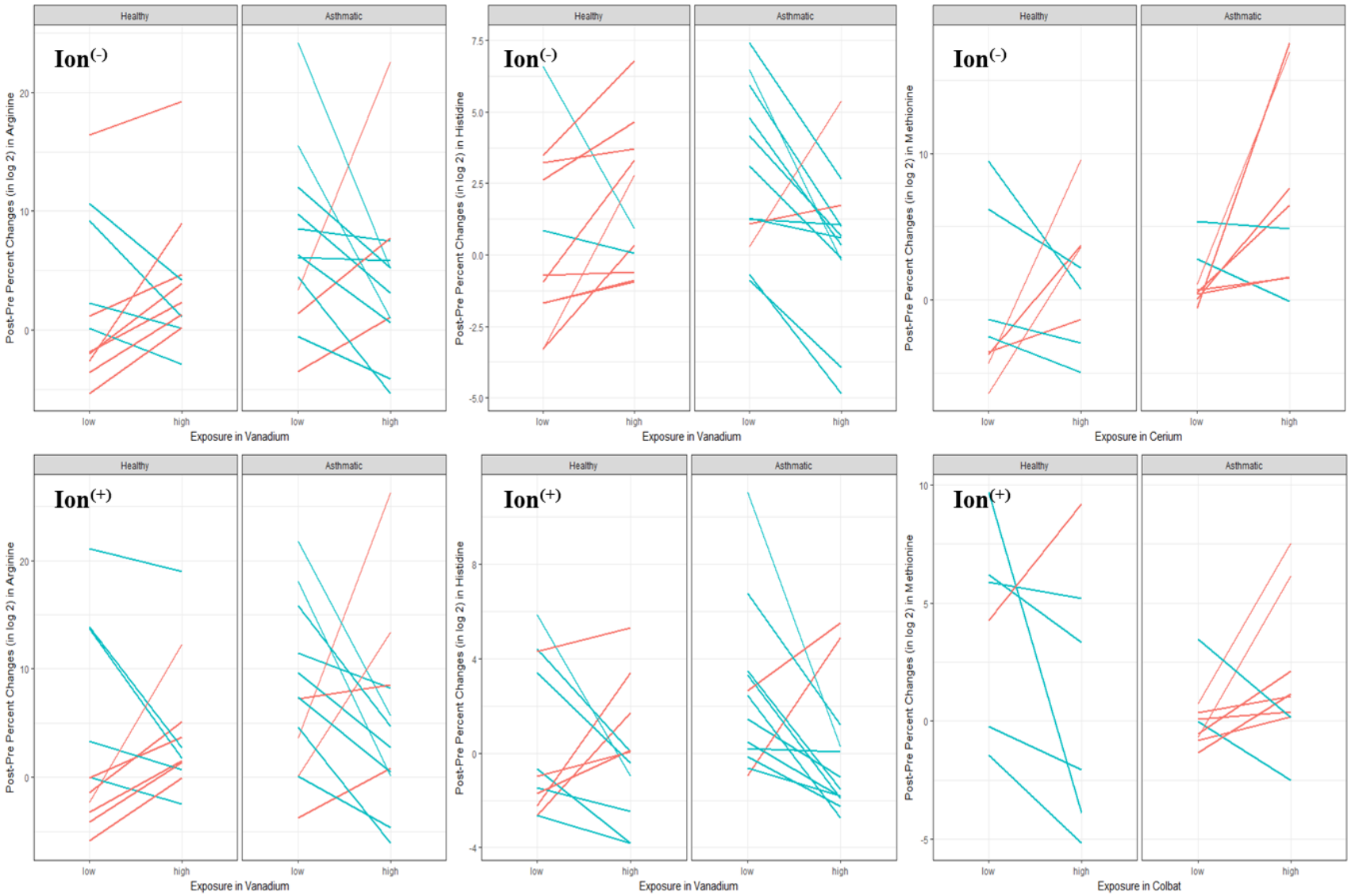

Figure 3.4 Differential associations between TRAP indicators and Arginine, Histidine, and Methionine among the asthmatic and healthy participants. $Ion^{(-)}$, metabolic features extracted using the negative ionization mode; $Ion^{(+)}$, metabolic features extracted using the positive ionization mode. Negative associations were presented in blue lines and positive associations were presented in red lines.

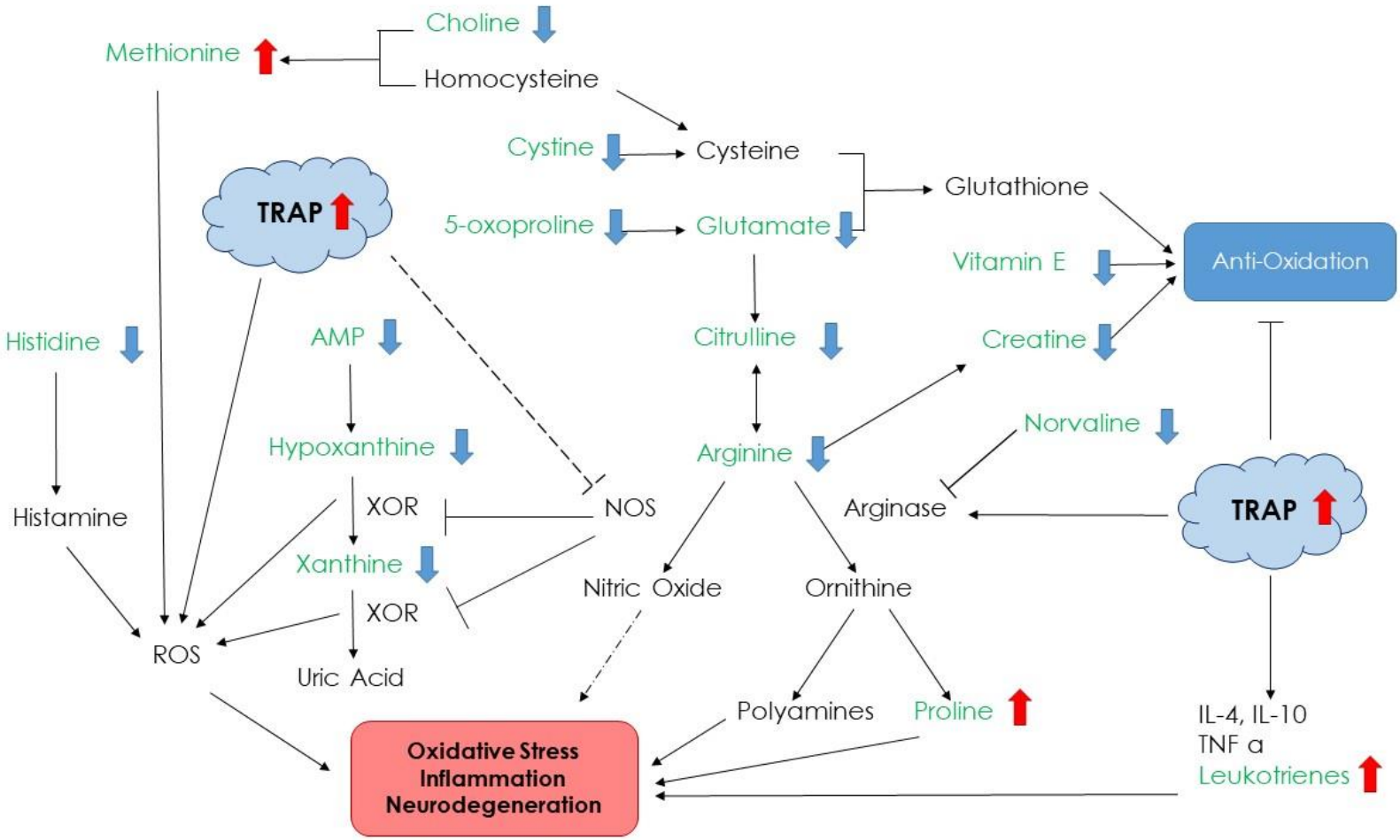

Figure 3.5 Potential molecular mechanisms on traffic-related air pollution toxicity elucidated using untargeted high-resolution metabolomics on the ACE-2 participants. Molecules in green denoted the metabolites detected and confirmed in the ACE-2 samples. Negative associations with elevated TRAP were presented in blue arrows and positive associations were presented in red arrows. Acronym: TRAP, traffic-related air pollutant; ROS, reactive oxygen species; NOS, nitric oxide synthases; XOR, xanthine oxidoreductase; IL-4, the interleukin 4; IL-10, the interleukin 10; TNF α, tumor necrosis factor alpha.

CHAPTER 3 SUPPLEMENTAL MATERIALS

Table S3.1 Number of significant features associated with TRAPs in each sets of MWAS models

Traffic related air pollutants	Main Effect		Asthmatic participants		Healthy participants		Effect modification of asthmatic status	
	$Ion^{(-)*}$	$Ion^{(+)}$	$Ion^{(-)}$	$Ion^{(+)}$	$Ion^{(-)}$	$Ion^{(+)}$	$Ion^{(-)}$	$Ion^{(+)}$
Particle Counts	177	71	123	51	248	104	657	189
Noise	173	77	150	56	287	122	477	178
pb-PAH	133	71	178	63	786	397	187	106
$PM_{2.5}$	157	58	128	45	227	86	286	100
Organic Components of $PM_{2.5}$								
EC	576	226	324	155	616	874	244	85
OC	242	79	73	26	553	180	335	122
WSOC	131	69	146	57	120	44	480	242
BC	188	80	149	54	230	92	239	112
Metal Components of $PM_{2.5}$								
Magnesium (Mg)	145	55	81	39	334	120	311	157
Aluminium (Al)	201	104	134	56	335	143	480	178
Phosphorus (P)	190	83	110	55	320	94	402	177
Potassium (K)	119	77	130	63	269	89	491	220
Calcium (Ca)	114	56	76	30	229	84	270	107
Titanium (Ti)	116	45	74	35	323	121	163	63
Vanadium (V)	569	193	370	157	995	400	261	111
Chromium (Cr)	288	101	141	56	464	242	861	325
Manganese (Mn)	123	47	75	31	244	85	292	131
Iron (Fe)	141	66	79	29	241	82	337	164
Cobalt (Co)	154	87	100	56	307	151	424	255
Nickle (Ni)	205	81	208	98	349	160	720	300
Zinc (Zn)	166	92	169	83	620	266	499	266
Arsenic (As)	193	85	102	34	304	95	313	127
Cadmium (Cd)	181	79	92	35	219	93	442	158
Antimony (Sb)	126	54	69	45	195	84	193	73
Barium (Ba)	179	82	80	24	198	73	350	215
Cerium (Ce)	224	99	118	58	682	298	248	142
Lead (Pb)	173	77	131	55	216	66	615	245

* $Ion^{(-)}$, features extracted (N=17,586) using the negative ionization mode; $Ion^{(+)}$, features extracted (N=9,087) using the positive ionization mode

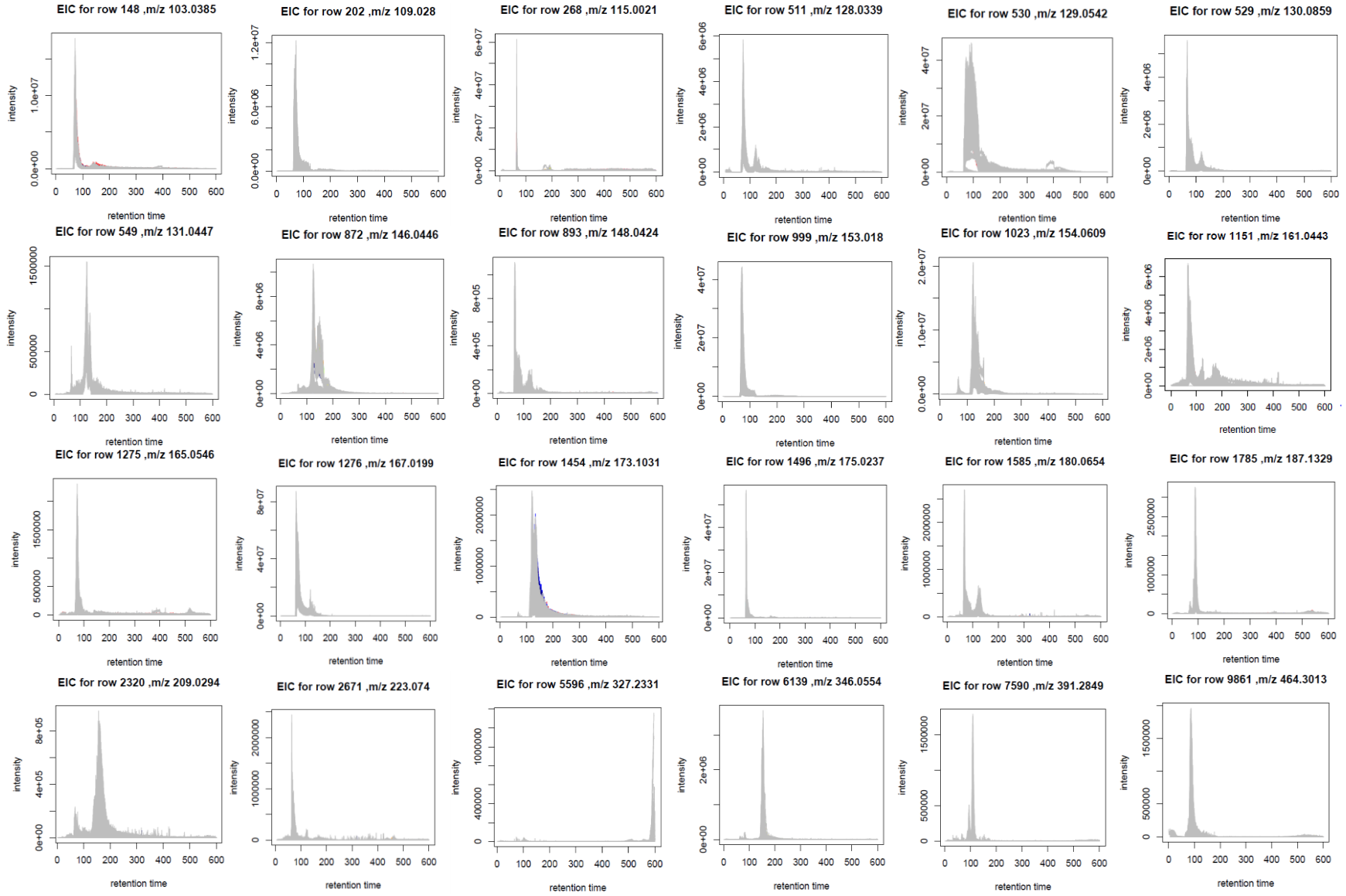

Figure S3.1a Extracted ion chromatographs (EICs) of the verified metabolic features in the negative ionization mode

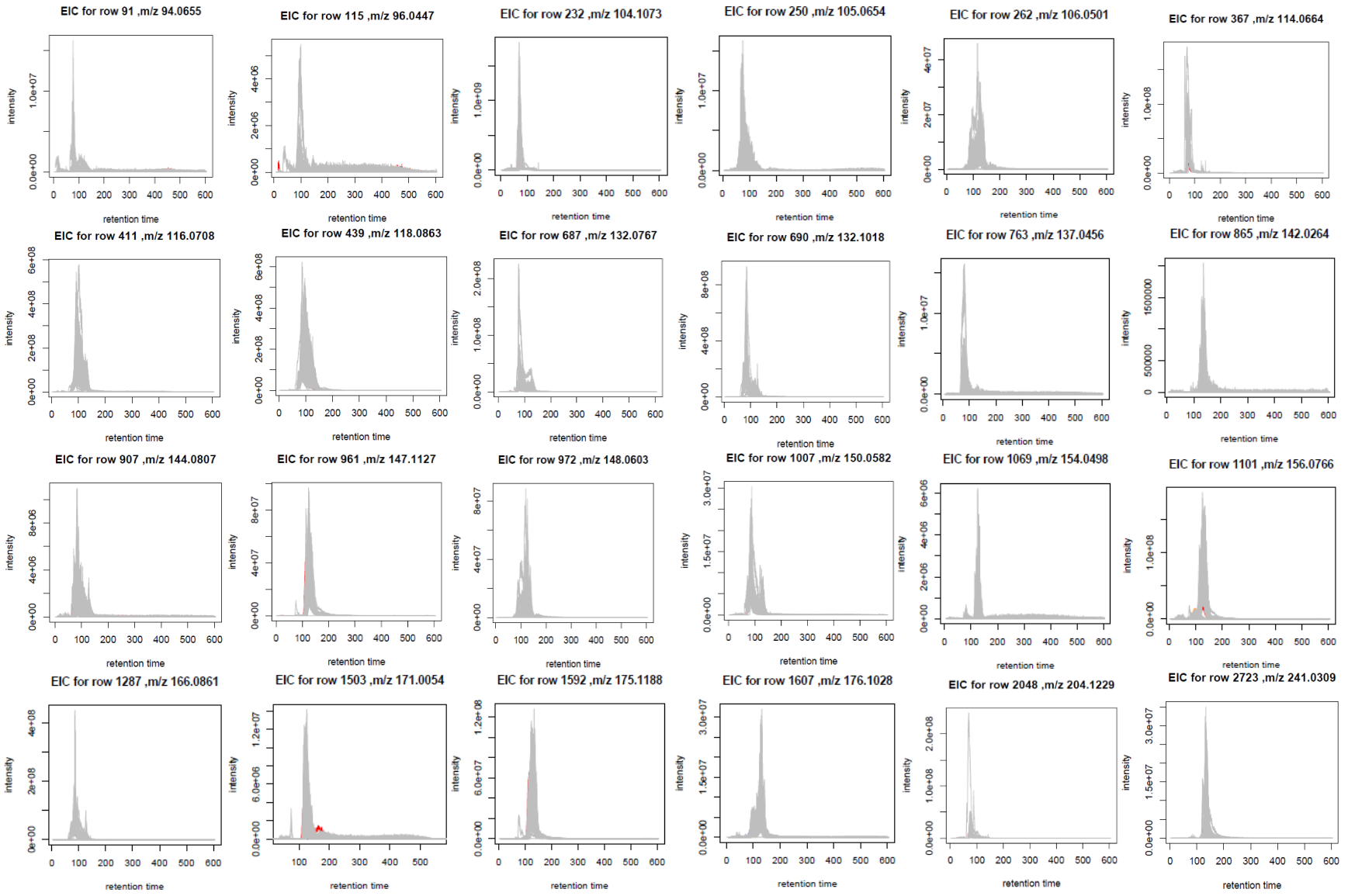

Figure S3.1b Extracted ion chromatographs (EICs) of the verified metabolic features in the positive ionization mode

CONCLUSIONS

To our knowledge, DRIVE study is among the first studies to quantify the effects of measurement error due to spatial and temporal variation of TRAPs and examine how well a near-road monitoring site can serve as a proxy to estimate traffic pollutant related health effects in epidemiology studies. Pollutant levels measured during DRIVE showed a relatively low impact of the 16-lane interstate highway compared to historic near-road field data. Spatial gradients of TRAPs varied substantially during the course of a day, with greater primary impacts from the highway occurring during morning rush hour periods. NO2, specifically, exhibited spatial trends that differed from other single-pollutant primary traffic indicators. This finding provides some indication of limitations in the use of NO2 as a primary traffic exposure indicator in panel-based health effect studies. Pronounced attenuation of observed changes in health effects was found when using measured pollutant level from the near-road monitor as a surrogate for true exposure. Moreover, the extent of attenuation associated with increasing distance from the traffic hotspot varied across pollutant species and over the course of the day. Together, results from the DRIVE monitoring and simulated epidemiologic analyses indicate that for panel-based studies, the use of near-road measurements as surrogates of exposure to primary traffic pollution may result in substantial under-estimates of health response and potential risk. This was observed to be true for even sites located within 20 m of the highway sources and increasing with distance from the highway and within indoor environments. Collectively, these results provide indication that caution should be taken when using near-road monitoring network to investigate health effects of traffic pollutants in future studies.

Recent advances in HRM support its use as a highly sensitive platform, capable of identifying thousands of small molecules, produced both endogenously and exogenously. The metabolomics analyses results from DRIVE study provided further evidence of HRM's ability to elucidate biologically-relevant pathways associated with exposures to key environmental pollutants and sources. The DRIVE results were broadly consistent with the limited number of similar studies, which have examined perturbations in the human

metabolome and ambient air pollution, in showing broad metabolomic perturbation associated with several oxidative stress and inflammatory pathways. Most intriguingly, however, were results from the DRIVE MWAS models, which point to the potential of HRM as tool for biomarker discovery. Here several metabolites were identified and validated in plasma and saliva that were directly associated with external traffic pollution measurements in DRIVE panel. Collectively, the current findings support the use of environmental metabolomics, as a sensitive means for conducting air pollution exposure and epidemiologic analyses, in panel-based designs.

Using the same high-resolution environmental metabolomics platform on ACE-2 study, thousands of significant and robust metabolic perturbations were found to be associated with TRAP exposure during commuting. Pathway analyses further elucidated a number of pathways predominantly associated with xenobiotic-mediated oxidative stress and acute inflammatory response, including leukotriene metabolism, vitamin E metabolism, cytochrome P450, pyrimidine metabolism, and tryptophan metabolism. In addition, the features enriched in these pathways responded differentially among asthmatic and healthy participants, indicative of their potential roles in asthma etiology. Our results were broadly consistent with the limited number of similar studies. More interestingly, we identified and validated 45 unique metabolites, many of which were not only significantly associated with multiple TRAP indicators, but also responded differently among participants with and without asthma. Most intriguingly, these confirmed metabolites were closely linked and connected in several inflammatory and redox pathways, elucidating the potential molecular mechanisms on traffic-related air pollution toxicity. Collectively, the current findings support the potential to develop some of these promising metabolic markers for reflecting TRAP exposures, their corresponding effects, and the asthma etiology.